

NACA TN 3016

# CASE FILE COPY

## NATIONAL ADVISORY COMMITTEE FOR AERONAUTICS

TECHNICAL NOTE 3016

### ANALYSIS OF TURBULENT HEAT TRANSFER AND FLOW IN THE ENTRANCE REGIONS OF SMOOTH PASSAGES

By Robert G. Deissler

Lewis Flight Propulsion Laboratory  
Cleveland, Ohio

PROPERTY BAIRDFIELD  
ENGINEERING LIBRARY

OCT 21 1953



Washington  
October 1953

2



NATIONAL ADVISORY COMMITTEE FOR AERONAUTICS

TECHNICAL NOTE 3016

ANALYSIS OF TURBULENT HEAT TRANSFER AND FLOW IN THE  
ENTRANCE REGIONS OF SMOOTH PASSAGES

By Robert G. Deissler

SUMMARY

A previous analysis for fully developed turbulent heat transfer and flow with variable fluid properties is extended and applied to the entrance regions of smooth tubes and parallel flat plates. Integral heat-transfer and momentum equations are used for calculating the thicknesses of the thermal and flow boundary layers. The effect of variable properties is determined for the case of uniform heat flux, uniform initial temperature distribution, and fully developed velocity distribution. A number of other cases in which the fluid properties are considered constant are analyzed. The predicted Nusselt numbers for air with a uniform wall temperature and uniform initial temperature and velocity distributions agree closely with experimentally determined values.

INTRODUCTION

Flow and heat transfer in the entrance regions of channels have been subjects of considerable interest. The laminar flow case has been analyzed in references 1 (pp. 299-310), 2, and 3 (pp. 451-464), for instance, and the turbulent case, in references 4 and 5. In these analyses constant fluid properties were assumed, and uniform wall temperature was postulated in the cases in which heat transfer was considered. In the turbulent flow cases the flow was assumed to be turbulent at all points along the passage.

The analysis in reference 4 is for a Prandtl number of 1 and is based on an assumed  $1/7$ -power velocity profile and the Blasius resistance formula. The relative changes in heat-transfer coefficient along the tube predicted in that analysis are approximately correct, but the absolute values of the heat-transfer coefficient at the end of the entrance region are about 20 percent too low. The analysis given in reference 5 is applicable to cases in which the heat transferred by turbulence can be neglected, as might occur at very low Prandtl numbers.

2857

1-20

The analysis given herein, which was made at the NACA Lewis laboratory, is an extension of the analysis given in reference 6 for fully developed heat transfer and flow with variable fluid properties to the entrance regions of smooth passages. In calculating the growth of the thermal and flow boundary layers in the entrance region, integral equations for heat transfer and momentum are used. For obtaining the velocity and temperature distributions in the boundary layers, the same assumptions are made for solving the turbulent transfer equations as were made in reference 6.

The flow is assumed to be turbulent at all points along the passage, as in previous analyses, so that the analysis should be applicable when disturbances occurring at the entrance are sufficient to produce a turbulent boundary layer. According to Prandtl's assumption, which is in reasonable agreement with experiment, in the presence of a laminar boundary layer near the entrance, the turbulent portion of the boundary layer behaves as though the boundary layer were turbulent all the way from the entrance (ref. 7, p. 74). The present calculations may therefore be applicable to the turbulent portion of the boundary layer even when a laminar boundary layer exists near the entrance.

The cases considered in the present analysis are given in the following table:

Phenomenon	Wall boundary condition	Initial temperature distribution	Initial velocity distribution	Passage	Prandtl number	Properties
Heat transfer	Uniform heat flux	Uniform	Fully developed	Tube	0.73	Variable
Heat transfer	Uniform heat flux	Uniform	Fully developed	Parallel flat plates	.73	Variable
Heat transfer	Uniform wall temperature	Uniform	Fully developed	Tube	.73	Constant
Heat transfer	Uniform heat flux	Uniform	Uniform	Tube	.73	Constant
Heat transfer	Uniform heat flux	Uniform	Uniform	Parallel flat plates	.73	Constant
Heat transfer	Uniform wall temperature	Uniform	Uniform	Tube	.73	Constant
Heat transfer	Uniform heat flux	Uniform	Fully developed	Tube	.01	Constant
Friction	-----	-----	Uniform	Tube	----	Constant
Friction	-----	-----	Uniform	Parallel flat plates	----	Constant

Although most of the cases in the preceding table are for constant fluid properties, the greater portion of the report is concerned with the first two cases, in which the properties are variable.

### ANALYSIS

For calculating heat transfer and friction in the entrance region of ducts, the usual boundary layer assumptions are made; that is, it is assumed that the effects of heat transfer and friction are confined to fluid layers close to the surface (thermal and flow boundary layers, respectively). The temperature and velocity distributions outside the boundary layers are assumed uniform, and the total temperature and total pressure are constant along the length of the duct for the region outside the boundary layers. More exact analyses (ref. 2) indicate that these assumptions are valid, even for laminar flow, except in the region at a distance from the entrance where the boundary layer fills a large portion of the tube. For that region, however, the Nusselt numbers and friction factors have values very close to the values for fully developed flow.

In the following analysis, flow in round tubes and between parallel flat plates will be considered. The effect of frictional heating will be neglected and then later investigated to some extent in the section Effect of frictional heating on entrance length.

#### Velocity and Temperature Distributions in Boundary Layers for Gases

For obtaining the velocities and temperatures in the flow and thermal boundary layers, the differential equations for shear stress and heat transfer can be written as follows:

$$\tau = \mu \frac{du}{dy} + \rho \epsilon \frac{du}{dy}$$

$$q = -k \frac{dt}{dy} - \rho c_p g \epsilon_h \frac{dt}{dy}$$

(The symbols used in this report are defined in appendix A.) In the preceding equations  $\epsilon$  and  $\epsilon_h$  are the eddy diffusivities for momentum and heat transfer, respectively, the values for which are dependent on the amount and kind of turbulent mixing at a point. When written in dimensionless form, these equations become

$$\frac{\tau}{\tau_0} = \frac{\mu}{\mu_0} \frac{du^+}{dy^+} + \frac{\rho}{\rho_0} \frac{\epsilon}{\mu_0/\rho_0} \frac{du^+}{dy^+}$$

2857

CZ-1 back

and

$$\frac{q}{q_0} = \left( \frac{k}{k_0} \frac{1}{Pr_0} + \frac{\rho}{\rho_0} \frac{c_p}{c_{p_0}} \frac{\epsilon_h}{\mu_0/\rho_0} \right) \frac{dt^+}{dy^+}$$

where the subscript 0 refers to values at the wall.

Assumptions. - The following assumptions are made in the use of the previous equations for obtaining velocity and temperature distributions in the flow and thermal boundary layers:

1. The eddy diffusivities for momentum  $\epsilon$  and heat transfer  $\epsilon_h$  are equal. Previous analyses for fully developed flow in tubes based on this assumption yielded heat-transfer coefficients and friction factors that agree with experiment for Reynolds numbers above 15,000 (ref. 6). At low Reynolds or Peclet numbers ( $Pe = Re \times Pr$ ), the ratio of eddy diffusivities appears to be a function of Peclet number (ref. 8); but for Reynolds numbers above 15,000, it is nearly constant for gases, at least for fully developed boundary layers. The same assumption is made here for developing boundary layers.

2. The eddy diffusivity  $\epsilon$  is given by

$$\epsilon = n^2 u y$$

in the region close to the wall ( $y^+ < 26$ ), and by the Kármán relation

$$\epsilon = \kappa^2 \frac{(du/dy)^3}{(d^2u/dy^2)^2}$$

in the region at a distance from the wall ( $y^+ > 26$ ). These expressions have been experimentally verified for fully developed boundary layers with variable properties in reference 6. It is assumed here that they apply also to developing boundary layers. The quantities  $n$  and  $\kappa$  are experimental constants having the values 0.109 and 0.36, respectively.

3. The variations across the flow and thermal boundary layers of the shear stress  $\tau$  and the heat transfer per unit area  $q$  have a negligible effect on the velocity and temperature distributions. It is shown in figure 12 of reference 6 that the assumption of a linear variation of shear stress and heat transfer across the boundary layers ( $\tau$  or  $q = 0$  at the edge of the thermal or flow boundary layer) gives very nearly the same velocity and temperature profiles as those obtained by assuming uniform shear stress and heat transfer across the boundary

layers for values of  $\delta^+$  or  $\delta_h^+$  between 500 and 5000.<sup>1</sup> For small values of  $\delta_h^+$ , such as occur very near the entrance, the effect of variable heat transfer will be checked in appendix B and in the section Effect of variation of heat transfer across boundary layer on Nusselt number for small  $\delta_h^+$  and constant fluid properties.

4. The molecular shear stress and heat-transfer terms in the equations can be neglected in the region at a distance from the wall (ref. 6, fig. 14).

5. The static pressure can be considered constant across the passage.

6. The Prandtl number and specific heat can be considered constant with temperature variation. The variations with temperature of the specific heat and Prandtl number of gases are of a lower order of magnitude than the variations of viscosity, thermal conductivity, and density. The variations of viscosity and thermal conductivity with temperature are assumed to be given by the equations

$$\mu/\mu_0 = k/k_0 = (t/t_0)^{0.68}$$

From the definitions of the quantities involved it can be shown that

$$t/t_0 = 1 - \beta t^+$$

Solution of equations. - The details of the solution of the equations for shear stress and heat transfer under the foregoing assumptions are given in reference 6. The resulting relations between  $t^+$  and  $y^+$  and  $u^+$  and  $y^+$  are given in figures 1 and 2. Positive values of  $\beta$  correspond to heat addition to the gas; negative values, to heat extraction. For the cases in which the fluid properties are considered constant, the curves for  $\beta = 0$  are used.<sup>2</sup> The plotted values of  $t^+$  and  $u^+$  are to be used in the thermal and flow boundary layers, that is, for values of  $y^+ < \delta_h^+$  or  $y^+ < \delta^+$ . For values of  $y^+$  greater

---

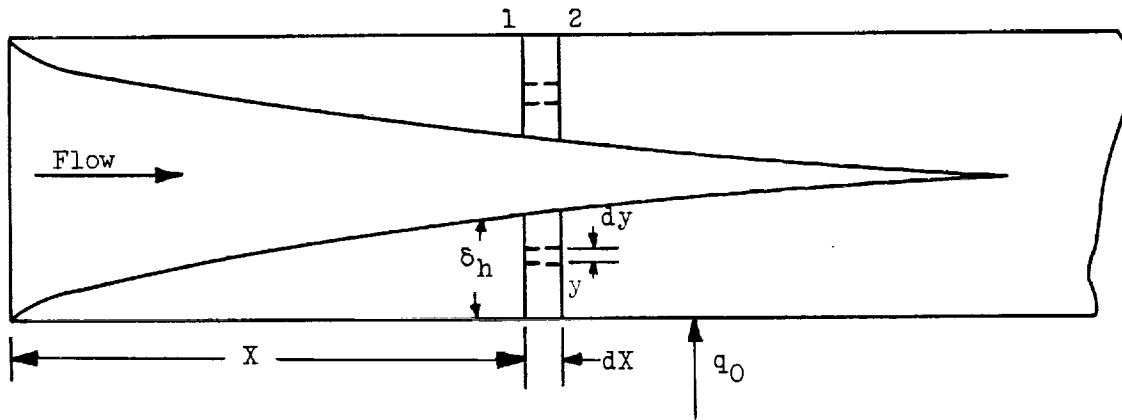
<sup>1</sup>Figure 12 of reference 6 applies to developing boundary layers if the symbols  $r_0^+$  in the figure are replaced by  $\delta^+$  or  $\delta_h^+$ .

<sup>2</sup>The case in which  $\beta = 0$  is a limiting one which can be approached as closely as desired by making the temperature difference small. In the limit, where the temperature difference is zero or infinitesimal, the properties must be constant.

than these values,  $t^+$  and  $u^+$  are constant and have the values at  $\delta_h^+$  and  $\delta^+$ . The relations between  $\delta_h^+$  and  $X/D$  and  $\delta^+$  and  $X/D$  will be obtained in the following sections.

### Development of Thermal Boundary Layers

Heat-flow equations for thermal boundary layers. - The heat-flow equation for the thermal boundary layer in a round tube can be obtained from the following diagram:



Energy flows into the differential annulus by convection through plane 1 and leaves through plane 2. In addition to this energy there is a radial flow of energy (heat) from the tube surface by conduction and a radial flow by convection at  $\delta_h$ . No radial heat flow due to temperature gradient takes place at  $\delta_h$  because the temperature gradient is, by definition of the thermal boundary layer, zero at the edge of the boundary layer.

Equating the heat energy entering the annulus to that leaving gives, for constant  $c_p$ ,

$$\begin{aligned}
 & q_0 2\pi r_0 dX + \left( \int_0^{\delta_h} t \rho u c_p g 2\pi r dy \right)_1 + \\
 & \left[ \left( \int_0^{\delta_h} \rho u 2\pi r dy \right)_2 - \left( \int_0^{\delta_h} \rho u 2\pi r dy \right)_1 \right] c_p g t_\delta \\
 & = \left( \int_0^{\delta_h} t \rho u c_p g 2\pi r dy \right)_2
 \end{aligned}$$



where the subscripts on the parentheses refer to planes 1 and 2 in the diagram, or

$$q_0 r_0 dX = d \left[ \int_0^{\delta_h} c_p g t \rho u (r_0 - y) dy \right] - c_p t_\delta g d \left[ \int_0^{\delta_h} \rho u (r_0 - y) dy \right] \quad (1)$$

where the differentials of the integrals indicate changes in the X-direction. Equation (1) is the desired equation for flow in tubes relating the thermal-boundary-layer thickness to the distance along the tube.

An equation corresponding to equation (1) can be easily derived for flow between flat plates. This equation is

$$q_0 dX = d \left( \int_0^{\delta_h} c_p g t \rho u dy \right) - c_p t_\delta g d \left( \int_0^{\delta_h} \rho u dy \right) \quad (2)$$

Equation (2) in the incompressible form has been used extensively for calculating the growth of the thermal boundary layer on a flat plate (ref. 7, p. 86).

Uniform heat flux, variable fluid properties (gases). - The total temperature outside the thermal boundary layer does not vary with X inasmuch as no heat penetrates the region outside the boundary layer. (The differences between total and static temperature are small except at high Mach numbers.) For uniform heat flux at the wall, equation (1) can then be integrated to give

$$\frac{q_0 r_0 X}{c_p g} = \int_0^{\delta_h} (t - t_\delta) \rho u (r_0 - y) dy \quad (3)$$

Equation (3) can be written in dimensionless form as

$$\frac{X}{D} = \frac{1}{2r_0^+{}^2} \int_0^{\delta_h^+} (t_\delta^+ - t^+) \frac{\rho}{\rho_0} u^+ (r_0^+ - y^+) dy^+ \quad (4)$$

where, from the definitions of the various quantities involved and the perfect gas law (constant pressure),

$$\rho/\rho_0 = 1/(1 - \beta t^+) \quad (5)$$

When equation (4) is to be used, values of  $r_0^+$  and  $\beta$  must first be fixed. Values of  $X/D$  can then be calculated for various values of  $\delta_h^+$ . The relations between  $t^+$  and  $y^+$  and  $u^+$  and  $y^+$  are obtained from figures 1 and 2.

The equation for flat plates corresponding to equation (4) is obtained from equation (2) and is found to be

$$\frac{X}{D} = \frac{1}{4r_0^+} \int_0^{\delta_h^+} (t_{\delta}^+ - t^+) \frac{\rho}{\rho_0} u^+ dy^+ \quad (6)$$

where  $D$  is the equivalent diameter for flow between flat plates, or twice the plate spacing.

Uniform wall temperature, constant fluid properties. - For flow in tubes, equation (1) can be written as

$$\frac{r_0 X}{c_p g} = \int_0^{[ ]} \frac{1}{q_0} d \left[ \int_0^{\delta_h} (t - t_{\delta}) \rho u (r_0 - y) dy \right] \quad (7)$$

where the quantity in brackets is also the upper limit on the integral. For constant fluid properties and uniform wall temperature, equation (7) can be written in dimensionless form as

$$\frac{X}{r_0} = \int_0^{[ ]} \frac{1}{r_0^+ \beta} d \left[ \frac{1}{r_0^+} \int_0^{\delta_h} (t_{\delta}^+ - t^+) \beta u^+ (r_0^+ - y^+) dy^+ \right] \quad (8)$$

where the shear stress  $\tau_0$  is allowed to vary with  $X$ . But

$$t_{\delta}/t_0 = t_1/t_0 = 1 - \beta t_{\delta}^+$$

since  $t_{\delta}$  does not vary with  $X$ . Therefore,

$$\beta = (1/t_{\delta}^+)(1 - t_1/t_0)$$

Substituting this expression for  $\beta$  into equation (8) results in

$$\frac{X}{D} = \frac{1}{2} \int_0^{\delta_h^+} \frac{t_{\delta^+}}{r_0^+} d \left[ \frac{1}{r_0^+} \int_0^{\delta_h^+} \frac{t_{\delta^+} - t^+}{t_{\delta^+}} u^+(r_0^+ - y^+) dy^+ \right] \quad (9)$$

Equation (9) gives the relation between  $X/D$  and  $\delta_h^+$  for round tubes with uniform wall temperature and constant fluid properties. Its use is similar to that of equation (4).

Nusselt numbers and Reynolds numbers. - It can easily be shown (see ref. 9) from the definitions of the quantities involved that the Nusselt number and Reynolds number (properties variable or constant) for circular tubes with the fluid properties evaluated at the wall temperature are given by

$$Nu_0 = \frac{2r_0^+ Pr}{t_b^+} \quad (10)$$

and

$$Re_0 = 2u_b^+ r_0^+ \quad (11)$$

where

$$t_b^+ = \frac{\int_0^{r_0^+} \frac{t^+ u^+(r_0^+ - y^+)}{1 - \beta t^+} dy^+}{\int_0^{r_0^+} \frac{u^+(r_0^+ - y^+)}{1 - \beta t^+} dy^+}$$

$$= \frac{\int_0^{\delta_h^+} \frac{t^+ u^+(r_0^+ - y^+)}{1 - \beta t^+} dy^+ + \frac{t_{\delta^+}}{1 - \beta t_{\delta^+}} \int_{\delta_h^+}^{r_0^+} u^+(r_0^+ - y^+) dy^+}{\int_0^{\delta_h^+} \frac{u^+(r_0^+ - y^+)}{1 - \beta t^+} dy^+ + \frac{1}{1 - \beta t_{\delta^+}} \int_{\delta_h^+}^{r_0^+} u^+(r_0^+ - y^+) dy^+} \quad (12)$$

and

$$u_b^+ = \frac{2}{r_0^{+2}} \int_0^{r_0^+} u^+(r_0^+ - y^+) dy^+$$

2857

CZ-2

which, by combination with equation (12), becomes

$$u_b^+ = \frac{2}{r_0^+} (1 - \beta t_b^+) \left[ \int_0^{\delta_h^+} \frac{u^+(r_0^+ - y^+)}{1 - \beta t^+} dy^+ + \frac{1}{1 - \beta t_{\delta}^+} \int_{\delta_h^+}^{r_0^+} u^+(r_0^+ - y^+) dy^+ \right] \quad (13)$$

The foregoing equations are for a circular tube. The corresponding equations for flow between flat plates are

$$Nu_0 = \frac{4r_0^+ Pr}{t_b^+} \quad (14)$$

and

$$Re_0 = 4u_b^+ r_0^+ \quad (15)$$

where

$$t_b^+ = \frac{\int_0^{\delta_h^+} \frac{t^+ u^+}{1 - \beta t^+} dy^+ + \frac{t_{\delta}^+}{1 - \beta t_{\delta}^+} \int_{\delta_h^+}^{r_0^+} u^+ dy^+}{\int_0^{\delta_h^+} \frac{u^+}{1 - \beta t^+} dy^+ + \frac{1}{1 - \beta t_{\delta}^+} \int_{\delta_h^+}^{r_0^+} u^+ dy^+} \quad (16)$$

and

$$u_b^+ = \frac{1}{r_0^+} (1 - \beta t_b^+) \left( \int_0^{\delta_h^+} \frac{u^+}{1 - \beta t^+} dy^+ + \frac{1}{1 - \beta t_{\delta}^+} \int_{\delta_h^+}^{r_0^+} u^+ dy^+ \right) \quad (17)$$

When values of  $Nu_0$  and  $Re_0$  are calculated, values of  $r_0^+$  and  $\beta$  must be fixed as in equation (4). Values of  $Nu_0$  and  $Re_0$  are thus obtained for given values of  $X/D$  and  $\beta$ .<sup>3</sup>

---

<sup>3</sup>Unfortunately,  $\beta$  varies along the passage. It will later be seen that  $q_1'$  is more convenient for use as a heat-flux parameter.

The temperature and velocity distributions from figures 1 and 2 can be used for these quantities except for the region outside the thermal boundary layer. The temperature distribution is, of course, uniform outside the thermal boundary layer ( $t^+ = t_\delta^+$ ). When the velocity distribution in that region is calculated for the case in which the velocity distribution is fully developed, it should be remembered that the properties are constant and have the values at  $\delta_h^+$ . For values of  $\delta_h^+ > 26$ , the velocity distribution curves outside the thermal boundary on the semilogarithmic plot are straight lines having the slope of the curves at  $\delta_h^+$ .

Nusselt numbers and Reynolds numbers with properties based on temperatures other than the wall temperature can be obtained by use of the relations

$$t_b/t_0 = 1 - \beta t_b^+$$

$$t_1/t_0 = 1 - \beta t_\delta^+$$

$$\rho_b/\rho_0 = 1/(1 - \beta t_b^+)$$

$$\mu_b/\mu_0 = k_b/k_0 = (1 - \beta t_b^+)^d$$

and so forth, where the perfect gas law with constant static pressure across the tube, constant Prandtl number, and constant specific heat have been assumed as in reference 6. The exponent  $d$  is obtained from viscosity data and is found to be about 0.68 for air and most gases. The following relations for Reynolds numbers then result:

$$Re_b = Re_0 \frac{1}{(t_b/t_0)^{d+1}} \quad (18)$$

$$Re_1 = Re_b \frac{(t_b/t_0)^d}{(t_1/t_0)^d} \quad (19)$$

where the continuity relation  $\rho_b u_b = \rho_1 u_1$  has been used. Similarly,

$$Nu_b = \frac{Nu_0}{(t_b/t_0)^d} \quad (20)$$

and

$$Nu_1 = \frac{Nu_b}{(t_1/t_b)^d} \quad (21)$$

Another useful parameter is  $q_1'$ , which can be calculated from

$$q_1' = \frac{\beta(t_b/t_0)}{u_b + (t_1/t_0)} \quad (22)$$

2857

Equation (22) can be obtained from the definition of  $q_1'$  and the perfect gas law for constant pressure,  $t_0/t_b = \rho_b/\rho_0$ , for  $\rho_b u_b$  is constant along the tube. The important property of  $q_1'$  is that it does not vary along the length of the tube.

It is desired to calculate the variation of bulk temperature and wall temperature along the tube for uniform heat flux. It can be shown, by use of the expressions  $q_0 = h(t_0 - t_b)$  and  $\pi DX q_0 = \rho g (\pi/4) D^2 u_b c_p (t_b - t_1)$ , that dimensionless bulk temperature and wall temperature parameters are given by

$$\left( \frac{t_b - t_1}{t_1} \right) \frac{1}{q_1'} = 4 \frac{X}{D} \quad (23)$$

and

$$\left( \frac{t_0 - t_1}{t_1} \right) \frac{1}{q_1'} = \frac{Re_1 Pr}{Nu_1} + 4 \frac{X}{D} \quad (24)$$

Equations (23) and (24) can be used for flow between flat plates as well as for tubes.

The average Nusselt number for a given  $X/D$  is calculated from

$$Nu_{1,av} = \frac{X/D}{\int_0^{X/D} \frac{d(X/D)}{Nu_1}} \quad (25)$$

This equation is consistent with the definition

$$(t_0 - t_b)_{av} \equiv \frac{\int_0^X (t_0 - t_b) dX}{X} \quad (26)$$

which is the usual way of defining the average difference between wall and bulk temperatures for uniform heat flux. For uniform wall temperature equation (26) is replaced by

$$(t_0 - t_b)_{av} = \frac{\int_0^X [(t_0 - t_b)/(q_0/q_{0av})] dX}{X}$$

which gives a Nusselt number consistent with equation (25). For points beyond the entrance region the Nusselt numbers and temperature distributions are calculated as outlined in appendix C.

#### Development of Flow Boundary Layer

Momentum equations for flow boundary layers. - The momentum equation for the fluid in a given space can be written for steady flow in vector notation as

$$\vec{F} = \iiint \vec{v}(\rho \vec{v} \cdot d\vec{A}) \quad (27)$$

or the force acting on the fluid in a space is equal to the rate of flow of momentum out of the space (ref. 10, p. 233). When the X component of equation (27) is written for the previously illustrated differential annulus ( $\delta_h$  replaced by  $\delta$ ), there results

$$dF_X = d\left(\int_0^\delta \rho u^2 2\pi r dy\right) - u_\delta d\left(\int_0^\delta \rho u 2\pi r dy\right) \quad (28)$$

where the differential of the second integral is the radial mass flow into the annulus at  $\delta$ . The force  $dF_X$  is composed of pressure forces on planes 1 and 2 and a shear force at the wall. There is no shear force at  $\delta$  because the velocity gradient is, by definition of the boundary layer, zero at the edge of the boundary layer. The force  $dF_X$  is then equal to

$$- [\pi r_0^2 - \pi(r_0 - \delta)^2] dp - 2\pi r_0 \tau_0 dX$$

Substituting for  $dF_X$  gives, for equation (28),

$$\delta(2r_0 - \delta)dp + 2r_0 \tau_0 dX = 2u_\delta d \left[ \int_0^\delta \rho u(r_0 - y) dy \right] - 2d \left[ \int_0^\delta \rho u^2(r_0 - y) dy \right] \quad (29)$$

In the region outside the boundary layer, the flow is frictionless, so that

$$dp = - \rho u_\delta du_\delta \quad (30)$$

Substituting equation (30) in equation (29), rearranging, and integrating between the tube entrance and  $X$  give

$$X = \int_{u_1}^{u_\delta} \frac{\delta(2r_0 - \delta)}{2\tau_0 r_0} \rho u_\delta du_\delta - \int_0^X \frac{d \left[ \int_0^\delta \rho u^2(r_0 - y) dy \right]}{\tau_0 r_0} + \int_0^X \frac{u_\delta d \left[ \int_0^\delta \rho u(r_0 - y) dy \right]}{\tau_0 r_0} \quad (31)$$

where the boundary-layer thickness has been taken as zero at  $X = 0$ . Equation (31) is the desired equation for flow in tubes relating the boundary-layer thickness to distance along the tube.

Equations corresponding to equations (29) and (31) can be derived for flow between flat plates. These equations are

$$\delta dp + \tau_0 dX = u_\delta d \left( \int_0^\delta \rho u dy \right) - d \left( \int_0^\delta \rho u^2 dy \right) \quad (32)$$

and

$$X = \int_{u_1}^{u_\delta} \frac{\delta \rho u_\delta}{\tau_0} du_\delta + \int_0^X \frac{u_\delta}{\tau_0} d \left[ \int_0^\delta \rho u dy \right] - \int_0^X \frac{1}{\tau_0} d \left[ \int_0^\delta \rho u^2 dy \right] \quad (33)$$



Equation (32) was first obtained by von Kármán and has been used extensively in the incompressible form for calculating the growth of the boundary layer for fluids flowing over surfaces (ref. 7, p. 66).

The value of  $\delta$  must be known in terms of  $u_\delta$  to solve equations (31) and (33). This relation will be obtained in the section Conservation of mass, constant properties.

Dimensionless form of momentum equations for constant properties. - Equation (31) for tubes can be written in dimensionless form for constant fluid properties as

$$\frac{X}{D} = \frac{1}{4} \int_{\frac{Re}{2}}^{u_\delta^+ r_0^+} \frac{(\delta^+/r_0^+)(2-\delta^+/r_0^+)}{r_0^+} u_\delta^+ d(u_\delta^+ r_0^+) -$$

$$\frac{1}{2} \int_0^{\delta^+} \frac{d \left[ \int_0^{\delta^+} u^{+2} (r_0^+ - y^+) dy^+ \right]}{r_0^{+2}} + \frac{1}{2} \int_0^{\delta^+} \frac{u_\delta^+ d \left[ \int_0^{\delta^+} u^+ \frac{(r_0^+ - y^+)}{r_0^+} dy^+ \right]}{r_0^+}$$

(34)

Equation (34) can be verified by substituting the definitions of the dimensionless quantities into the equation. Equation (34) can be put into a form more convenient for computation by using the definition for the differential of a product. Thus

$$r_0^+ u_\delta^+ d \left[ \int_0^{\delta^+} u^+ \frac{(r_0^+ - y^+)}{r_0^+} dy^+ \right] \equiv d \left[ r_0^+ u_\delta^+ \int_0^{\delta^+} u^+ \frac{(r_0^+ - y^+)}{r_0^+} dy^+ \right] -$$

$$d(r_0^+ u_\delta^+) \int_0^{\delta^+} u^+ \frac{(r_0^+ - y^+)}{r_0^+} dy^+$$

(35)

Substitution of equation (35) into the last term of equation (34) (the substitution can be more easily made if eq. (34) is first differentiated with respect to  $X$ ) and simplification give

$$\frac{X}{D} = \int_{\frac{Re}{2}}^{u_{\delta^+} r_0^+} \left[ \frac{1}{4} \left( \frac{\delta^+}{r_0^+} \right) \frac{1}{r_0^+} (2 - \delta^+/r_0^+) u_{\delta^+} - \frac{1}{2r_0^{+3}} \int_0^{\delta^+} u^+(r_0^+ - y^+) dy^+ \right] d(r_0^+ u_{\delta^+}) + \int_0^{[\ ]} \frac{1}{2r_0^{+2}} d \left[ \int_0^{\delta^+} (u_{\delta^+} - u^+) u^+(r_0^+ - y^+) dy^+ \right] \quad (36)$$

Equation (36) relates  $X/D$  to  $\delta^+$  for various values of  $Re$  for tubes. The relation between  $u^+$  and  $y^+$  is obtained from the curve for  $\beta = 0$  in figure 2. The value of  $r_0^+$  for a given  $Re$  and  $\delta^+$  will be obtained in the next section. The corresponding equation for flow between flat plates is found from equation (33) to be

$$\frac{X}{D} = \frac{1}{4} \int_{\frac{Re}{4}}^{u_{\delta^+} r_0^+} \left( \frac{\delta^+ u_{\delta^+}}{r_0^{+2}} - \frac{1}{r_0^{+2}} \int_0^{\delta^+} u^+ dy^+ \right) d(r_0^+ u_{\delta^+}) + \frac{1}{4} \int_0^{[\ ]} \frac{1}{r_0^{+2}} d \left[ r_0^+ \int_0^{\delta^+} (u_{\delta^+} - u^+) u^+ dy^+ \right] \quad (37)$$

Conservation of mass, constant properties. - In order to solve equations (36) and (37),  $u_{\delta^+}$  must be known in terms of  $Re$ . This relation can be obtained from the law of conservation of mass. For a constant-area duct and constant density, the law of conservation of mass gives

$$u_1 = u_b \quad (38)$$

or the bulk velocity is constant and equal to the uniform initial velocity. For a tube, equation (38) can be written

$$\begin{aligned} u_1 &= \frac{2}{r_0^2} \int_0^{r_0} u(r_0 - y) dy \\ &= \frac{2}{r_0^2} \int_0^{\delta} u(r_0 - y) dy + \frac{u_{\delta}}{r_0^2} (r_0 - \delta)^2 \end{aligned} \quad (39)$$

Equation (39) can be written in dimensionless form as

$$Re = \frac{4}{r_0^+} \int_0^{\delta^+} u^+(r_0^+ - y^+) dy^+ + \frac{2u_{\delta^+}(r_0^+ - \delta^+)^2}{r_0^+} \quad (40)$$

The equation corresponding to equation (40) for flow between flat plates is

$$Re = 4 \int_0^{\delta^+} u^+ dy^+ + 4u_{\delta^+}(r_0^+ - \delta^+) \quad (41)$$

Equation (40) or (41) gives the relation between  $Re$  and  $\delta^+$  or  $u_{\delta^+}$  for a given value of  $r_0^+$ .

Nusselt numbers, Reynolds numbers, and friction factors; constant fluid properties. - Nusselt numbers for a developing velocity distribution as well as a developing temperature distribution can be calculated from equations (10) and (12) or (14) and (16) as before. If the assumption is made that the thermal- and flow-boundary-layer thicknesses are equal ( $\delta_h^+ \approx \delta^+$  for  $Pr \approx 1$ )<sup>4</sup>, equation (12) for tubes can be simplified, and for constant fluid properties ( $\beta = 0$ ) becomes

$$t_b^+ = \frac{\int_0^{\delta_h^+} t^+ u^+(r_0^+ - y^+) dy^+ + \frac{t_{\delta^+} u_{\delta^+}}{2} (r_0^+ - \delta_h^+)^2}{\int_0^{\delta_h^+} u^+(r_0^+ - y^+) dy^+ + \frac{u_{\delta^+}}{2} (r_0^+ - \delta_h^+)^2} \quad (42)$$

A similar equation can be obtained for flow between flat plates.

Reynolds numbers for flow in tubes and between plates can be calculated from equations (40) and (41). For constant fluid properties the Reynolds number is constant along the length of the tube.

The pressure drop between the entrance and a given section, which is required to calculate the friction factor, is obtained by integrating equation (30).

$$p_1 - p = \frac{\rho u_{\delta}^2}{2} - \frac{\rho u_1^2}{2} \quad (43)$$

Or, in dimensionless form,

$$p' = 2(u_{\delta^+} r_0^+)^2 - \frac{1}{2} Re^2 \quad (44)$$

<sup>4</sup>This assumption is used only for determining  $t_b^+$  for the case where the initial velocity and temperature distributions are uniform.

for tubes, or

$$p' = 8(u_0^+ r_0^+)^2 - \frac{1}{2} Re^2 \quad (45)$$

for flat plates. The pressure-drop parameter  $p'$  in these equations is defined as

$$p' \equiv \frac{(p_1 - p)\rho D^2}{\mu^2} \quad (46)$$

The average friction factor based on the pressure drop for a given  $X/D$  is defined by

$$f_{av} \equiv \frac{D(p_1 - p)}{2X\rho u_b^2} \quad (47)$$

or

$$f_{av} = \frac{1}{2} \frac{p'}{(X/D)Re^2} \quad (48)$$

This equation includes momentum changes caused by velocity profile development.

The local friction factor based on the local pressure gradient is defined by

$$f \equiv - \frac{D(dp/dX)}{2\rho u_b^2} \quad (49)$$

or

$$f = \frac{1}{2} \frac{dp'/d(X/D)}{Re^2} \quad (50)$$

When  $f$  is to be found from equation (50), the curve for  $p'$  against  $X/D$  can be differentiated; or the curves, calculated from equation (36) or (37), for  $u_0^+ r_0^+$  against  $X/D$  can be differentiated and  $dp'/d(X/D)$  calculated from equation (44). The latter procedure proved to be the more accurate.

The local friction factor based on the local shear stress at the wall and excluding momentum changes due to a developing velocity profile is defined by

$$f_\tau \equiv \frac{2\tau_0}{\rho u_b^2} \quad (51)$$

or

$$f_{\tau} = \frac{2}{u_b^{+2}} \quad (52)$$

and, since  $Re$  is constant along the tube and equal to  $2u_b^{+} r_0^{+}$ ,

$$f_{\tau} = \frac{8r_0^{+2}}{Re^2} \quad (53)$$

where the relation between  $r_0^{+}$  and  $Re$  for a given  $\delta^{+}$  is obtained from equation (40) or (41).

## RESULTS AND DISCUSSION

### Heat Transfer with Uniform Heat Flux, Uniform Initial Temperature Distribution, Fully Developed Velocity Distribution, and Variable Fluid Properties for Gases; Prandtl Number of 0.73

Development of thermal boundary layer. - Figure 3 illustrates the development of the temperature profile in a tube for uniform heat flux and a fully developed velocity profile. The distance along the tube for various thermal-boundary-layer thicknesses is calculated from equation (4) and the temperature distribution in figure 1. The temperature distribution in the thermal boundary layer is obtained from figure 1; the temperature outside the boundary layer is uniform, inasmuch as no heat penetrates that region. The Reynolds numbers are calculated from equations (11) and (13). Figure 3 indicates that for a fixed tube diameter at a given distance from the entrance, the boundary-layer thickness is less for high Reynolds numbers than for low ones, or the distance required for a given degree of temperature profile development is greater for high Reynolds numbers than for low ones.

Although the temperature distributions in figure 3 are for  $\beta = 0$ , or constant fluid properties, similar distributions are obtained for variable fluid properties with large amounts of heat transfer, as may be inferred from figure 4. The variation of the thermal entrance length, defined as the length required for the thermal boundary layers from the opposite walls to meet at the center of the passage, with Reynolds number and heat flux  $q_1'$  is shown in figure 4. The quantity  $q_1'$  was calculated from equation (22). The quantity  $q_1'$  rather than  $\beta$  is used as a heat-flux parameter inasmuch as it is constant along the length of the tube. For the range of  $q_1'$  shown,  $t_0/t_b$  varies from about 0.4 to 3. Figure 4 indicates that heat flux has but a slight effect on the thermal entrance length.

2857

CZ-3 back

Local Nusselt numbers for tubes. - Local Nusselt numbers  $hD/k_i$  with properties evaluated at the inlet temperature are plotted against  $X/D$  for various values of  $Re_1$  and  $q_1'$  (heat flux) in figure 5. The heat-transfer coefficient in the Nusselt number is based on the difference between wall and bulk temperature (see appendix A). For obtaining the curves Nusselt numbers were calculated from equations (10), (20), and (21); Reynolds numbers, from equations (11), (18), and (19);  $q_1'$ , from equation (22); and  $X/D$ , from equation (4) for various values of the parameters  $\delta_h^+$ ,  $r_0^+$ , and  $\beta$ . Interpolation was necessary for obtaining the variation of  $Nu_1$  with  $X/D$  for constant values of  $Re_1$  and  $q_1'$ .

The curves in figure 5 indicate, as might be expected, that the Nusselt numbers (heat-transfer coefficients) close to the entrance are very high in comparison with the fully developed values farther down the tube at the ends of the curves. These values are high because the thermal boundary layer is thin and the temperature gradients consequently are severe near the entrance. At  $X/D = 0$  the boundary-layer thickness  $\delta_h$  is zero, so that the heat-transfer coefficient is infinite at the entrance. For uniform heat flux this means that the temperature difference  $t_0 - t_b$  must be zero at  $X/D = 0$ ; for a finite temperature difference at  $X/D = 0$  the heat transfer per unit area could not be uniform, since it would be infinite at the entrance.

Inspection of the curves in figure 5 shows that the Nusselt numbers very nearly reach their fully developed values long before the thermal boundary layers have met at the ends of the curves. For instance, for  $q_1' = 0$  (constant fluid properties) and  $Re_1 = 100,000$ , the Nusselt number at  $X/D$  of 9 is within 2 percent of its fully developed value at  $X/D$  of 18.8. This indicates that, for practical purposes, the thermal entrance lengths can be considered to be less than half the values given in figure 4.

Comparison of the curves for  $q_1' = 0$ , 0.004, and -0.0025 indicates a decrease in  $Nu_1$  at a given  $X/D$  for heat addition to the gas and an increase for heat extraction from the gas. For both heat addition and extraction,  $Nu_1$  increases with  $X/D$  for large values of  $X/D$ . These trends are clearly shown in figure 6, where  $Nu_1$  is plotted for  $q_1' = 0.004$  and -0.0025 for large values of  $X/D$ . For  $q_1' = 0$  (constant properties) the Nusselt numbers are constant beyond the entrance length. The Nusselt numbers for values of  $X/D$  beyond the entrance region were calculated by the method described in appendix C. For heat extraction from the gas the curves are cut at the points shown because the wall temperature reaches absolute zero at those points. The portions of the curves for which the temperature is below the liquefaction temperature of the gas should, of course, be disregarded because the properties no longer have the assumed variations with temperature. The increases in

Nusselt number with  $X/D$  are caused by the variation of properties along the tube and across the tube. The increases are due principally to the variation of  $t_0/t_b$ , which decreases along the tube for both heat addition to and extraction from the gas.

It is clear from figure 6 that fully developed heat transfer, in the sense that the heat-transfer coefficient becomes independent of  $X/D$ , cannot be obtained when the properties are variable. Fully developed heat transfer can, however, be obtained in the sense that the relation between the Nusselt number and Reynolds number becomes independent of  $X/D$  for sufficiently large values of  $X/D$  when the properties are evaluated at the proper reference temperature, as shown in figure 7. The curves in figure 7 were obtained by cross-plotting the curves for  $q_1' = 0$  from figure 4. They can be used for  $q_1' \neq 0$  by evaluating the properties, including density, in the Nusselt number and Reynolds number at the reference temperatures  $t_x \equiv x(t_0 - t_b) + t_b$  given in figure 8. The values of  $x$  were computed by selecting values of  $t_x$  such that the values of  $Nu_x$  and  $Re_x$ , calculated from the curves in figure 5, from equations (18) to (21), and from the definition of  $t_x$ , fall on the lines for  $q_1' = 0$  in figure 7. The curves in figure 8 indicate that the reference temperature for points close to the entrance is slightly closer to the bulk temperature than the reference temperature for fully developed heat transfer, although its variation with  $X/D$  is not large.

Effect of variation of heat transfer across boundary layer on Nusselt number for small  $\delta_h^+$  and constant fluid properties. - For large values of  $\delta_h^+$  ( $r_0^+$  for fully developed flow), the effect of the radial variation of heat transfer on temperature distributions was checked in reference 2 and found to be small. However, for low values of  $\delta_h^+$ , such as occur very close to the entrance, the flow is nearly laminar, so that the temperature profile in the boundary layer is not flat as it is for higher values of  $\delta_h^+$ . The temperature distribution in the thermal boundary layer for laminar heat transfer from a flat plate can be closely represented by a cubic parabola (ref. 7, p. 89), which means that the heat transfer per unit area varies as  $1 - y^2/\delta_h^2$ , as shown in appendix B. This variation of heat transfer is used herein for turbulent heat transfer for small  $\delta_h^+$  in order to obtain the effect of variation of  $q/q_0$  on the Nusselt numbers in the entrance region. The expression for the temperature distribution with this variation of  $q/q_0$  is obtained in appendix B.

The variation of  $Nu$  with  $X/D$  for variable heat transfer per unit area across the boundary layer ( $q/q_0 = 1 - y^2/\delta_h^2$ ) is shown in figure 9. For comparison, the curves from figure 5(a) for constant heat transfer ( $q/q_0 = 1$ ) are shown by dotted lines. The curves in figure 9 indicate that the variation of heat transfer per unit area across the boundary layer has a negligible effect on the relation between Nusselt number and  $X/D$ , so that the use of the temperature distributions in figure 1 appears justified, even for low values of  $\delta_h^+$ .

Wall and bulk temperature distributions for tubes. - Wall and bulk temperatures along a tube with uniform heat transfer as calculated from equations (23) and (24) are plotted in dimensionless form in figure 10. As mentioned previously, the wall and bulk temperatures are equal at the entrance for uniform heat transfer. The bulk temperature varies linearly with  $X/D$  inasmuch as the specific heat is assumed constant. For  $q_1' = 0$  the wall and bulk temperature curves are parallel beyond the entrance region. For both heat addition ( $q_1' = 0.004$ ) and heat extraction ( $q_1' = -0.0025$ ) from the gas, the wall and bulk temperature curves converge beyond the entrance region because of the increase in heat-transfer coefficient with  $X/D$  for those portions of the curves.

Average Nusselt numbers for tubes. - The variation of average Nusselt number  $Nu_{1,av}$  with  $X/D$  as calculated from equation (25) is shown in figure 11. The trends are similar to those for local Nusselt numbers but the changes are more gradual.

The relation between  $Nu_{x,av}$  and  $Re_{x,av}$  for various values of  $X/D$  is given in figure 12. The curves were obtained by cross-plotting the curves for  $q_1' = 0$  in figure 11(a) and can be used for  $q_1' \neq 0$  by evaluating the properties in the Nusselt number and Reynolds number at  $t_{x,av} = x(t_{0,av} - t_{b,av}) + t_{b,av}$ , where  $x$  is given in figure 13. The values of  $x$  were computed by selecting values of  $t_{x,av}$  such that the values of  $Nu_{x,av}$  and  $Re_{x,av}$  calculated as outlined in appendix C fall on the lines for  $q_1' = 0$  in figure 12. Figure 13 indicates that the value of  $x$  increases continuously with  $X/D$  for both heat addition to and extraction from the gas. These trends are indicated experimentally for heat addition in reference 11, where a constant reference temperature used for a range of values of  $X/D$  was found to give average Nusselt numbers for high heat fluxes at low values of  $X/D$  which were slightly higher than those for low heat fluxes. The values of  $x$  given in figure 13 indicate that for large values of  $X/D$ ,  $x > 1$ , so that for heat addition  $t_{x,av}$  is higher than the average wall temperature although not necessarily higher than the exit wall temperature. The variation of  $x$  with  $X/D$  is caused by the variation of properties along the tube. A more satisfactory correlation would perhaps be obtained by



using  $x$  only to account for the variation of properties across the tube and using another factor to account for the variation along the tube. The curves in figures 12 and 13 might, however, provide a convenient means of utilizing the results of the analysis for some purposes.

Nusselt numbers and temperature distributions for flow between flat plates. - Nusselt numbers, wall temperature distributions, and bulk temperature distributions for flow between flat plates with uniform heat transfer and fully developed velocity distribution are plotted in figures 14 to 16. The curves agree closely with the corresponding curves for flow in a tube. For instance, the curves for local Nusselt numbers plotted in figure 14 are between  $3\frac{1}{2}$  and 5 percent higher in the fully developed portions of the curves than the corresponding curves for tubes in figure 5. The portions of the curves close to the entrance agree even more closely. This agreement indicates that results for turbulent heat transfer in tubes can be used, with small error, for flat plates when an equivalent diameter equal to twice the plate spacing is used.

It should be emphasized that in applying the results of the foregoing analysis the same assumptions regarding the variation of properties with temperature should be made as were made in the analysis, that is, constant specific heat, and viscosity and thermal conductivity both proportional to  $t^{0.68}$ .

It should also be mentioned that the results in this analysis do not include the low Peclet number effect described in reference 8 inasmuch as the temperature distributions in figure 1 do not include that effect. The Nusselt numbers at  $Re_1 = 10,000$  may therefore be slightly high, but the ratios of local to fully developed Nusselt numbers should be accurate.

Effect of frictional heating on entrance length. - The effect of frictional heating on the  $X/D$  for a given  $\delta_h^+$  can be approximately accounted for by replacing  $t_\delta^+$  and  $t^+$  by  $T_\delta^+$  and  $T^+$ , respectively, in equation (4) and setting  $\rho/\rho_0 = 1/(1 - \beta T^+ - \alpha u^{+2})$  (ref. 9). In using that procedure it is assumed that the total-temperature gradient is zero at the edge of the thermal boundary layer, a good assumption for Prandtl numbers close to unity.

The variation of thermal entrance length  $(X/D)_{he}$  with Reynolds number and heat flux with frictional heating ( $\alpha = 0.00025$ ) is shown in figure 17. Mach numbers for air at the tube center at  $(X/D)_{he}$  are indicated in the figure. The Mach numbers were calculated from

$$M = \sqrt{\frac{2}{\gamma-1} \left( \frac{1}{\frac{1}{a_{c^+}^2} - 1} \right)}$$

which can be obtained from the definitions of  $M$ ,  $T_c$ ,  $u_c^+$ , and  $\alpha$ . Comparison of figure 17 with figure 4 indicates that frictional heating increases the entrance length, although the increase is not large for subsonic flow. Inasmuch as Nusselt numbers for fully developed heat transfer are not affected by frictional heating (ref. 9), the effect of frictional heating on the relations between Nusselt number and  $X/D$  probably is slight when the total rather than the static bulk temperature is used in the definition of the heat-transfer coefficient.

2857

Heat Transfer with Uniform Wall Temperature, Uniform Initial  
Temperature Distribution, Fully Developed Velocity  
Distribution, and Constant Fluid Properties for

Gases; Prandtl Number of 0.73

Relations among Nusselt number, Reynolds number, and  $X/D$  for the case of tubes, as calculated from equations (9) to (11), are plotted in figure 18. Comparison of figure 18 with figure 5 indicates that the Nusselt numbers for uniform wall temperature are very slightly lower than those for uniform heat flux. The heat transfer per unit area  $q_0$  must be infinite at  $X/D = 0$  for uniform wall temperature. This occurs only for an infinitesimal distance  $dX$ , however, so that a finite amount of heat is transferred.

Heat Transfer with Uniform Heat Flux, Uniform Initial Velocity and  
Temperature Distributions, and Constant Fluid Properties

for Gases; Prandtl Number of 0.73

For calculating the variation of Nusselt number with  $X/D$  for this case the flow-boundary-layer thickness as well as the thermal-boundary-layer thickness should be known for various values of  $X/D$ . However, in the calculation of Nusselt numbers, it is considered sufficiently accurate to assume the thicknesses of the thermal and flow boundary layers to be equal, inasmuch as the Prandtl number is close to unity.

Relations among Nusselt number, Reynolds number, and  $X/D$  for tubes, as calculated from equations (10), (42), (40), and (4), are plotted in figure 19. Comparison of figure 19 with figure 5 indicates

that the Nusselt numbers for a uniform initial velocity distribution are higher than those for a fully developed velocity distribution. This result might be expected because of the higher friction in the case of the uniform initial velocity profile.

Average Nusselt numbers as calculated from equation (25) are plotted in figure 20. Figure 20(b), which is a logarithmic plot, compares the predicted relations between  $Nu_{av}$  and  $X/D$  with the empirical relation  $Nu \propto (X/D)^{-0.1}$ . Curves having a slope of  $-0.1$  on the log-log plot agree closely with the predicted lines for  $X/D$  between 6 and 60. The agreement of the data given in reference 11 with the empirical relation for values of  $X/D$  as high as 120 might be due to the use of a constant rather than a variable reference temperature as given in figure 13.

Nusselt numbers for flow between flat plates are given in figure 21. Comparison of figure 21 with figure 19 indicates very close agreement between the Nusselt numbers for tubes and flat plates.

#### Heat Transfer with Uniform Wall Temperature, Uniform Initial

#### Velocity and Temperature Distributions, and Constant Fluid

#### Properties for Gases; Prandtl Number of 0.73;

#### and Comparison with Experimental Data

The variation of Nusselt number with  $X/D$  for this case is given in figure 22. The curves agree closely with those for the corresponding case for uniform heat flux given in figure 19. The Nusselt numbers for uniform wall temperature are slightly lower than those for uniform heat flux.

A comparison between analytical and experimental results for uniform wall temperature and uniform initial velocity and temperature distributions is given in figure 23. The experimental curves represent data from reference 12 for air flowing in a tube at uniform temperature with a bellmouth entrance and a screen at the entrance and should represent the case analyzed in this section. The screen at the entrance should insure a turbulent boundary layer throughout the tube. The figure shows that the agreement between analytical and experimental results for this case is very good.

The lack of a comparison of the present analytical results for a uniform wall temperature and a fully developed velocity distribution with the data from reference 12, which were taken with a long approach section at the entrance, should perhaps be explained. It appears that the sharp edge at the beginning of the long approach section produced

2857

CZ-4

large disturbances which were not damped out in the length of approach section used. The data in reference 12 for heat-transfer coefficients with a sharp entrance without an approach section indicate such results. For that case the heat-transfer coefficients are higher throughout the tube than those obtained with a bellmouth entrance.

Average Nusselt numbers calculated from equation (25) are plotted in figure 24. As in the case of local Nusselt numbers, the average Nusselt numbers for a uniform wall temperature in figure 24 are slightly lower than those for a uniform heat flux in figure 20.

Heat Transfer with Uniform Heat Flux, Uniform Initial  
Temperature Distribution, Fully Developed Velocity  
Distribution, and Constant Fluid Properties for  
Liquid Metals; Prandtl Number of 0.01

Temperature distributions for fully developed flow calculated as described in reference 8 and plotted in figure 25 were used in the thermal boundary layer for calculating the variation of Nusselt number with  $X/D$  for liquid metals. The velocity distributions were obtained from the curve for  $\beta = 0$  in figure 2. The curves for  $Nu$  against  $X/D$  in figure 26 were calculated from equations (4) and (10) to (12) ( $\beta = 0$ ). An unexpected feature of these curves is the slight increase of Nusselt number with  $X/D$  at large values of  $X/D$  and Reynolds number. This increase is due to the change in shape of the temperature profile with  $\delta_h^+$  for low Prandtl numbers. Thus, as  $\delta_h^+$  increases, the temperature gradient at the wall increases slightly in some instances because of the added turbulence in the boundary layer at higher values of  $\delta_h^+$ . This effect is indicated experimentally by the data in reference 13.

A plot of Nusselt number against  $Pe/(X/D)$  for various Peclet numbers is given in figure 27. If the heat transfer contributed by eddy diffusion were neglected, the curves for various Reynolds numbers would fall essentially on a single line as in reference 5. Examination of the curves in figure 27 indicates that for Reynolds numbers below 1000 the curves could be represented approximately by a single line. This line is slightly higher than the one obtained in reference 5 inasmuch as a uniform wall temperature rather than a uniform heat flux was postulated in that reference.

### Friction Factors with Uniform Initial Velocity Distribution and Constant Fluid Properties

Three friction factors are discussed in this section:  $f_\tau$ , based on the shear stress at the wall;  $f$ , based on the static-pressure gradient; and  $f_{av}$ , based on the pressure drop along the tube. The friction factor  $f_\tau$  is calculated from equation (53);  $f$ , from equation (50); and  $f_{av}$ , from equation (48). The Reynolds numbers and values of  $X/D$  corresponding to these friction factors are calculated from equations (41) and (36). The velocity distributions in the flow boundary layer are obtained from the curve for  $\beta = 0$  in figure 2.

The friction factors for a tube based on the shear stress at the wall and on the static-pressure gradient are plotted in figures 28 and 29, respectively. The friction factors based on the pressure gradient are higher than those based on the shear stress in the entrance region because the former include the pressure decrease caused by the increase in momentum of the fluid as the velocity profile develops as well as the pressure decrease caused by the shear stress at the wall. For fully developed flow the two friction factors are identical. Average friction factors based on the pressure drop are plotted in figure 30 and are, of course, higher than the local values.

The computed values of  $f$  and  $f_{av}$  are subject to some inaccuracy because of errors associated with measuring the slope of a curve (eq. (50)) and because the two terms in equation (44), which are subtracted, are nearly equal close to the entrance. The results presented should, however, be well within the limits of accuracy of experimentally determined friction factors.

Friction factors for flow between flat plates are plotted in figures 31 to 33 and are found to be very similar to those for a tube.

### Comparison of Local Nusselt Numbers and Friction Factors

A comparison of local Nusselt numbers and friction factors for various cases is presented in figure 34, where the ratio of local Nusselt number or friction factor to the fully developed value is plotted against  $X/D$  for a Reynolds number of 100,000. The quantity  $Nu/Nu_d$  is smaller than  $f/f_d$  for a given  $X/D$  in all cases except that of heat transfer to a liquid metal ( $Pr = 0.01$ ). The larger values of  $Nu/Nu_d$  for a liquid metal are apparently caused by the fact that the temperature profile at low Prandtl numbers is similar to that for

19857

CZ-4 back

laminar flow. At very high Reynolds numbers, where the dip occurs in the curves for Nusselt number plotted against  $X/D$ , and at very low Reynolds numbers, the values of  $Nu/Nu_d$  may be lower than  $f/f_d$  for liquid metals (fig. 26). For gases the values of  $Nu/Nu_d$  are lower than  $f/f_d$  for a given value of  $X/D$  because of the momentum pressure loss for velocity profile development included in the friction factor  $f$ ; there is no counterpart for this momentum pressure loss in heat transfer.

It should be mentioned that the preceding conclusions may apply only to the case analyzed, that is, to the case where the boundary layer is turbulent throughout the tube. The turbulent boundary layer might be produced by a bellmouth with a strip of sand paper at the entrance or by screens. For flow in which the boundary layer is partially laminar, or for which there are large disturbances at the entrance, such as might be caused by a right-angle-edge entrance, the conclusions might be altered.

#### SUMMARY OF RESULTS

The following results were obtained from the analytical investigation of the entrance region for turbulent heat transfer and flow in smooth tubes and between parallel flat plates:

1. The thin thermal boundary layers and consequently severe temperature gradients at the wall near the entrance produced high heat transfer near the entrance. Approximately fully developed heat transfer was, in general, attained in an entrance length less than 10 diameters.
2. The effect of variable properties on the local Nusselt number correlation for gases with fully developed velocity profiles was to decrease the Nusselt number with conductivity based on the inlet temperature for heat addition to the gas and to increase it for heat extraction from the gas at a given ratio of distance from the entrance to tube diameter  $X/D$  and inlet Reynolds number. For large values of  $X/D$ , the Nusselt number with conductivity based on the inlet temperature increased continuously with  $X/D$  for both heat addition to and extraction from the gas. A heat-transfer coefficient which is independent of  $X/D$  is therefore not obtained for heat transfer with variable properties, even in the fully developed region.
3. The reference temperature used for evaluating the properties in order to eliminate the effect of heat flux on the curves for local Nusselt number against Reynolds number at various values of  $X/D$  varied only slightly with  $X/D$ . The reference temperature for average Nusselt numbers, however, increased continuously with  $X/D$  for heat addition to the gas and was higher than the average wall temperature but lower than the exit wall temperature at very large values of  $X/D$ .

4. The variation of Nusselt number with  $X/D$  for a gas with uniform initial temperature and velocity distributions and uniform heat flux agreed with the experimentally determined relation,  $Nu \propto (X/D)^{-0.1}$ , for values of  $X/D$  between 6 and 60.

5. The predicted variation of Nusselt number with  $X/D$  for air with a uniform wall temperature and uniform initial velocity and temperature distributions agreed very well with the experimental values from reference 12.

6. The variation of Nusselt number with Graetz number for liquid metals (Prandtl number of 0.01) was represented approximately by a single line for Peclet numbers below 1000.

7. The ratio of friction factor based on the static-pressure gradient in the entrance region to the fully developed value was greater than the corresponding ratio of Nusselt numbers for gases in the entrance region because of the momentum pressure loss associated with the velocity profile development.

8. Essentially the same variations of Nusselt number and friction factor with  $X/D$  were obtained for flow between parallel flat plates as were obtained for a tube when the equivalent diameter equal to twice the plate spacing was used for the plates.

Lewis Flight Propulsion Laboratory  
National Advisory Committee for Aeronautics  
Cleveland, Ohio, July 21, 1953

## APPENDIX A

## SYMBOLS

The following symbols are used in this report:

A	area, sq ft
$c_p$	specific heat of fluid at constant pressure, Btu/(lb)(°F)
$c_{p0}$	specific heat of fluid at constant pressure at wall, Btu/(lb)(°F)
D	inside diameter of tube, ft
d	exponent; value depends on variation of viscosity of fluid with temperature
g	acceleration due to gravity, 32.2 ft/sec <sup>2</sup>
h	local heat-transfer coefficient, $q_0/t_0 - t_b$ , Btu/(sec)(sq ft)(°F)
$h_{av}$	average heat-transfer coefficient, $q_{0,av}/(t_0 - t_b)_{av}$
J	mechanical equivalent of heat, 778 ft-lb/Btu
k	thermal conductivity of fluid, Btu/(sec)(sq ft)(°F/ft)
$k_b$	thermal conductivity of fluid evaluated at $t_b$ , Btu/(sec)(sq ft)(°F/ft)
$k_1$	thermal conductivity of fluid evaluated at $t_1$ , Btu/(sec)(sq ft)(°F/ft)
$k_0$	thermal conductivity of fluid evaluated at $t_0$ , Btu/(sec)(sq ft)(°F/ft)
$k_x$	thermal conductivity of fluid evaluated at $t_x$ , Btu/(sec)(sq ft)(°F/ft)
$k_{x,av}$	thermal conductivity of fluid evaluated at $t_{x,av}$ , Btu/(sec)(sq ft)(°F/ft)



2857

M	Mach number at tube center at $X/D$
n	constant
p	static pressure
$p_1$	static pressure at inlet, lb/sq ft abs
q	rate of heat transfer toward tube center per unit area, Btu/(sec)(sq ft)
$q_0$	rate of heat transfer at inside wall toward tube center per unit area, Btu/(sec)(sq ft)
$q_{0,av}$	average rate of heat transfer at inside wall toward tube center per unit area for a given $X/D$ , Btu/(sec)(sq ft)
r	radius, distance from tube center, ft
$r_0$	inside tube radius or one-half distance between plates, ft
T	absolute total temperature, $^{\circ}R$
$T_c$	absolute total temperature at tube center, $^{\circ}R$
$T_\delta$	total temperature outside thermal boundary layer, $^{\circ}R$
t	absolute static temperature, $^{\circ}R$
$t_b$	bulk static temperature of fluid at cross section of tube, $^{\circ}R$
$t_{b,av}$	average bulk temperature, $^{\circ}R$
$t_1$	inlet static temperature of fluid, $^{\circ}R$
$t_x$	reference temperature for local Nusselt and Reynolds numbers, $x(t_0 - t_b) + t_b$ , $^{\circ}R$
$t_{x,av}$	reference temperature for average Nusselt and Reynolds numbers, $x(t_{0,av} - t_{b,av}) + t_{b,av}$
$t_\delta$	temperature of fluid outside thermal boundary layer

$t_0$	absolute wall temperature, $^{\circ}\text{R}$
$t_{0,av}$	average wall temperature, $^{\circ}\text{R}$
$(t_0 - t_b)_{av}$	average difference between wall and bulk temperature, $^{\circ}\text{R}$
$u$	time-average velocity parallel to axis of channel, ft/sec
$u_b$	bulk velocity at cross section of tube, ft/sec
$u_i$	velocity of fluid at inlet, ft/sec
$u_{\delta}$	velocity outside flow boundary layer, ft/sec
$\vec{v}$	velocity vector, ft/sec
$X$	distance from entrance, ft
$x$	number used in evaluating arbitrary temperature in tube, $t_x$ or $t_{x,av}$
$y$	distance from wall, ft
$\delta$	flow-boundary-layer thickness, ft
$\delta_h$	thermal-boundary-layer thickness, ft
$\epsilon$	coefficient of eddy diffusivity, sq ft/sec
$\mu$	absolute viscosity of fluid, (lb)(sec)/sq ft
$\mu_b$	absolute viscosity of fluid evaluated at $t_b$ , (lb)(sec)/sq ft
$\mu_i$	absolute viscosity of fluid evaluated at $t_i$ , (lb)(sec)/sq ft
$\mu_x$	absolute viscosity of fluid evaluated at $t_x$ , (lb)(sec)/sq ft
$\mu_{x,av}$	absolute viscosity of fluid evaluated at $t_{x,av}$ , (lb)(sec)/sq ft
$\mu_0$	absolute viscosity of fluid evaluated at $t_0$ , (lb)(sec)/sq ft
$\rho$	mass density of fluid, (lb)(sec <sup>2</sup> )/ft <sup>4</sup>

$\rho_b$	mass density of fluid evaluated at $t_b$ , (lb)(sec <sup>2</sup> )/ft <sup>4</sup>
$\rho_{b,av}$	mass density of fluid evaluated at $t_{b,av}$ , (lb)(sec <sup>2</sup> )/ft <sup>4</sup>
$\rho_1$	mass density of fluid evaluated at $t_1$ , (lb)(sec <sup>2</sup> )/ft <sup>4</sup>
$\rho_x$	mass density of fluid evaluated at $t_x$ , (lb)(sec <sup>2</sup> )/ft <sup>4</sup>
$\rho_{x,av}$	mass density of fluid evaluated at $t_{x,av}$ , (lb)(sec <sup>2</sup> )/ft <sup>4</sup>
$\rho_0$	mass density of fluid evaluated at $t_0$ , (lb)(sec <sup>2</sup> )/ft <sup>4</sup>
$\tau$	shear stress in fluid, lb/sq ft
$\tau_0$	shear stress in fluid at wall, lb/sq ft

## Dimensionless groups:

$f$	friction factor based on static-pressure gradient, $-\frac{D}{2\rho} \frac{dp/dx}{u_b^2}$
$f_{av}$	friction factor based on static-pressure drop, $\frac{D(p_1 - p)}{2 X \rho u_b^2}$
$f_d$	fully developed friction factor
$f_\tau$	friction factor based on shear stress at wall, $2\tau_0/(\rho u_b^2)$
$Gz$	Graetz number, $Re Pr/(X/D)$
$Nu$	Nusselt number, $h D/k$
$Nu_{av}$	average Nusselt number for constant properties defined by eq. (25)
$Nu_b$	Nusselt number with thermal conductivity evaluated at $t_b$ , $h D/k_b$
$Nu_d$	fully developed Nusselt number
$Nu_1$	Nusselt number with conductivity evaluated at $t_1$

2857

5-20

$Nu_{1,av}$	average Nusselt number defined by eq. (25) with conductivity evaluated at $t_1$
$Nu_x$	Nusselt number with conductivity evaluated at $t_x$
$Nu_{x,av}$	average Nusselt number with conductivity evaluated at $t_{x,av}$
$Nu_0$	Nusselt number with thermal conductivity evaluated at $t_0$
$p'$	pressure-drop parameter, $(p_1 - p)\rho D^2/\mu^2$
$Pe$	Peclet number, $Re Pr$
$Pr$	Prandtl number, $c_p g \mu/k$
$Pr_0$	Prandtl number with properties evaluated at $t_0$
$q_1'$	heat-transfer parameter, $q_0/(c_p g \rho_1 u_1 t_1)$
$Re$	Reynolds number, $\rho u_b D/\mu$
$Re_b$	Reynolds number with density and viscosity evaluated at $t_b$ , $\rho_b u_b D/\mu_b$
$Re_1$	Reynolds number with density and viscosity evaluated at $t_1$ , $\frac{\rho_1 u_b D}{\mu_1}$
$Re_x$	Reynolds number with density and viscosity evaluated at $t_x$ , $\rho_x u_b D/\mu_x$
$Re_{x,av}$	Reynolds number with density and viscosity evaluated at $t_{x,av}$ , $Re_1 \frac{\rho_{x,av}}{\rho_{b,av}} \frac{\mu_1}{\mu_{x,av}}$
$Re_0$	Reynolds number with density and viscosity evaluated at $t_0$ , $\rho_0 u_b D/\mu_0$
$r_0^+$	tube radius parameter, $\frac{\sqrt{\tau_0/\rho_0}}{\mu_0/\rho_0} r_0$

$T^+$  total-temperature parameter,  $\frac{(t_0 - T)c_p \int \tau_0}{q_0 \sqrt{\tau_0/\rho_0}} = \frac{1 - T/t_0}{\beta}$

$T_\delta^+$   $\frac{1}{\beta} \left( 1 - \frac{T_\delta}{t_0} \right)$

$t^+$  temperature parameter,  $\frac{(t_0 - t)c_p \int \tau_0}{q_0 \sqrt{\tau_0/\rho_0}} = \frac{1 - t/t_0}{\beta}$

$t_b^+$  bulk-temperature parameter,  $\frac{1}{\beta} \left( 1 - \frac{t_b}{t_0} \right)$

$t_\delta^+$   $\frac{1}{\beta} \left( 1 - \frac{t_\delta}{t_0} \right)$

$u^+$  velocity parameter,  $\frac{u}{\sqrt{\tau_0/\rho_0}}$

$u_b^+$  bulk-velocity parameter,  $\frac{u_b}{\sqrt{\tau_0/\rho_0}}$

$u_c^+$  value of  $u^+$  at tube center

$u_\delta^+$   $\frac{u_\delta}{\sqrt{\tau_0/\rho_0}}$

$\left( \frac{X}{D} \right)_{he}$  thermal entrance length divided by diameter

$y^+$  wall distance parameter,  $\frac{\sqrt{\tau_0/\rho_0}}{\mu_0/\rho_0} y$

$\alpha$  compressibility or frictional heating parameter,  $\tau_0/(2gJc_p t_0 \rho_0)$

$\beta$  heat-transfer parameter,  $q_0 \sqrt{\tau_0/\rho_0} / (c_p \int \tau_0 t_0)$

$\delta^+$  dimensionless flow-boundary-layer thickness,  $\frac{\sqrt{\tau_0/\rho_0}}{\mu_0/\rho_0} \delta$

$\delta_h^+$  dimensionless thermal-boundary-layer thickness,  $\frac{\sqrt{\tau_0/\rho_0}}{\mu_0/\rho_0} \delta_h$

An integral sign having open brackets for the upper limit  $\int [ ]$  indicates that the variable of integration should be used as the upper limit.

2857

CZ-5 back

## APPENDIX B

## ANALYSIS INCLUDING EFFECT OF VARIATION OF HEAT TRANSFER

ACROSS BOUNDARY LAYER FOR SMALL  $\delta_h^+$  WITH

## CONSTANT FLUID PROPERTIES

As was mentioned in the section Effect of variation of heat transfer across boundary layer on Nusselt number for small  $\delta_h^+$  and constant fluid properties, the effect of variation of  $q/q_0$  across the boundary layer for small  $\delta_h^+$  should be checked. For laminar flow over a flat plate the temperature distribution in the thermal boundary layer can be closely approximated by a cubic parabola. For a cubic parabola,  $q/q_0 = 1 - y^2/\delta_h^2$  as shown in the following:

For laminar flow,

$$q = -k \, dt/dy = q_0(1 - y^2/\delta_h^2) \quad (C1)$$

Integration of equation (C1) gives

$$y - \frac{y^3}{3\delta_h^2} = \frac{k}{q_0} (t_0 - t) \quad (C2)$$

Evaluation of equation (C2) at the edge of the boundary layer gives

$$\frac{k}{q_0} (t_0 - t_\delta) = \frac{1}{3} \delta_h \quad (C3)$$

Combination of equations (C2) and (C3) results in

$$\frac{t_0 - t}{t_0 - t_\delta} = \frac{3}{2} \frac{y}{\delta_h} - \frac{1}{2} \left( \frac{y}{\delta_h} \right)^3 \quad (C4)$$

which is the same as the equation on page 89 in reference 7. The assumption that  $q/q_0 = 1 - y^2/\delta_h^2$  therefore leads to a cubic parabola for the temperature distribution for laminar flow. The same assumption is used herein for turbulent flow for small  $\delta_h^+$ . The equation for turbulent heat transfer can be written

$$q = - (k + c_p g \rho \epsilon) dt/dy \quad (C5)$$

With the assumption for  $q/q_0$  and  $\epsilon = n^2 u y$  for flow close to the wall (ref. 6), equation (C5) becomes, in dimensionless form,

$$1 - \frac{y^{+2}}{\delta_h^{+2}} = \left( \frac{1}{Pr} + n^2 u^+ y^+ \right) \frac{dt^{+'}}{dy^+} \quad (C6)$$

where  $t^{+'}$  represents the temperature distribution with  $q/q_0 = 1 - y^{+2}/\delta_h^{+2}$  as distinguished from  $t^+$ , which is the dimensionless temperature parameter for  $q/q_0 = 1$ . Separation of variables and integration of equation (C6) result in

$$t^{+'} = \int_0^{y^+} \frac{dy^+}{\frac{1}{Pr} + n^2 u^+ y^+} - \frac{1}{\delta_h^{+2}} \int_0^{y^+} \frac{y^{+2} dy^+}{\frac{1}{Pr} + n^2 u^+ y^+} \quad (C7)$$

The first term on the right side of equation (C7) is  $t^+$  for constant properties (ref. 6), so that

$$t^{+'} = t^+ - \frac{1}{\delta_h^{+2}} \int_0^{y^+} \frac{y^{+2} dy^+}{\frac{1}{Pr} + n^2 u^+ y^+} \quad (C8)$$

The values of  $t^+$  are obtained from figure 1. For obtaining the Nusselt numbers the values of  $t^{+'}$  from equation (C8) are used in equations (12) and (4) in place of  $t^+$ .

## APPENDIX C

## CALCULATION OF NUSSELT NUMBERS, REYNOLDS NUMBERS, AND TEMPERATURE

## DISTRIBUTIONS FOR FLOW BEYOND ENTRANCE REGION

For points beyond the entrance region the relation between Nusselt number and Reynolds number with the properties, including density, evaluated at the reference temperature  $t_x \equiv x(t_0 - t_b) + t_b$ , where  $x = 0.4$  for heat addition and 0.6 for heat extraction from the gas, can be obtained from the curve for fully developed flow in figure 7. From equations (18) to (21) and the definition of  $t_x$  it can be shown that

$$Re_x = Re_1 \left[ \frac{1}{x \left( \frac{t_0}{t_b} - 1 \right) + 1} \right]^{d+1} \left( \frac{t_1}{t_b} \right)^d \quad (B1)$$

and

$$Nu_1 = Nu_x \left( \frac{t_b}{t_1} \right) \left[ x \left( \frac{t_0}{t_b} - 1 \right) + 1 \right]^d \quad (B2)$$

where  $d = 0.68$  for air and most other gases. The value of  $Nu_1$  for a given value of  $Re_1$  can be obtained from equations (B1) and (B2) provided the values of  $t_b/t_1$  and  $t_0/t_b$  are known. The quantities  $t_b/t_1$  and  $t_0/t_b$  can be written in terms of the quantities plotted in figure 10 as

$$\frac{t_b}{t_1} = q_1' \left[ \left( \frac{t_b - t_1}{t_1} \right) \frac{1}{q_1'} \right] + 1 = 4 \frac{X}{D} + 1 \quad (B3)$$

(see eq. (23)) and

$$\frac{t_0}{t_b} = \frac{q_1' \left[ \left( \frac{t_0 - t_1}{t_1} \right) \frac{1}{q_1'} \right] + 1}{q_1' \left[ \left( \frac{t_b - t_1}{t_1} \right) \frac{1}{q_1'} \right] + 1} \quad (B4)$$

In the procedure for obtaining the value of  $t_0/t_b$ , the quantity in brackets in the numerator is first determined by extrapolating a known



curve for that quantity plotted against  $X/D$ . The value of  $Nu_1$  can then be obtained from equation (B2). With that value of  $Nu_1$  a new and more accurate value of  $[(t_0 - t_1)/t_1] \frac{1}{q_1'}$  can be calculated from equation (24). The calculation of  $Nu_1$  can then be repeated using the new value of

$$[(t_0 - t_1)/t_1] \frac{1}{q_1'}$$

Average Nusselt numbers with the conductivity evaluated at the inlet temperature  $Nu_{1,av}$  can be calculated from equation (25), where the values of  $Nu_1$  are calculated as outlined previously. It is desirable to calculate average Nusselt numbers and Reynolds numbers with properties evaluated at the average bulk or the average wall temperature for given values of  $X/D$ . The average bulk temperature rise for a given  $X/D$  is one-half the temperature rise at  $X/D$ , since the specific heat is assumed constant. Therefore,

$$\left( \frac{t_{b,av} - t_1}{t_1} \right) \frac{1}{q_1'} = \frac{1}{2} \left[ \left( \frac{t_b - t_1}{t_1} \right) \frac{1}{q_1'} \right]$$

or

$$\frac{t_{b,av}}{t_1} = \frac{q_1'}{2} \left[ \left( \frac{t_b - t_1}{t_1} \right) \frac{1}{q_1'} \right] + 1 \quad (B5)$$

From the definitions of  $h_{av}$ ,  $Nu_{1,av}$ ,  $Re_1$ , and  $Pr$ , it can be shown that

$$\frac{t_{0,av}}{t_1} = \frac{t_{b,av}}{t_1} + \frac{q_1' Re_1 Pr}{Nu_{1,av}} \quad (B6)$$

Average Nusselt numbers and Reynolds numbers with properties evaluated at  $t_{b,av}$ ,  $t_{0,av}$ , or any arbitrary temperature

$$t_{x,av} \equiv x(t_{0,av} - t_{b,av}) + t_{b,av}$$

can be calculated by use of equations (B5) and (B6).

## REFERENCES

1. Goldstein, Sidney: Modern Developments in Fluid Dynamics. Clarendon Press (Oxford), 1938.
2. Langhaar, H. L.: Steady Flow in the Transition Length of a Straight Tube. Jour. Appl. Mech., vol. 9, no. 2, June 1942, pp. A55-A58.
3. Jacob, Max: Heat Transfer. Vol. 1. John Wiley & Sons, Inc., 1929.
4. Latzko, H.: Heat Transfer in a Turbulent Liquid or Gas Stream. NACA TM 1068, 1944.
5. Poppendiek, H. F., and Palmer, L. D.: Forced Convection Heat Transfer in Thermal Entrance Regions, Part II. ORNL 914 Metallurgy and Ceramics, Reactor Exp. Eng. Div., Oak Ridge National Lab., Oak Ridge (Tenn.), May 26, 1952. (Contract No. W-7405, eng. 26.)
6. Deissler, R. G., and Eian, C. S.: Analytical and Experimental Investigation of Fully Developed Turbulent Flow of Air in a Smooth Tube with Heat Transfer with Variable Fluid Properties. NACA TN 2629, 1952.
7. Eckert, E. R. G.: Introduction to the Transfer of Heat and Mass. First ed., McGraw-Hill Book Co., Inc., 1950.
8. Deissler, Robert G.: Analysis of Fully Developed Turbulent Heat Transfer at Low Peclet Numbers in Smooth Tubes with Application to Liquid Metals. NACA RM E52F05, 1952.
9. Deissler, Robert G.: Analytical Investigation of Turbulent Flow in Smooth Tubes with Heat Transfer with Variable Fluid Properties for Prandtl Number of 1. NACA TN 2242, 1950.
10. Prandtl, L., and Tietjens, O. G.: Fundamentals of Hydro and Aero-Mechanics. First ed., McGraw-Hill Book Co., Inc., 1934.
11. Weiland, Walter F., and Lowdermilk, Warren H.: Measurements of Heat-Transfer and Friction Coefficients for Air Flowing in a Tube of Length-Diameter Ratio of 15 at High Surface Temperatures. NACA RM E53E04, 1953.
12. Boelter, L. M. K., Young, G., and Iversen, H. W.: An Investigation of Aircraft Heaters. XXVII - Distribution of Heat-Transfer Rate in the Entrance Section of a Circular Tube. NACA TN 1451, 1948.
13. Stromquist, W. K., and Boarts, R. M.: Effect of Wetting on Liquid Metal Heat Transfer. Prog. Rep., Dept. Chem. Eng., The University of Tennessee, Sept. 30, 1952. (AEC Contract No. AT-(40-1)-1310.)

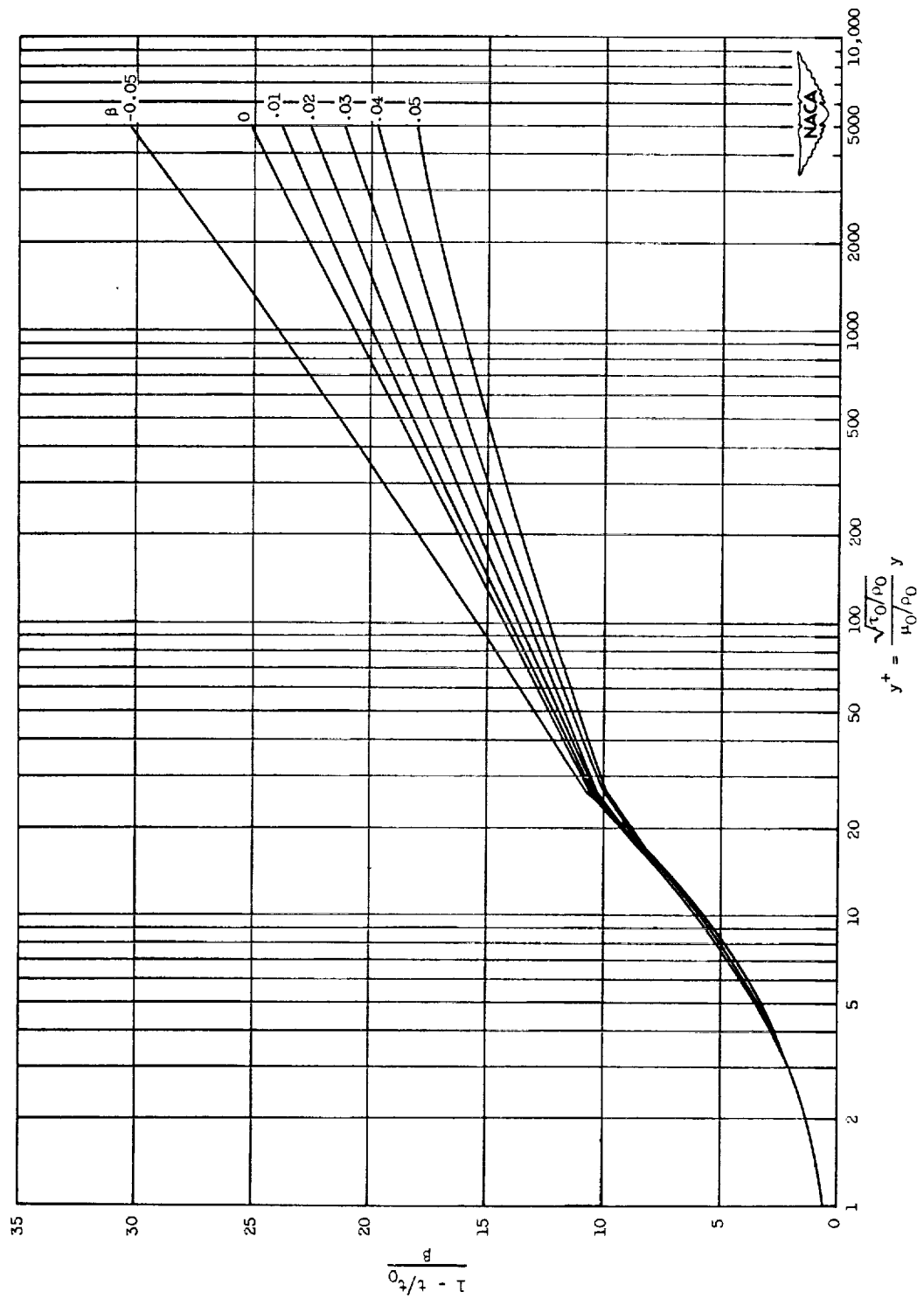


Figure 1. - Predicted generalized temperature distribution for flow of gases with heat transfer at Prandtl number of 0.73 from reference 6.

2857

CZ-6

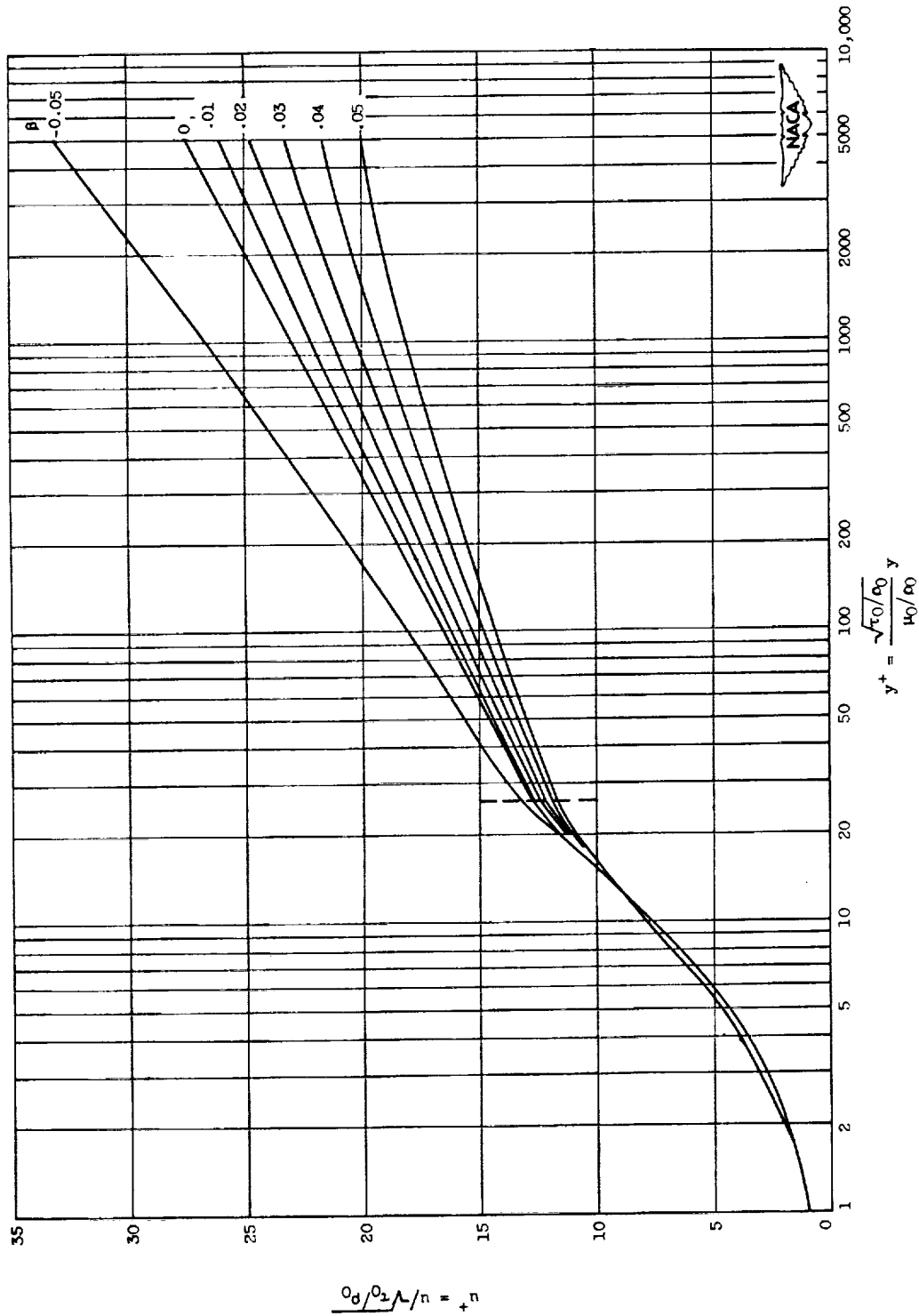
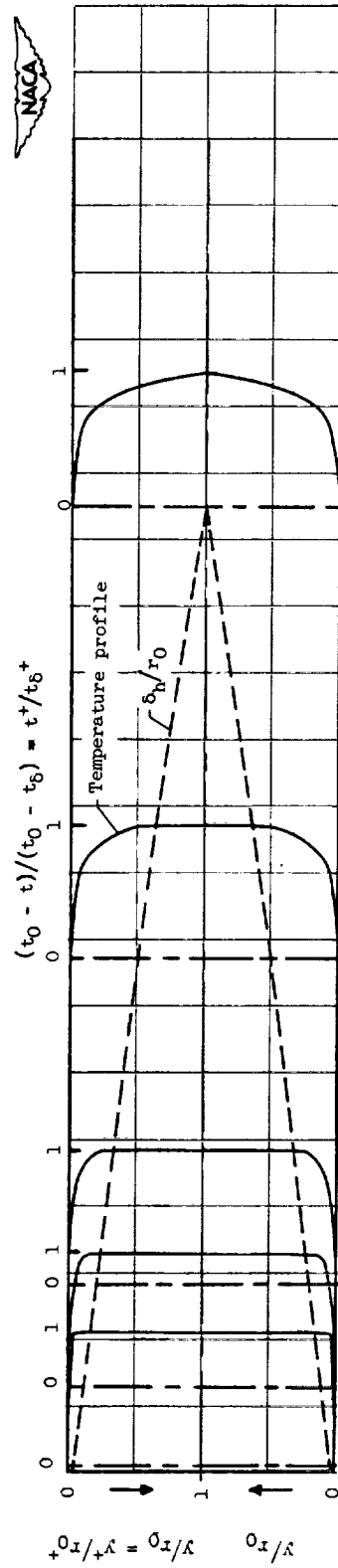


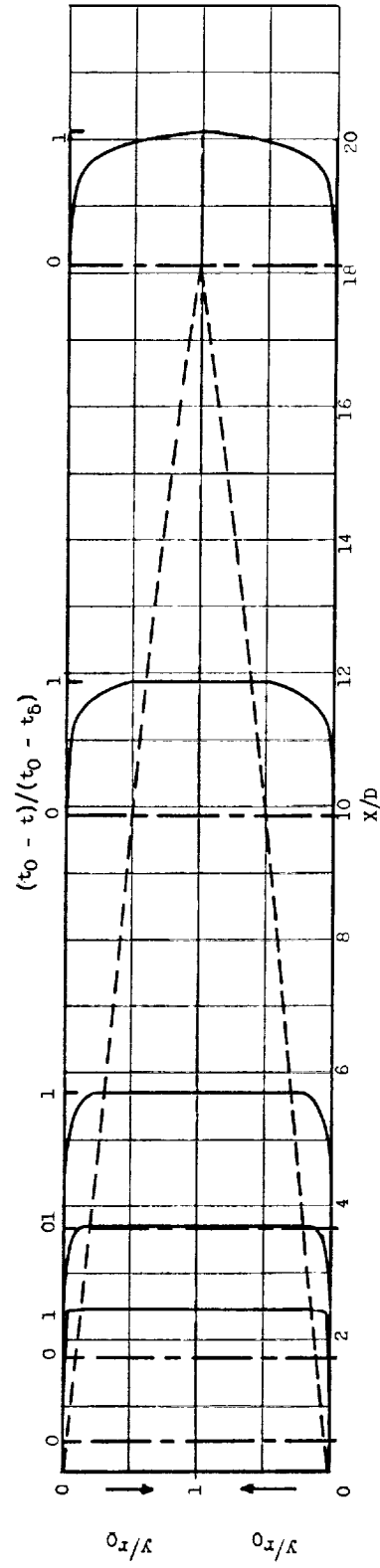
Figure 2. - Predicted generalized velocity distribution for flow of gases with heat transfer at Prandtl number of 0.73 from reference 6.

2857

CZ-6 back



(a) Reynolds number, 16,700 ( $r_0^+, 500$ ).



(b) Reynolds number, 83,000 ( $r_0^+, 2000$ ).

Figure 3. - Development of thermal boundary layer in entrance region of tube for a gas.  $Pr, 0.73; q_1', 0$ . Uniform heat flux, uniform initial temperature distribution, and fully developed velocity distribution.

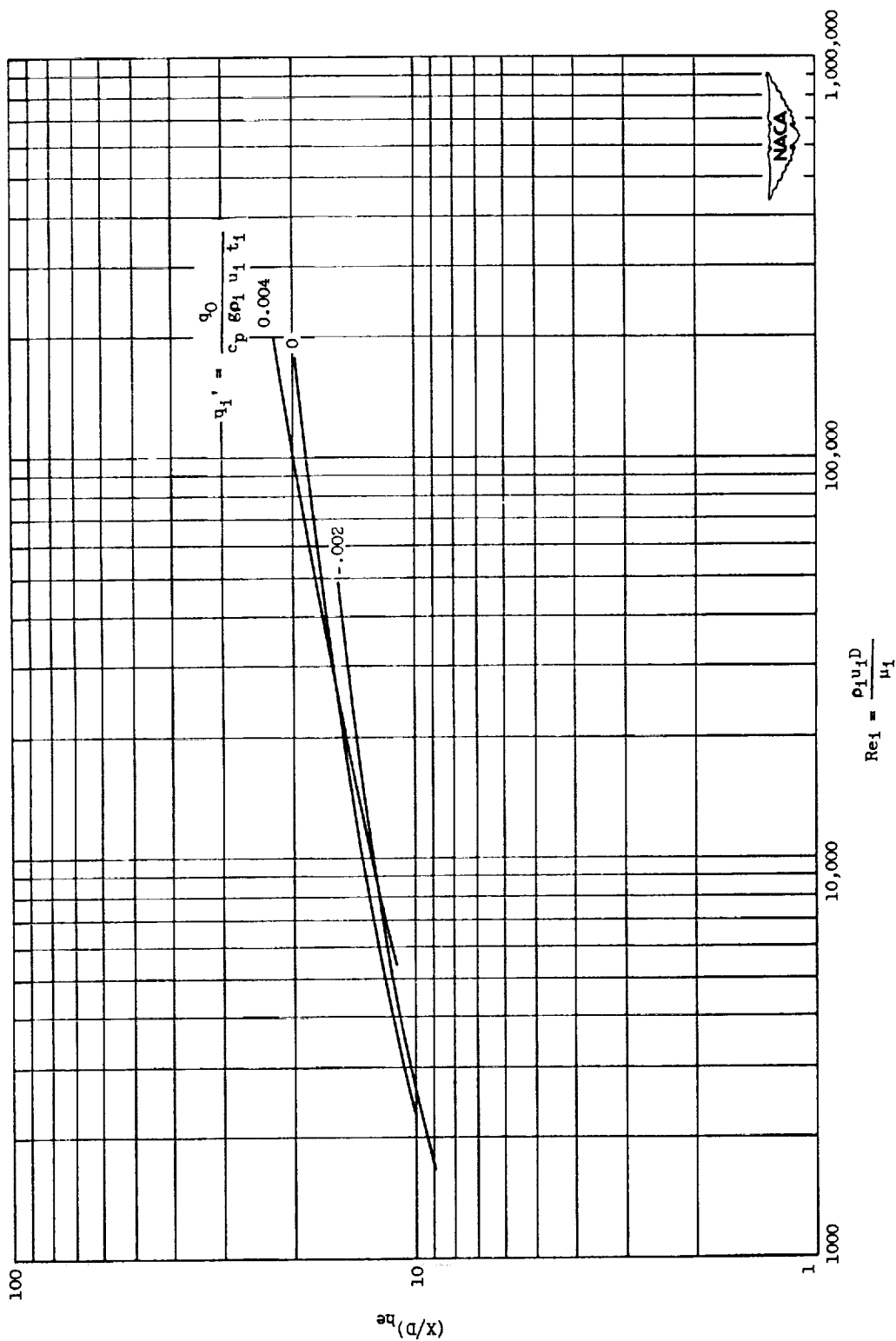
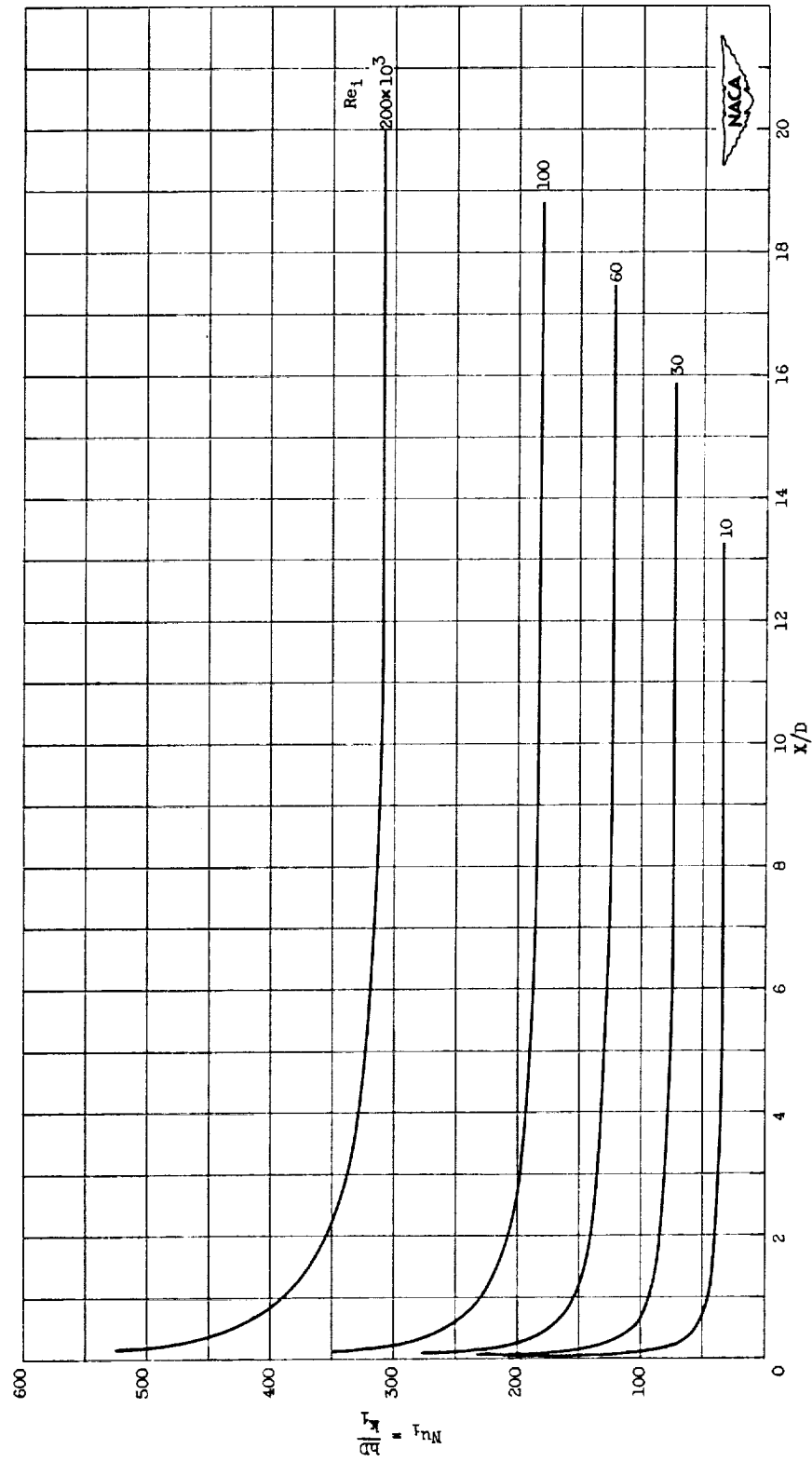
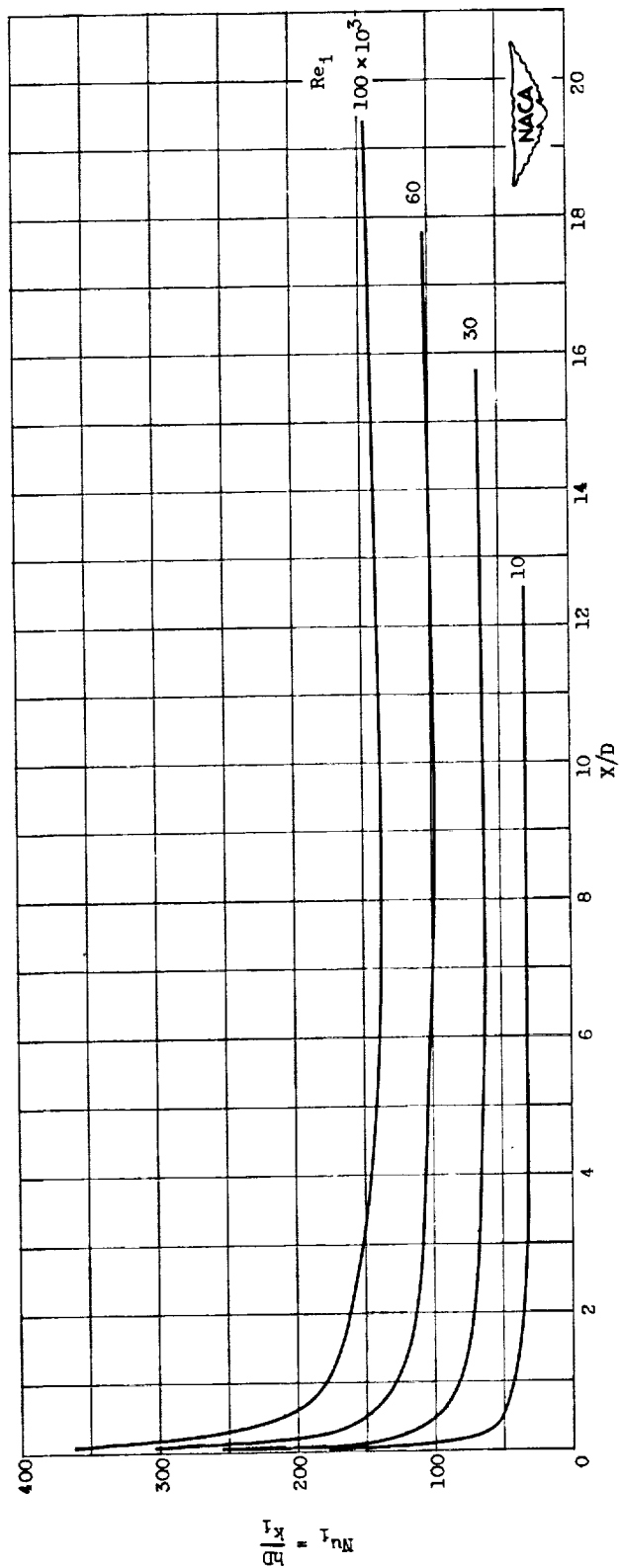


Figure 4. - Variation of thermal entrance length with Reynolds number and heat flux for gas flowing in a tube.  $Pr, 0.73$ . Uniform heat flux, uniform initial temperature distribution, and fully developed velocity distribution.



(a)  $q_1' = 0$  (constant properties).

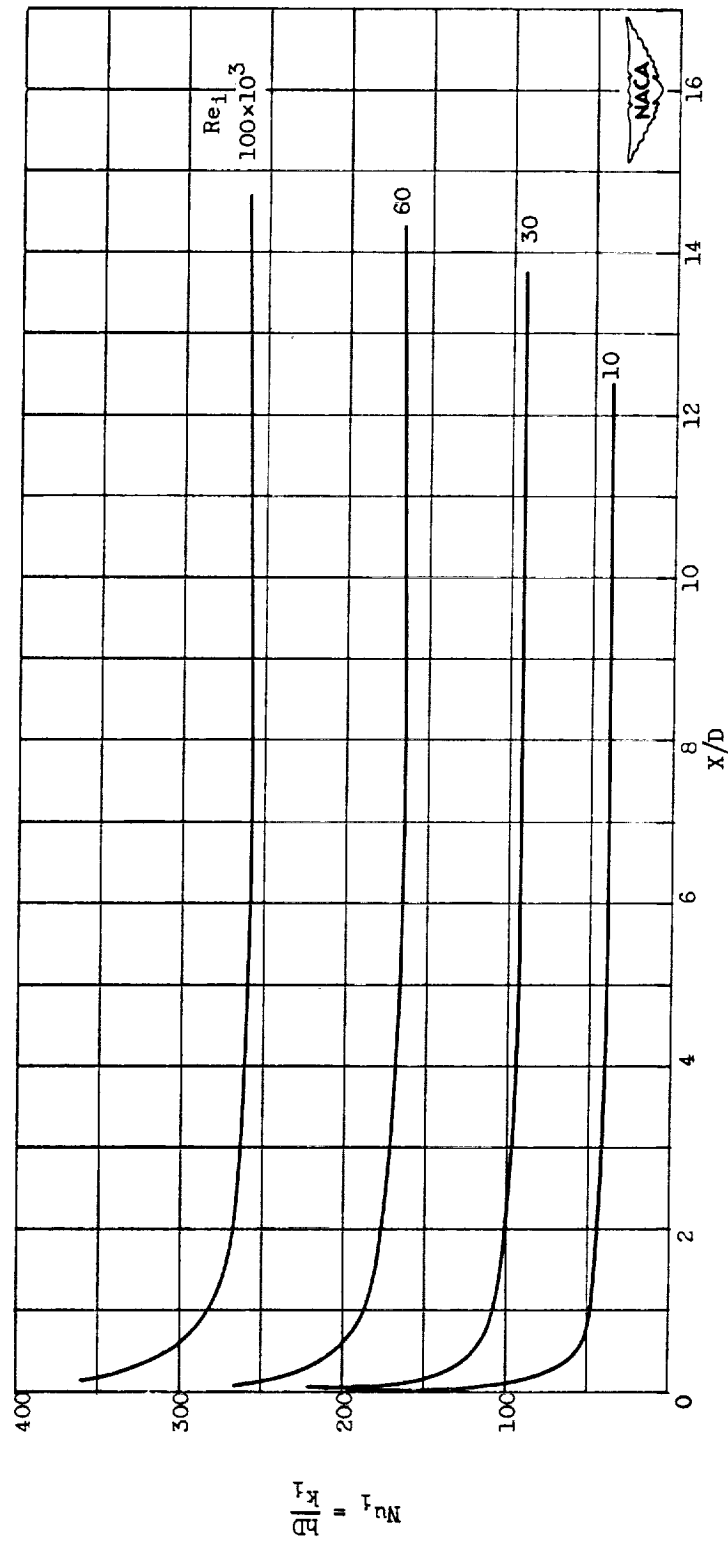
Figure 5. - Variation of Nusselt number  $Nu_1$  with  $X/D$  and Reynolds number for gas flowing in a tube.  $Pr, 0.73$ . Uniform heat flux, uniform initial temperature distribution, and fully developed velocity distribution.



(b)  $q_1' = 0.004$  (heat addition to gas).

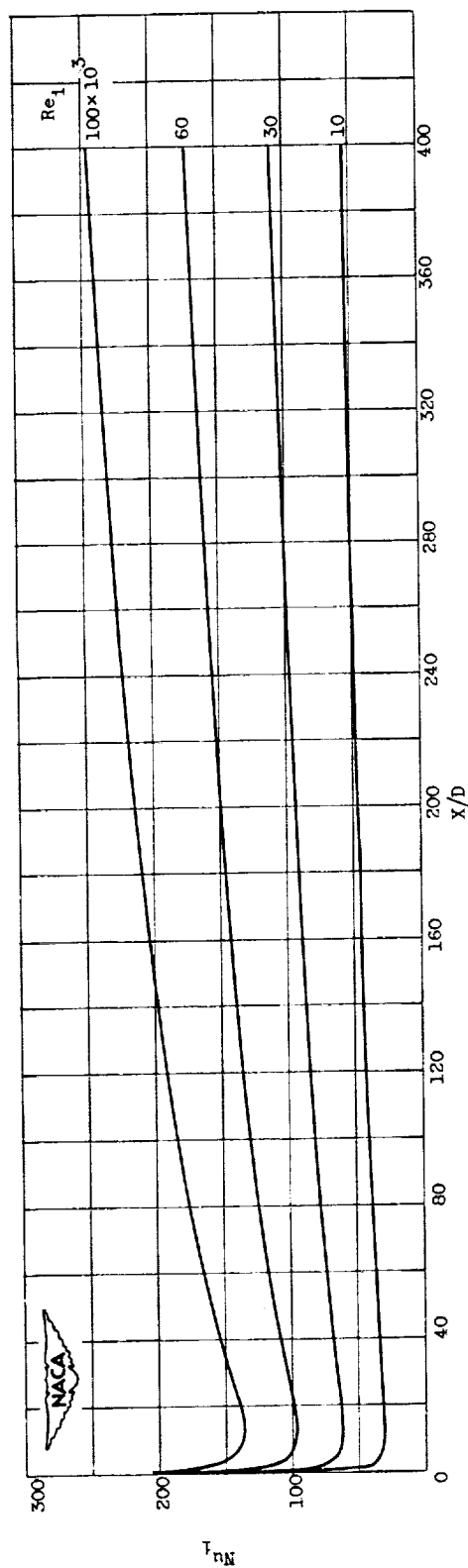
Figure 5. - Continued. Variation of Nusselt number  $Nu_x$  with  $x/d$  and Reynolds number for gas flowing in a tube.  $Pr, 0.73$ . Uniform heat flux, uniform initial temperature distribution, and fully developed velocity distribution.





(c)  $q_1' = -0.0025$  (heat extraction from gas).

Figure 5. - Concluded. Variation of Nusselt number  $Nu_1$  with  $X/D$  and Reynolds number for gas flowing in a tube.  $Pr, 0.73$ . Uniform heat flux, uniform initial temperature distribution, and fully developed velocity distribution.

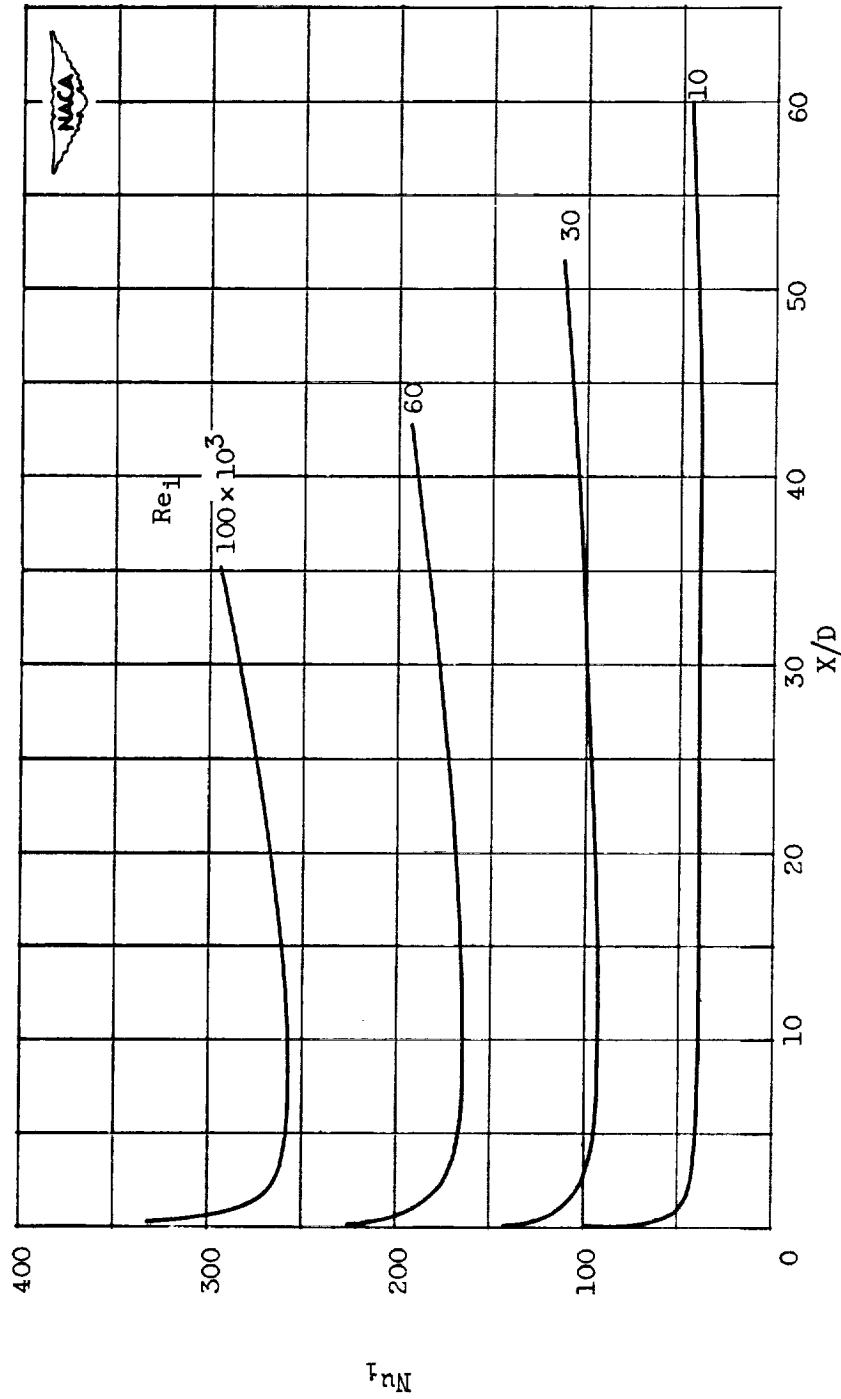


(a)  $q_1' = 0.004$ .

Figure 6. - Variation of Nusselt number  $Nu_i$  with  $x/d$  and Reynolds number for gas flowing in a tube for large values of  $x/d$ .  $Pr, 0.73$ . Uniform heat flux, uniform initial temperature distribution, and fully developed velocity distribution.

2857

CZ-7



(b)  $q_i' = -0.0025$ .

Figure 6. - Concluded. Variation of Nusselt number  $Nu_i$  with  $X/D$  and Reynolds number for gas flowing in a tube for large values of  $X/D$ .  $Pr, 0.73$ . Uniform heat flux, uniform initial temperature distribution, and fully developed velocity distribution.

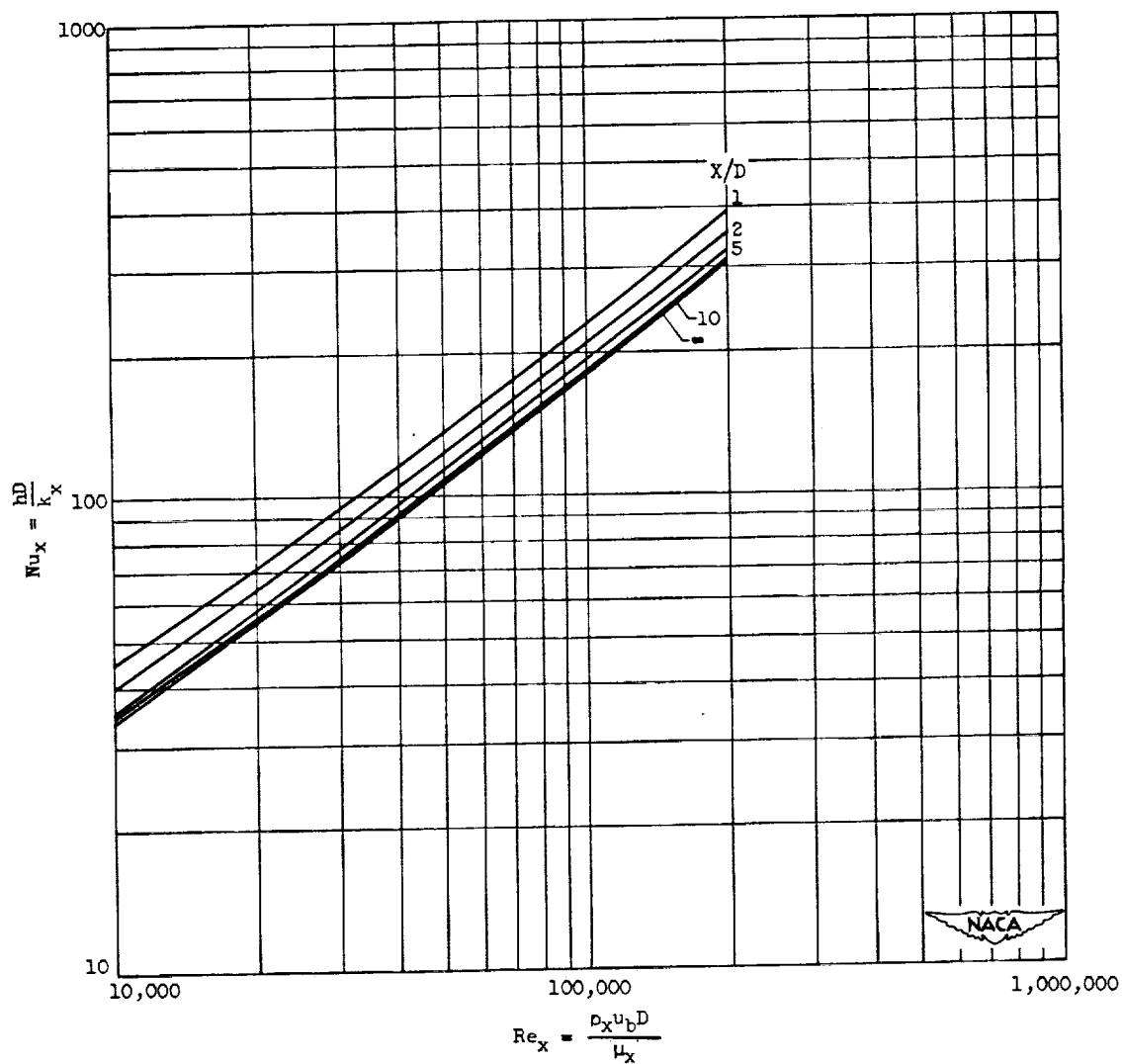


Figure 7. - Variation of local Nusselt number with Reynolds number for various values of  $X/D$  for gas flowing in a tube with properties evaluated at  $t_x = x(t_0 - t_b) + t_b$ , where  $x$  is determined from figure 8.  $Pr, 0.73$ . Uniform heat flux, uniform initial temperature distribution, and fully developed velocity distribution.

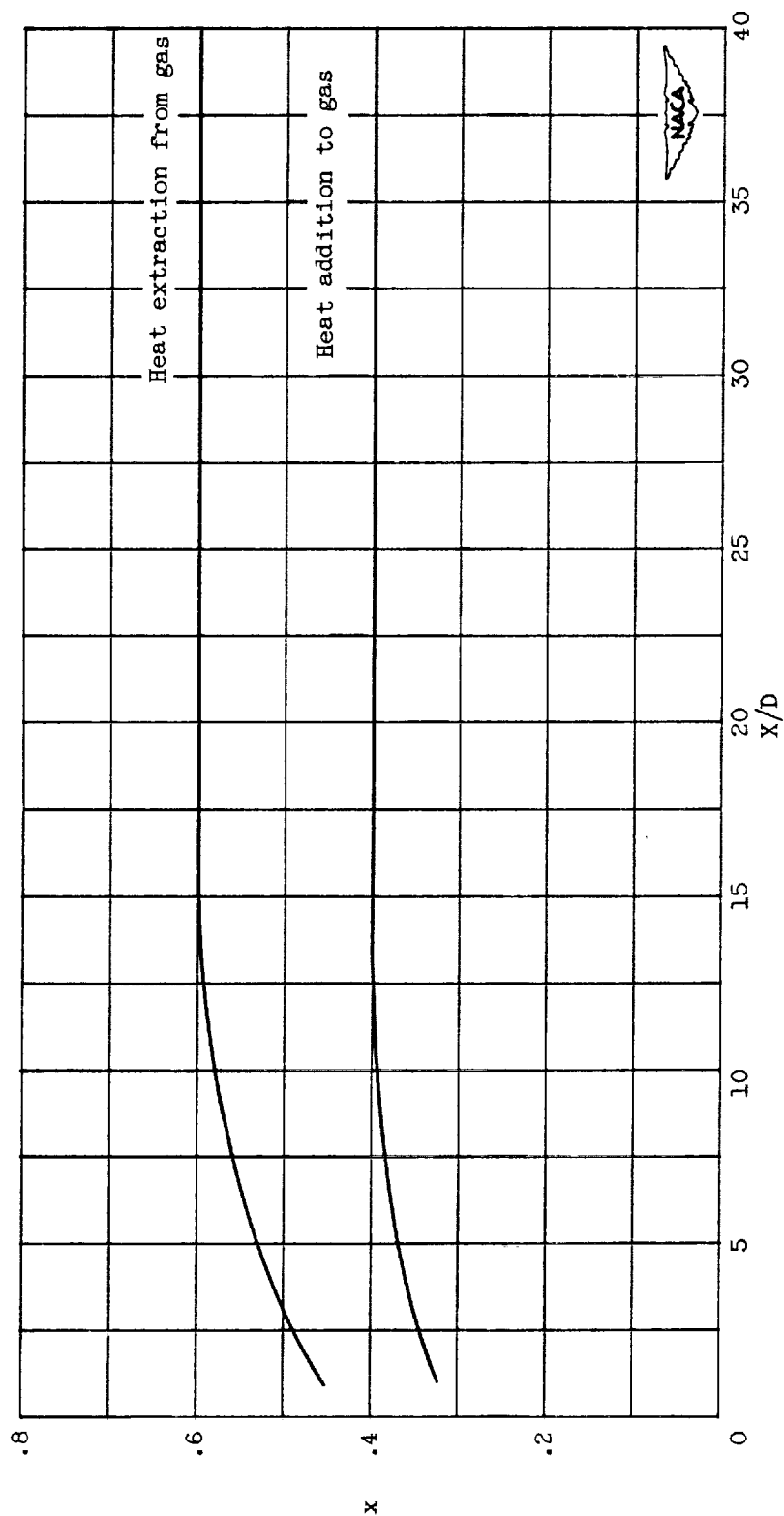


Figure 8. - Variation of  $x$ , defined by  $t_x = x(t_0 - t_b) + t_b$ , with  $X/D$  for use with figure 7.

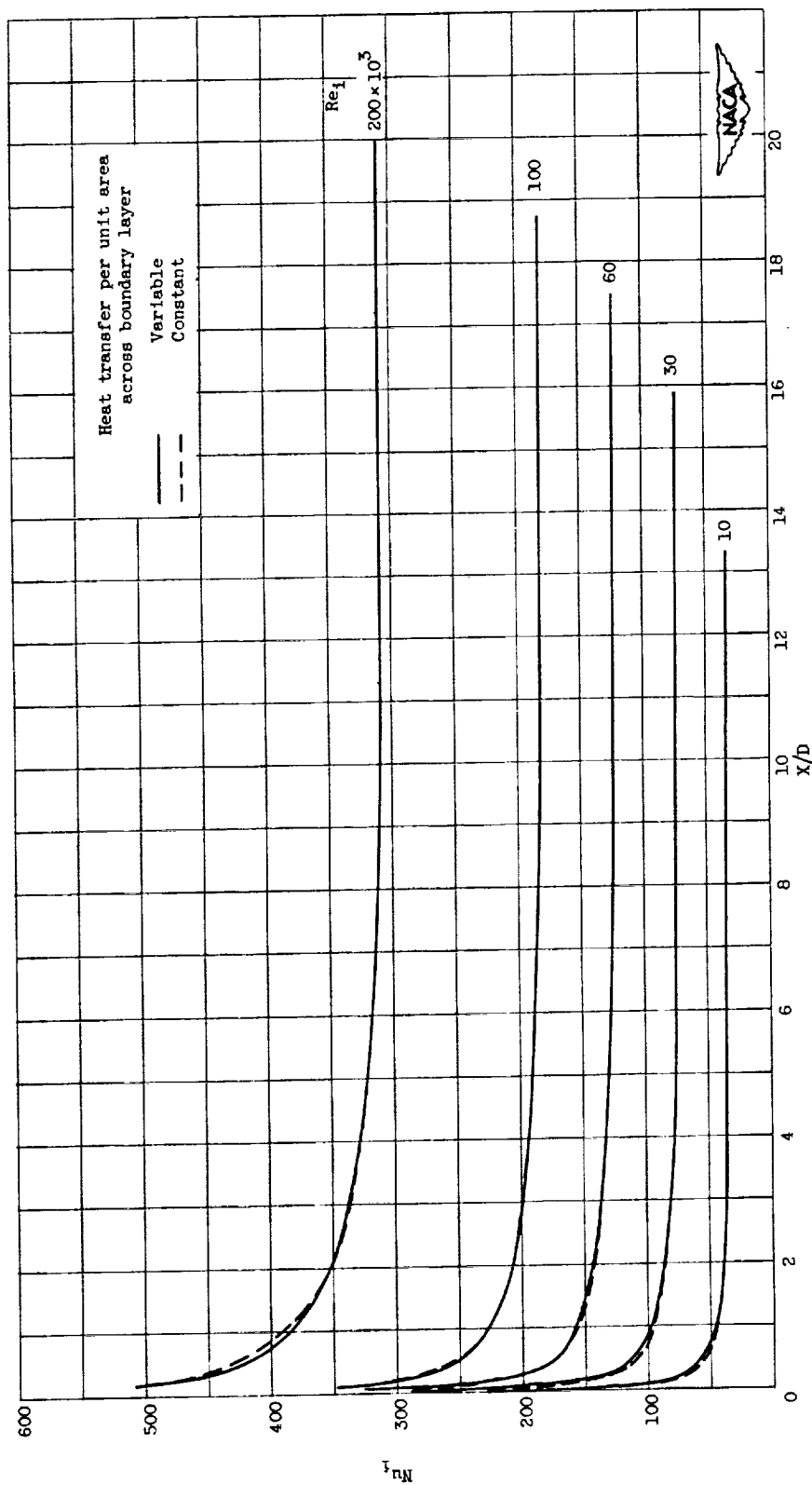
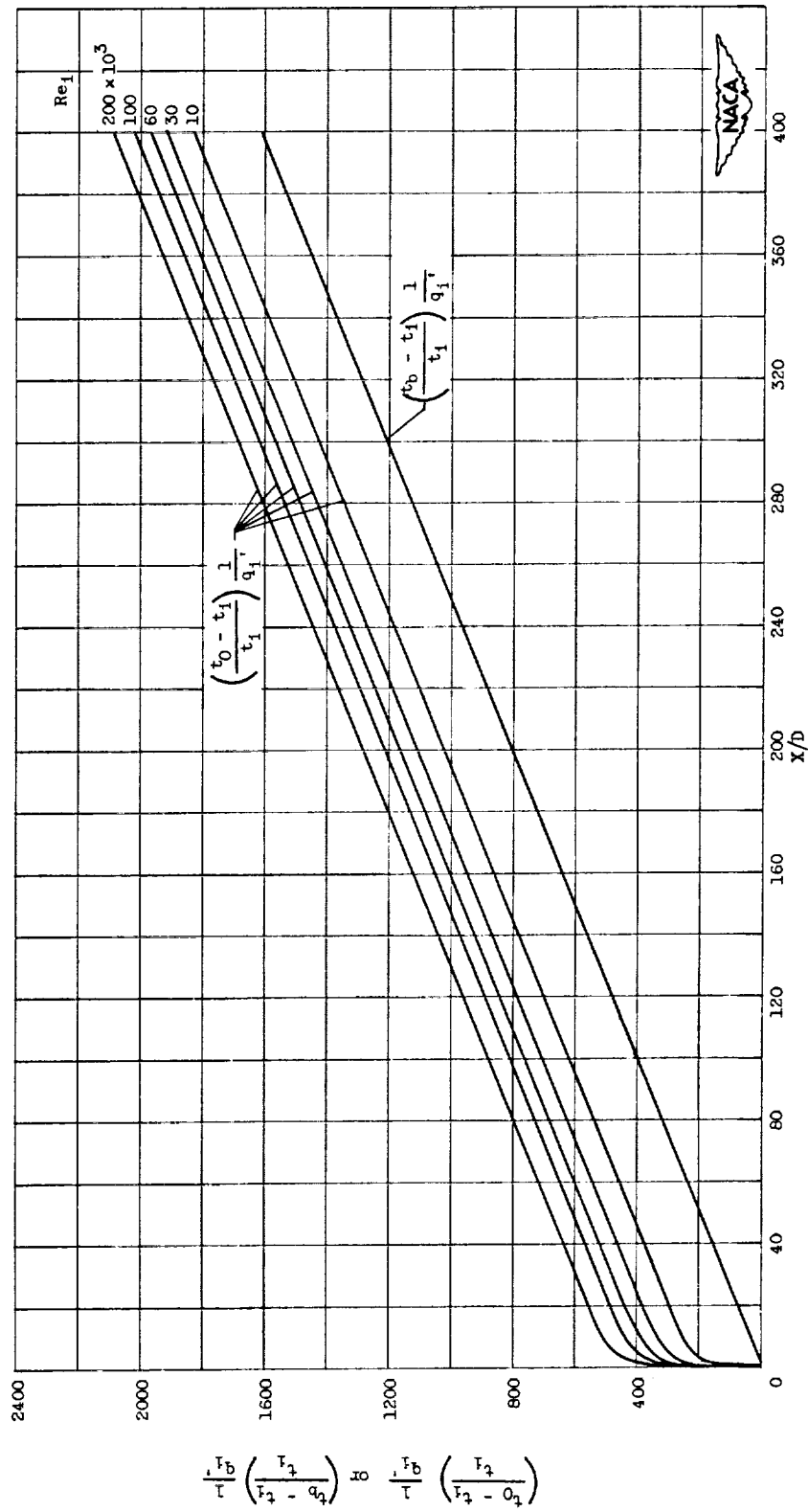


Figure 9. - Curves showing effect of variable heat flux across boundary layer on Nusselt numbers in entrance region of tube.  $Pr, 0.73$ . Uniform wall heat flux, uniform initial temperature distribution, and fully developed velocity distribution.  $q_1' = 0$ .

2857



(a)  $q_1' = 0$  (constant properties).

Figure 10. - Variation of dimensionless wall and bulk temperatures with  $X/d$  and Reynolds number for gas flowing in a tube.  $Pr = 0.73$ . Uniform heat flux, uniform initial temperature distribution, and fully developed velocity distribution.

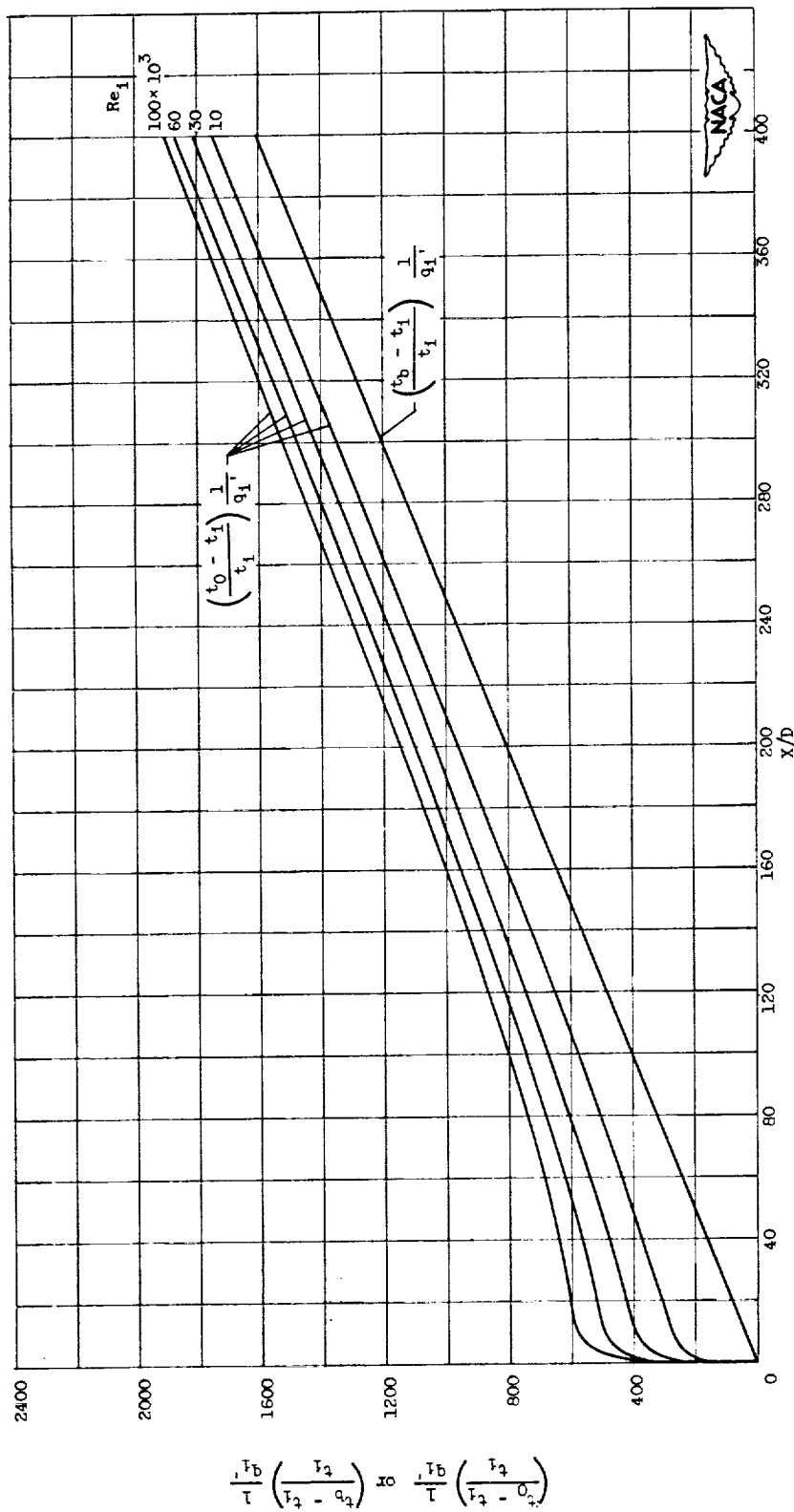
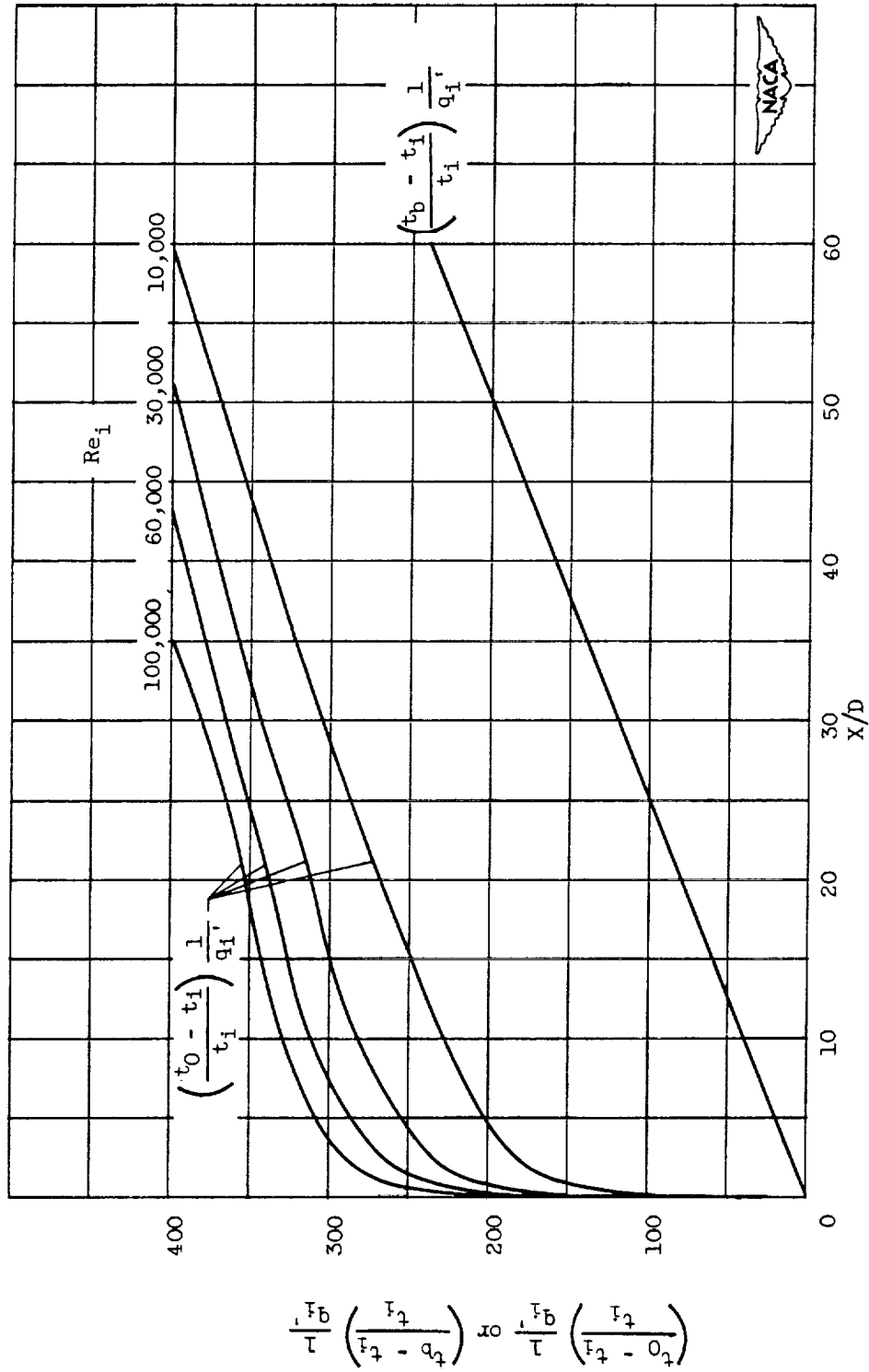


Figure 10. - Continued. Variation of dimensionless wall and bulk temperatures with  $X/d$  and Reynolds number for gas flowing in a tube.  $Pr, 0.73$ . Uniform heat flux, uniform initial temperature distribution, and fully developed velocity distribution.

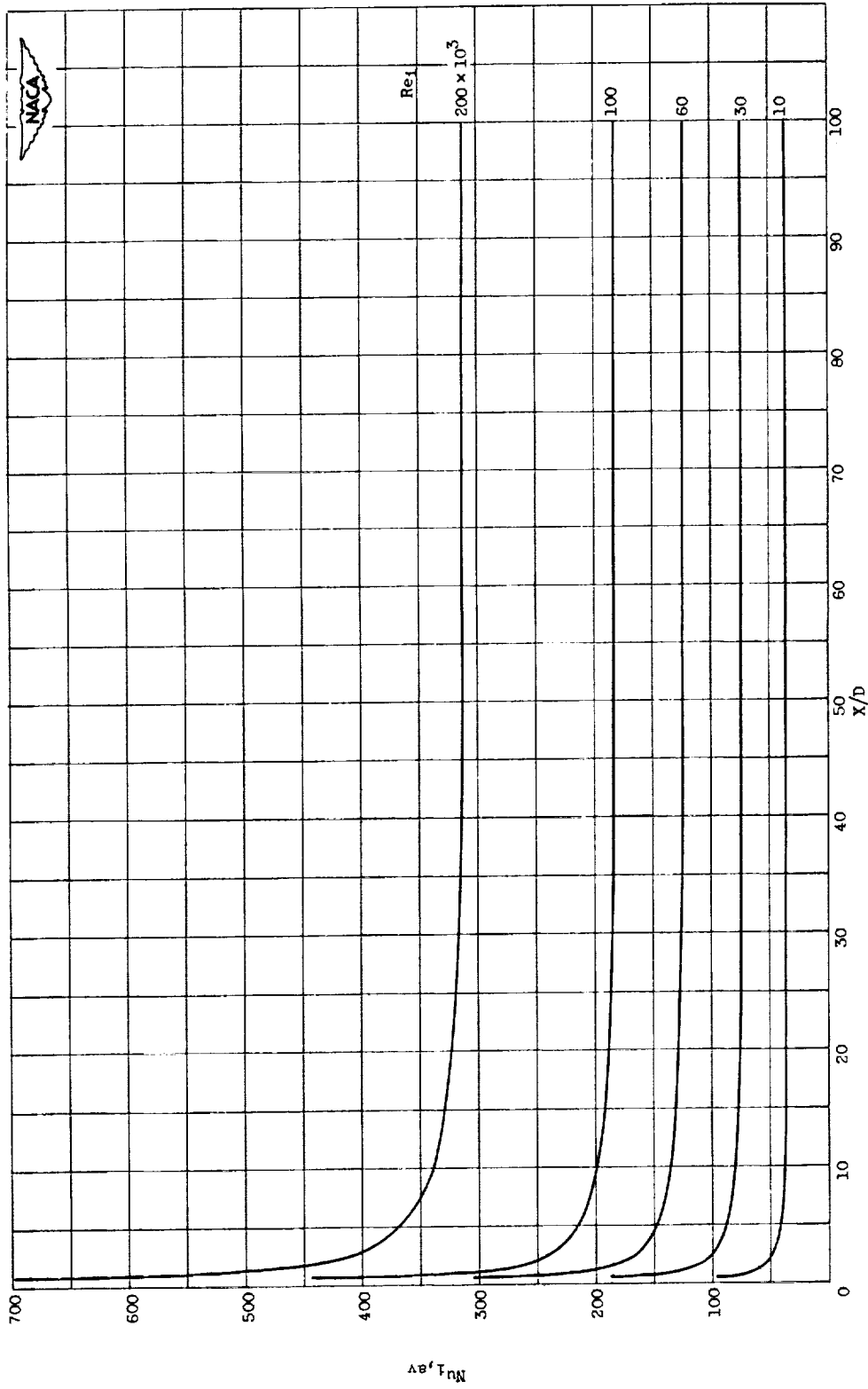
(b)  $q_1' = 0.004$  (heat addition to gas).





(c)  $q_i' = -0.0025$  (heat extraction from gas).

Figure 10. - Concluded. Variation of dimensionless wall and bulk temperatures with  $X/D$  and Reynolds number for gas flowing in a tube.  $Pr, 0.73$ . Uniform heat flux, uniform initial temperature distribution, and fully developed velocity distribution.



(a)  $q_{1,i} = 0$  (constant properties).

Figure 11. - Variation of average Nusselt number defined by equation (25) with  $X/D$  and Reynolds number for gas flowing in a tube.  $Pr, 0.73$ . Uniform heat flux, uniform initial temperature distribution, and fully developed velocity distribution.

CZ-8

2857

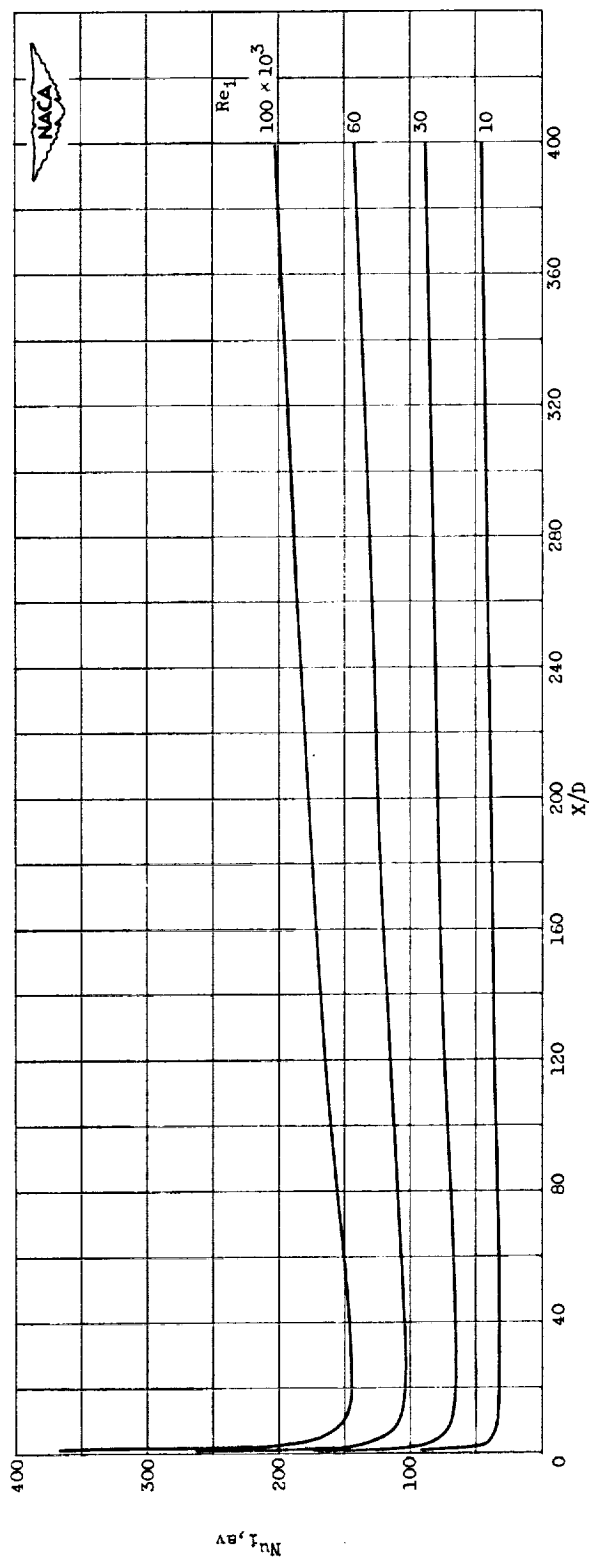
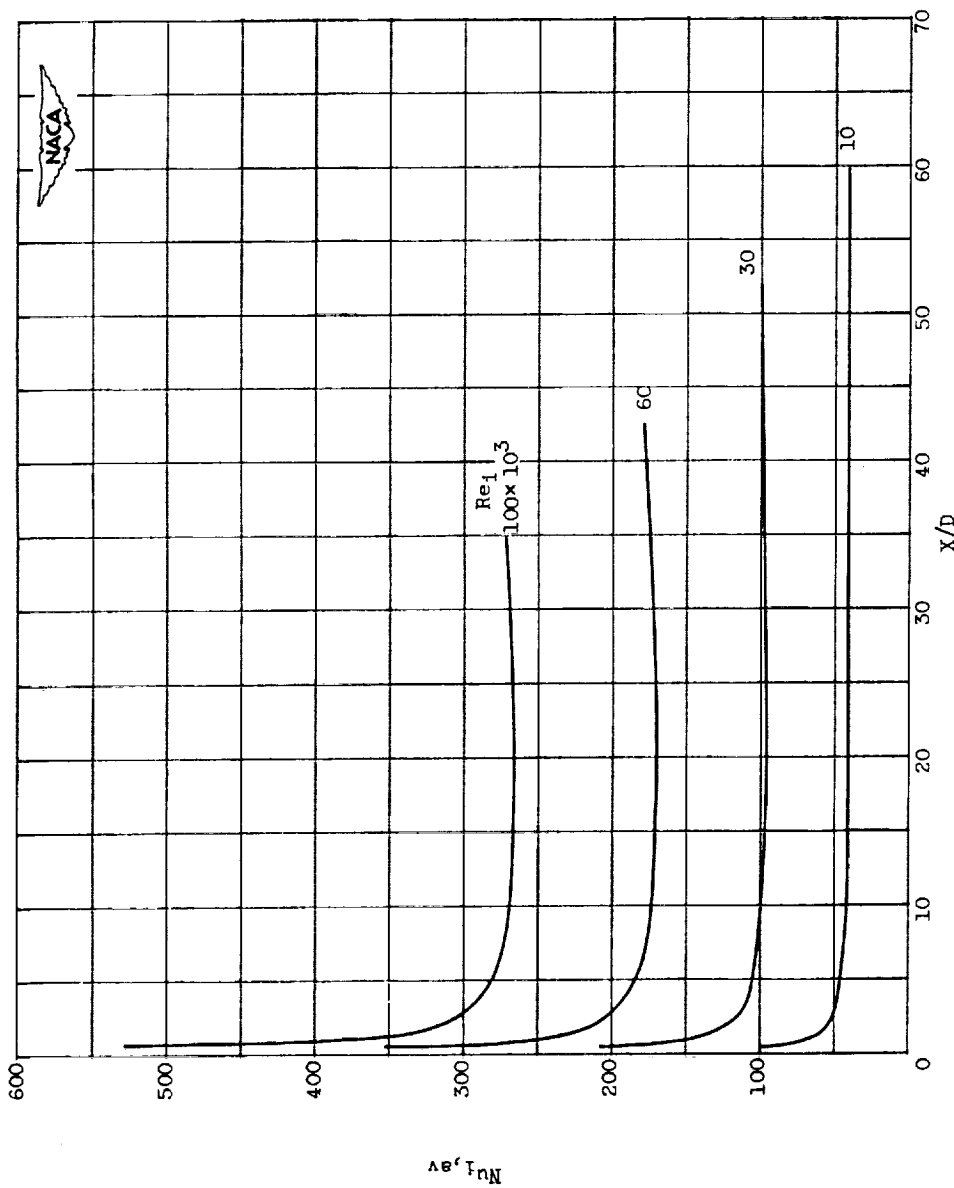
(b)  $q_1' = 0.004$  (heat addition to gas).

Figure 11. - Continued. Variation of average Nusselt number defined by equation (25) with  $X/D$  and Reynolds number for gas flowing in a tube.  $Pr, 0.73$ . Uniform heat flux, uniform initial temperature distribution, and fully developed velocity distribution.



(c)  $q_1' = -0.0025$  (heat extraction from gas).

Figure 11. - Concluded. Variation of average Nusselt number defined by equation (25) with  $X/D$  and Reynolds number for gas flowing in a tube.  $Pr, 0.73$ . Uniform heat flux, uniform initial temperature distribution, and fully developed velocity distribution.

2857

CZ-8 back

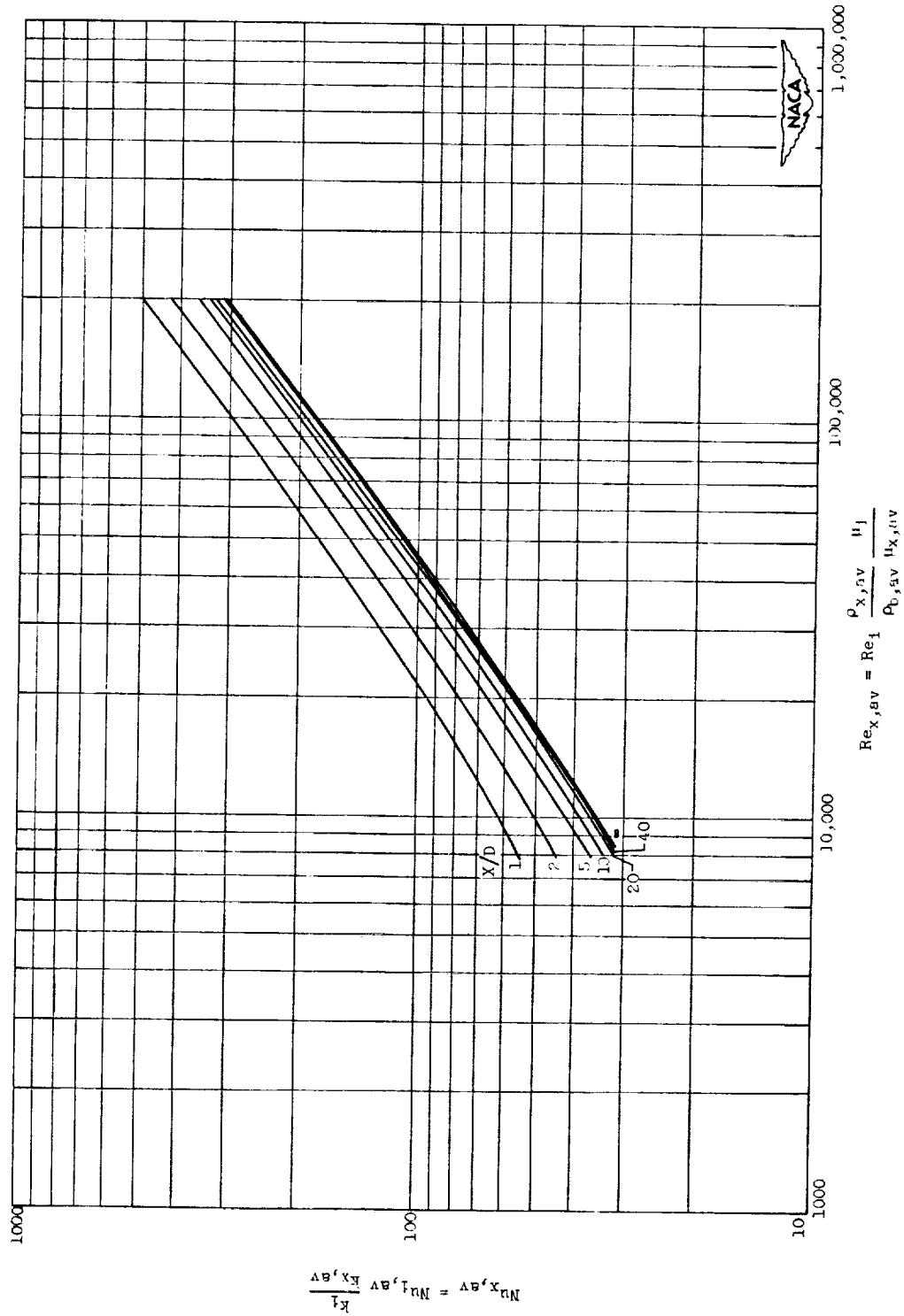


Figure 12. - Variation of average Nusselt number with average Reynolds number for various values of  $X/D$  for gas flowing in a tube with properties evaluated at  $t_{x,av} = x(t_{0,av} - t_{b,av}) + t_{b,av}$ , where  $x$  is obtained from figure 13.  $Pr, 0.73$ . Uniform heat flux, uniform initial temperature distribution, and fully developed velocity distribution.

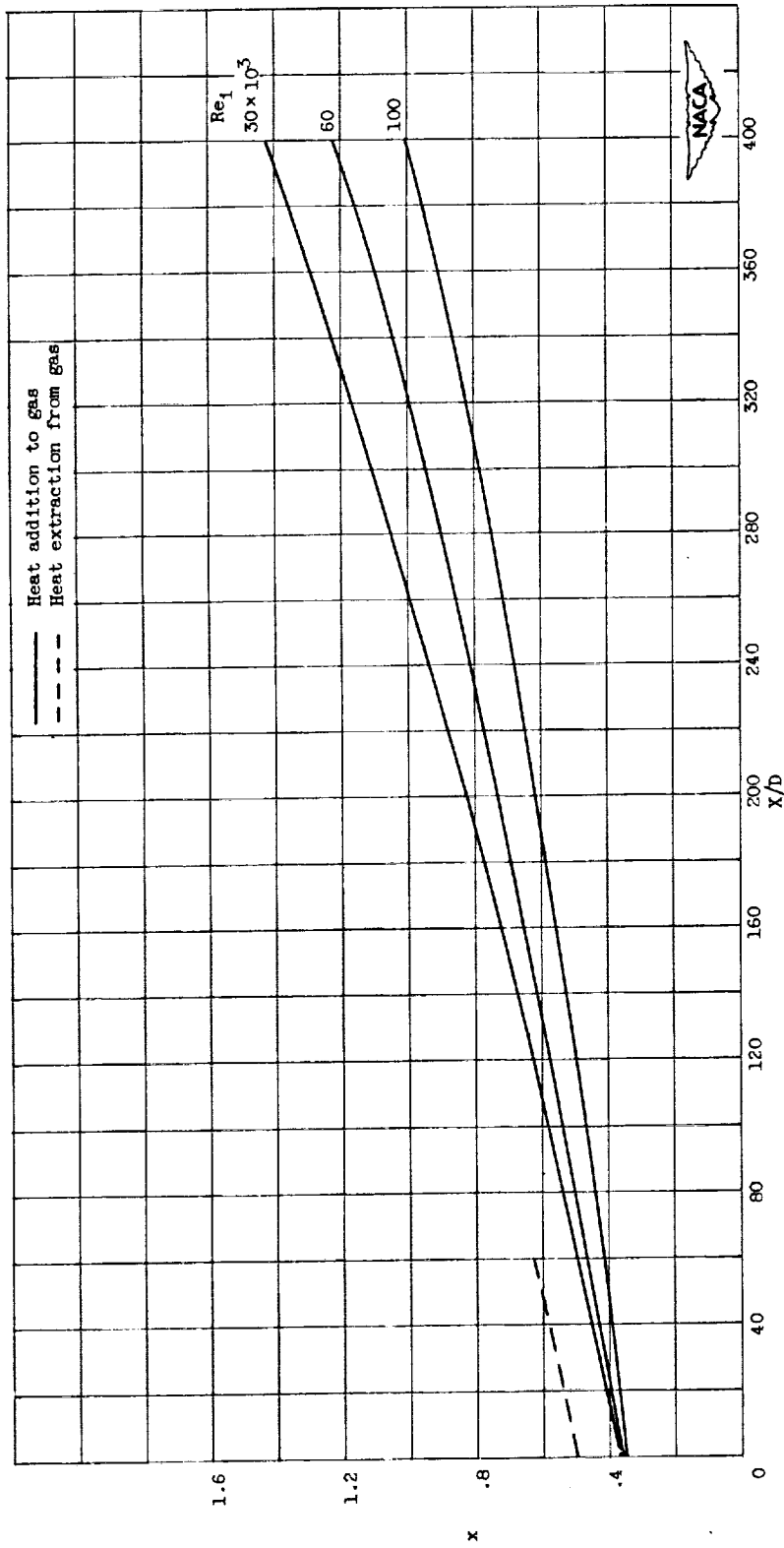
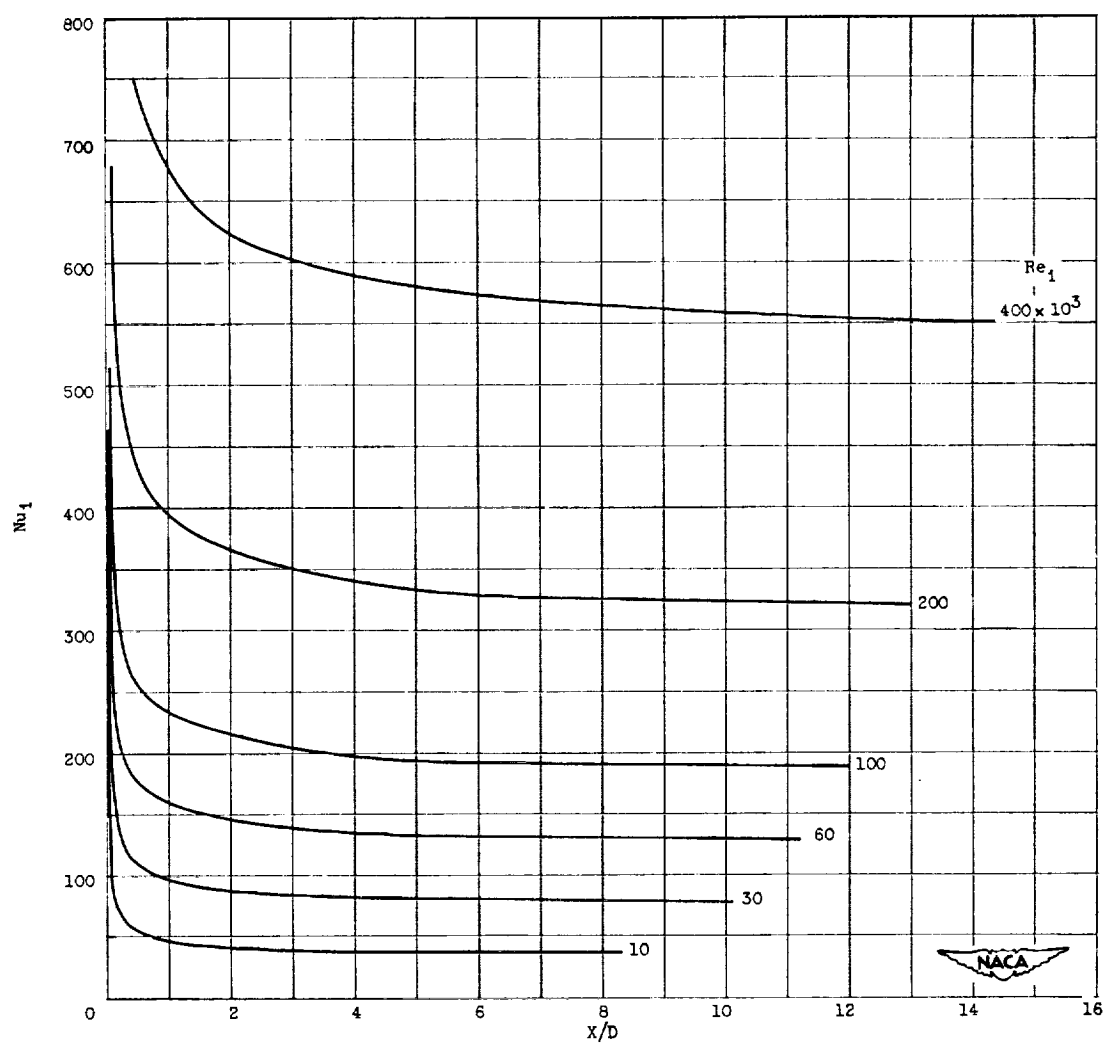
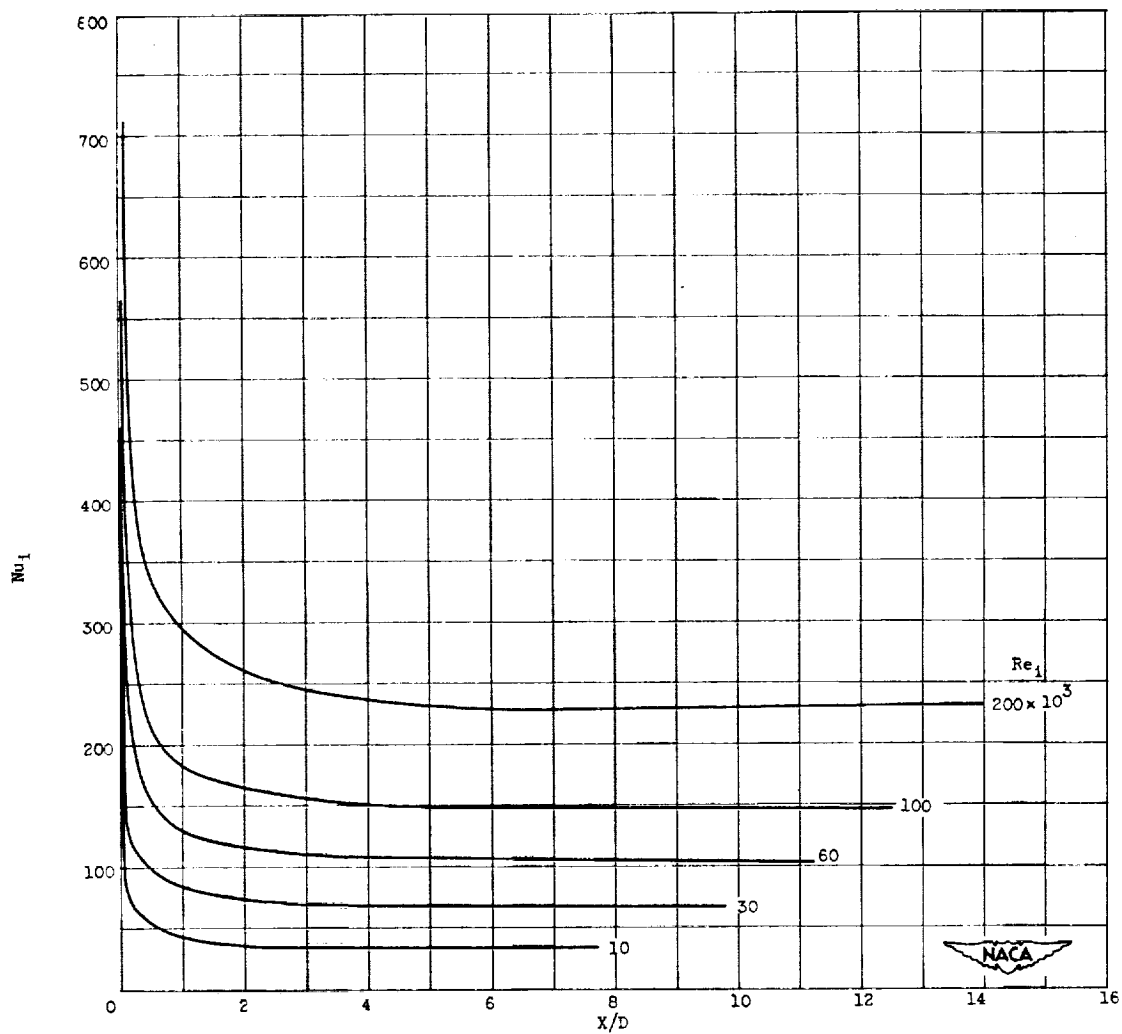


Figure 13. - Values of  $x$  as defined by  $t_{x,av} = x(t_{0,av} - t_{b,av}) + t_{b,av}$  for use with figure 12.



(a)  $q_1' = 0$  (constant properties).

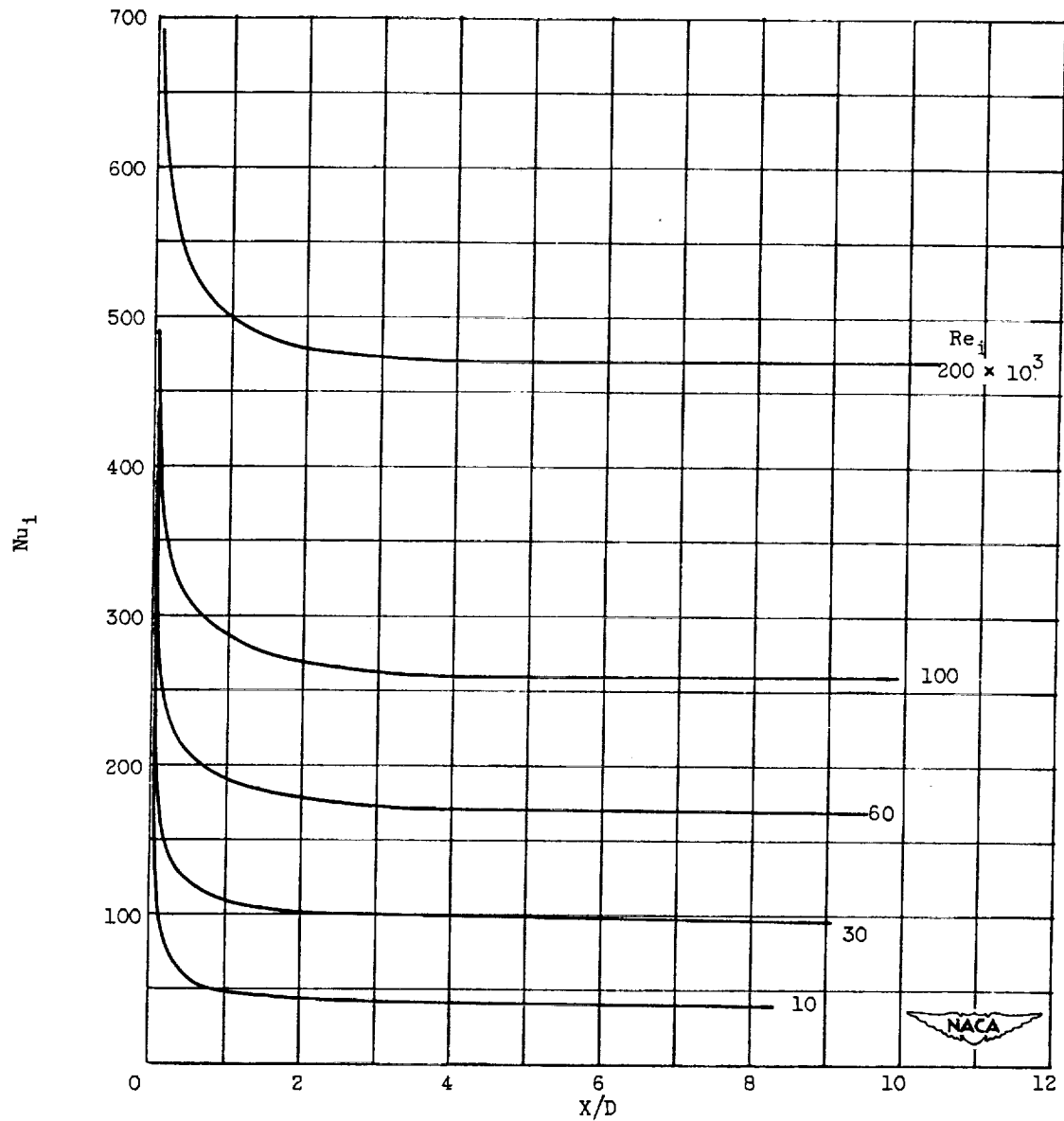
Figure 14. - Variation of Nusselt number with  $X/D$  and Reynolds number for gas flowing between parallel flat plates.  $Pr, 0.73$ . Uniform heat flux, uniform initial temperature distribution, and fully developed velocity distribution.



(b)  $q_1' = 0.004$  (heat addition to gas).

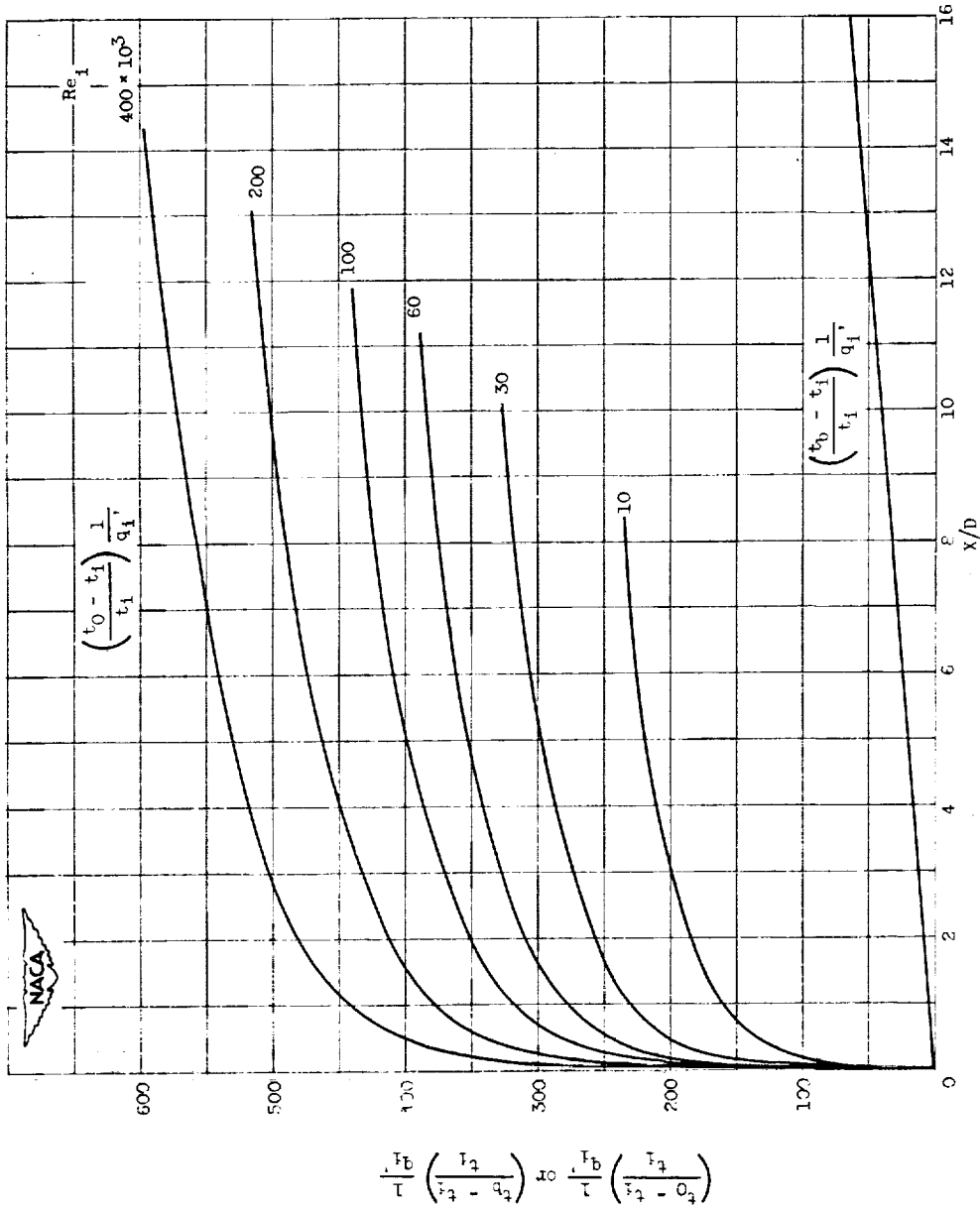
Figure 14. - Continued. Variation of Nusselt number with  $X/D$  and Reynolds number for gas flowing between parallel flat plates.  $Pr, 0.73$ . Uniform heat flux, uniform initial temperature distribution, and fully developed velocity distribution.





(c)  $q_1' = -0.0025$  (heat extraction from gas).

Figure 14. - Concluded. Variation of Nusselt number with  $X/D$  and Reynolds number for gas flowing between parallel flat plates.  $Pr, 0.73$ . Uniform heat flux, uniform initial temperature distribution, and fully developed velocity distribution.

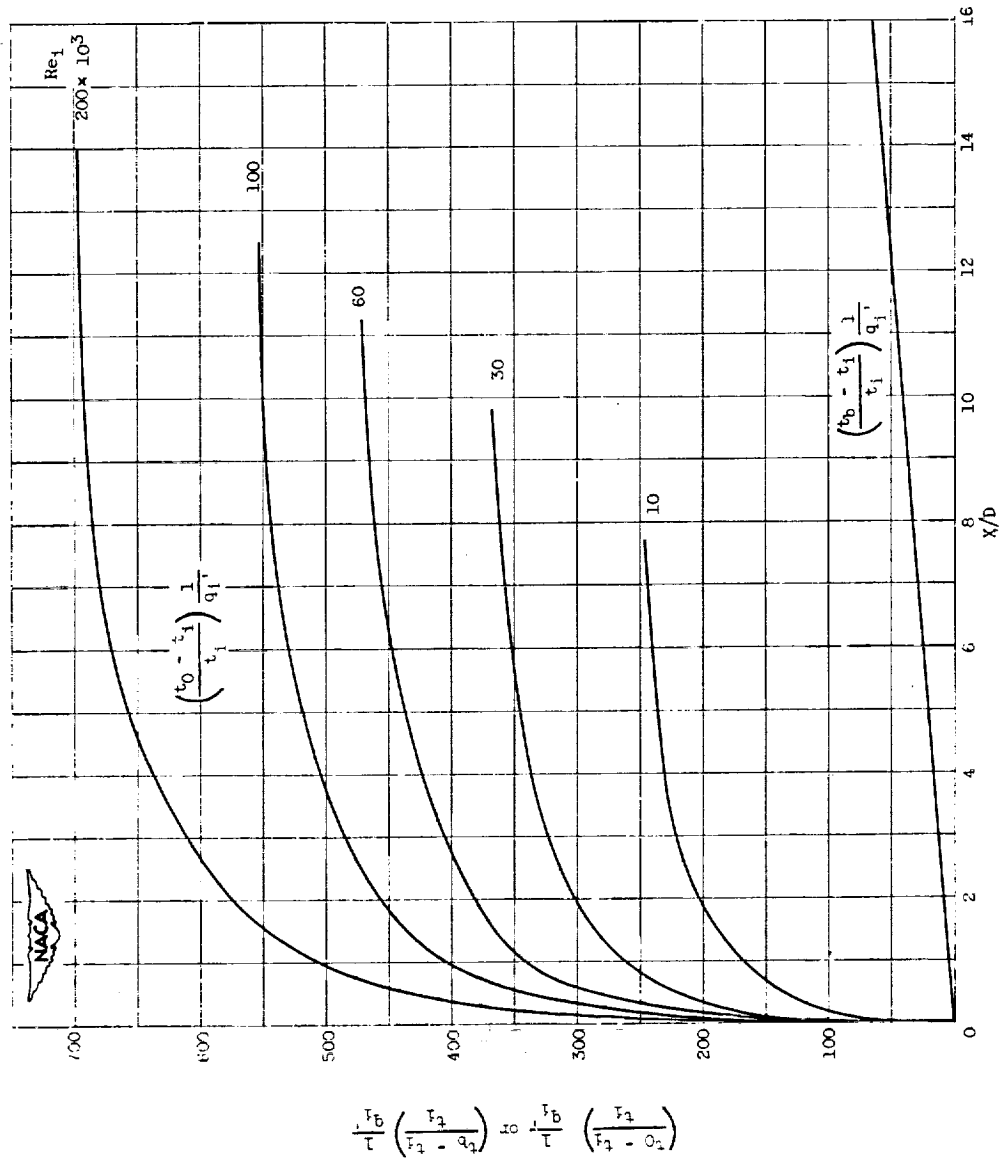


(a)  $q_1' = 0$  (constant properties).

Figure 15. - Variation of dimensionless wall and bulk temperatures with  $X/D$  and Reynolds number for gas flowing between parallel flat plates.  $Pr, 0.73$ . Uniform initial temperature distribution and fully developed velocity distribution.

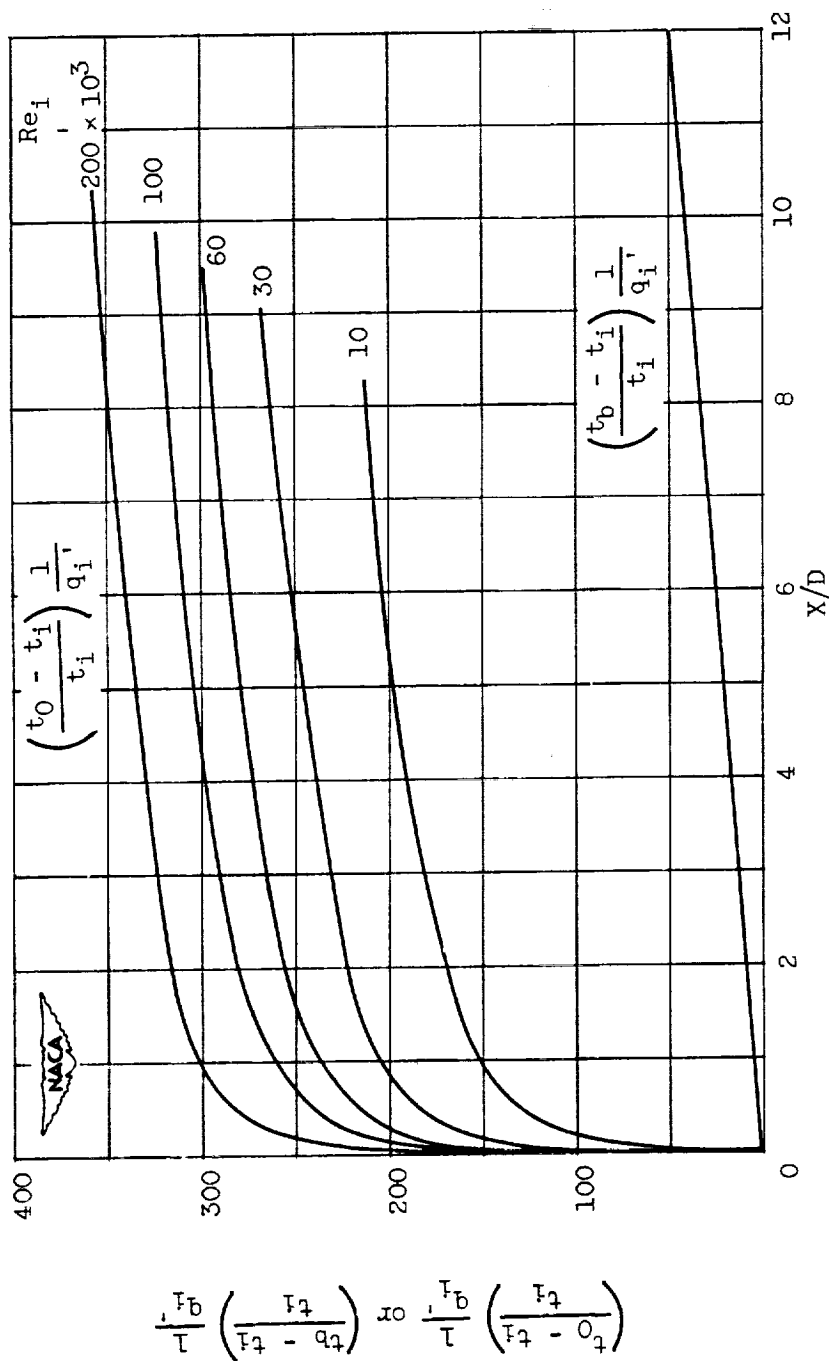
2857

CZ-9



(b)  $q_1' = 0.004$  (heat addition to gas).

Figure 15. - Continued. Variation of dimensionless wall and bulk temperatures with  $X/D$  and Reynolds number for gas flowing between parallel flat plates.  $Pr, 0.73$ . Uniform initial temperature distribution and fully developed velocity distribution.



(c)  $q_i' = -0.0025$  (heat extraction from gas).

Figure 15. - Concluded. Variation of dimensionless wall and bulk temperatures with  $X/D$  and Reynolds number for gas flowing between parallel flat plates,  $Pr, 0.73$ . Uniform initial temperature distribution and fully developed velocity distribution.

2857

CZ-9 back

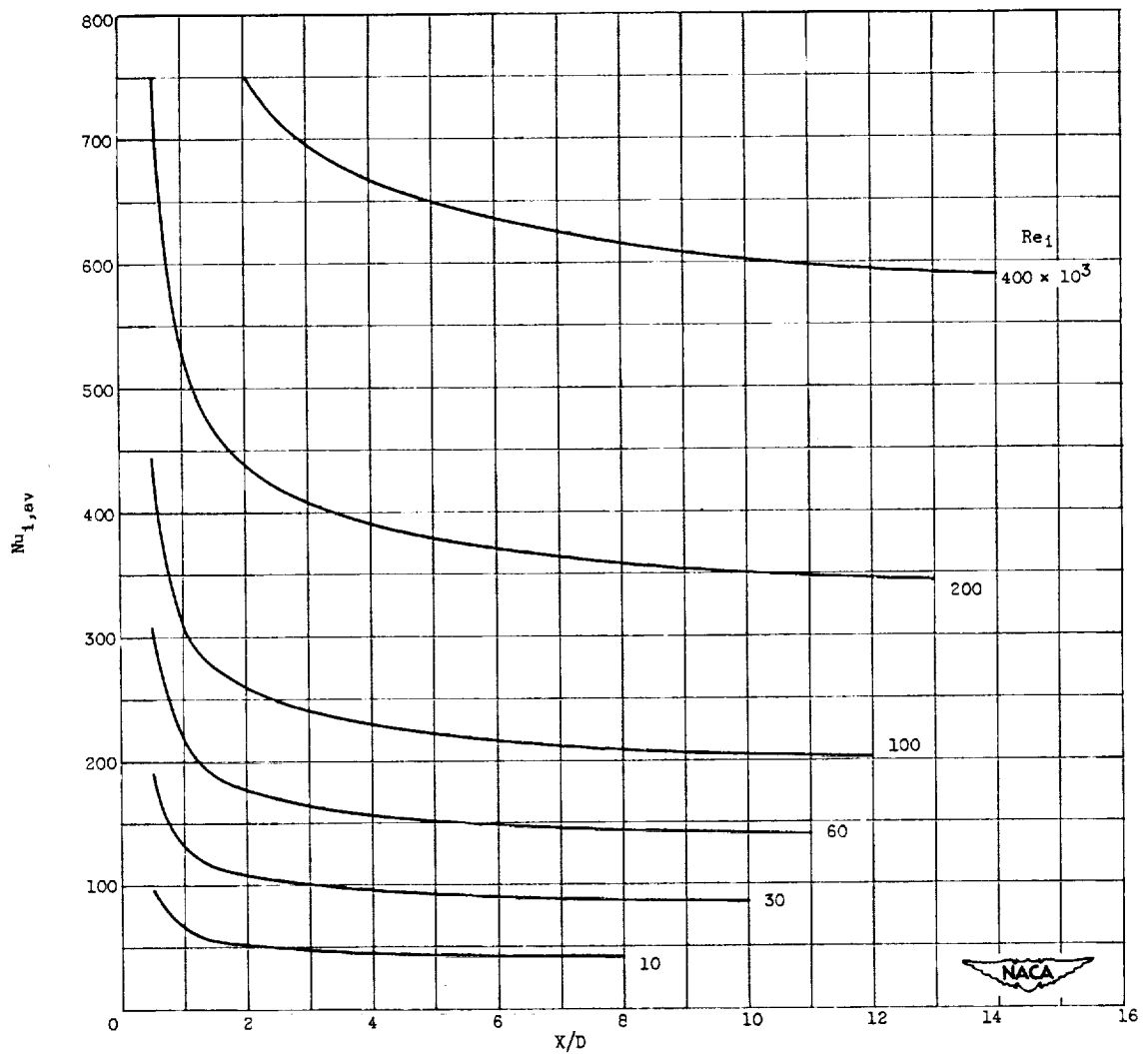
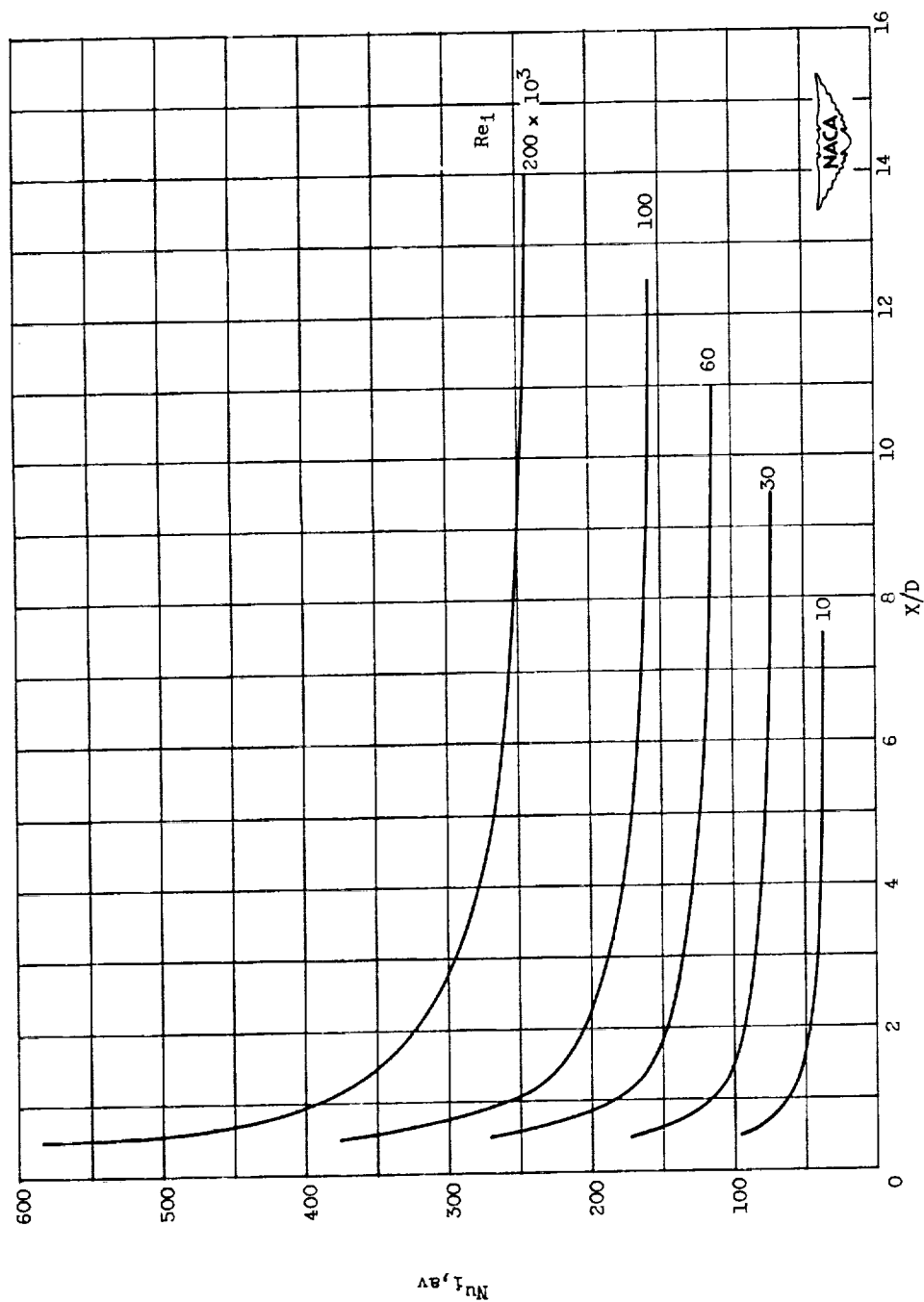
(a)  $q_1' = 0$  (constant properties).

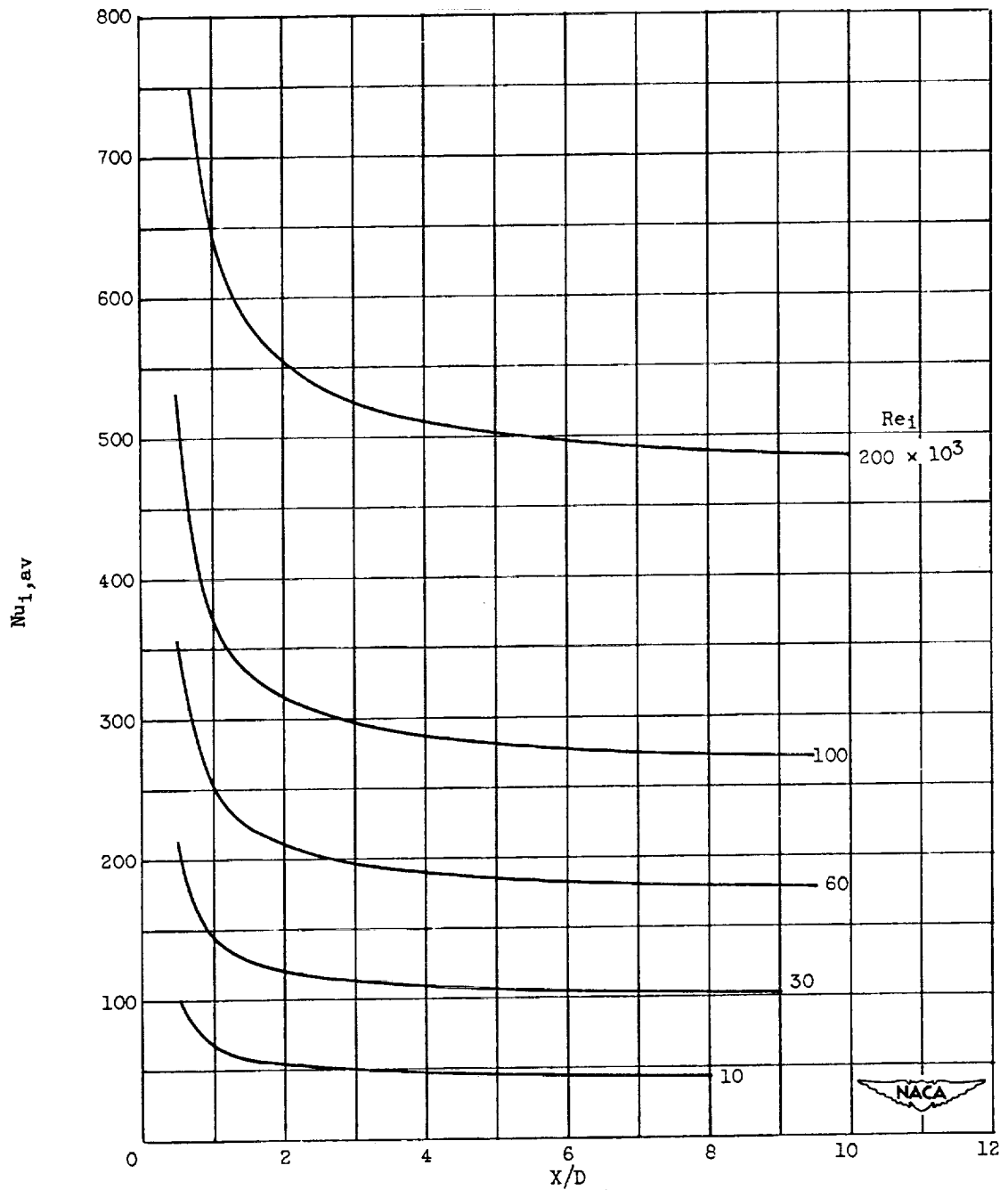
Figure 16. - Variation of average Nusselt number defined by equation (25) with  $X/D$  and Reynolds number for gas flowing between parallel flat plates.  $Pr, 0.73$ . Uniform heat flux, uniform initial temperature distribution, and fully developed velocity distribution.



(b)  $q_1' = 0.004$  (heat addition to gas).

Figure 16. - Continued. Variation of average Nusselt number defined by equation (25) with  $X/D$  and Reynolds number for gas flowing between parallel flat plates.  $Pr, 0.73$ . Uniform heat flux, uniform initial temperature distribution, and fully developed velocity distributions.

2857



(c)  $q_1' = -0.0025$  (heat extraction from gas).

Figure 16. - Concluded. Variation of average Nusselt number defined by equation (25) with  $X/D$  and Reynolds number for gas flowing between parallel flat plates.  $Pr, 0.73$ . Uniform heat flux, uniform initial temperature distribution, and fully developed velocity distribution.

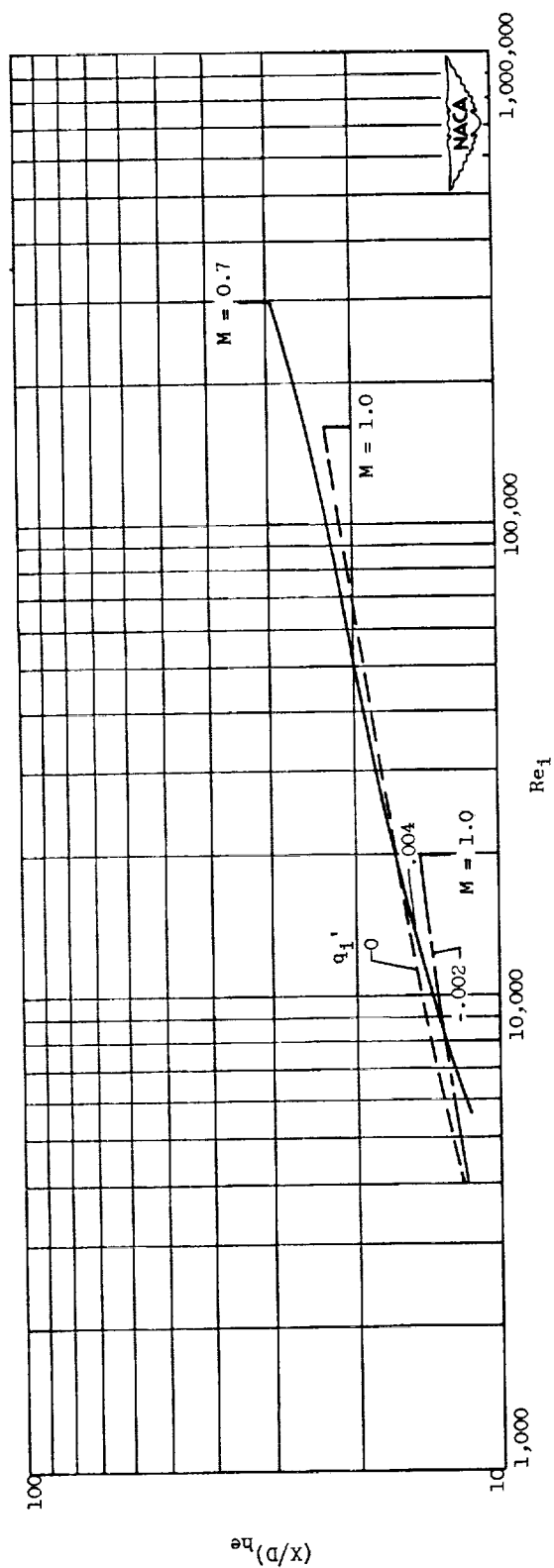


Figure 17. - Variation of thermal entrance length with Reynolds number for gas flowing in a tube with frictional heating.  $\alpha = 0.00025$ ;  $Pr = 0.73$ . Uniform heat flux, uniform initial temperature distribution, and fully developed velocity distribution.



2857

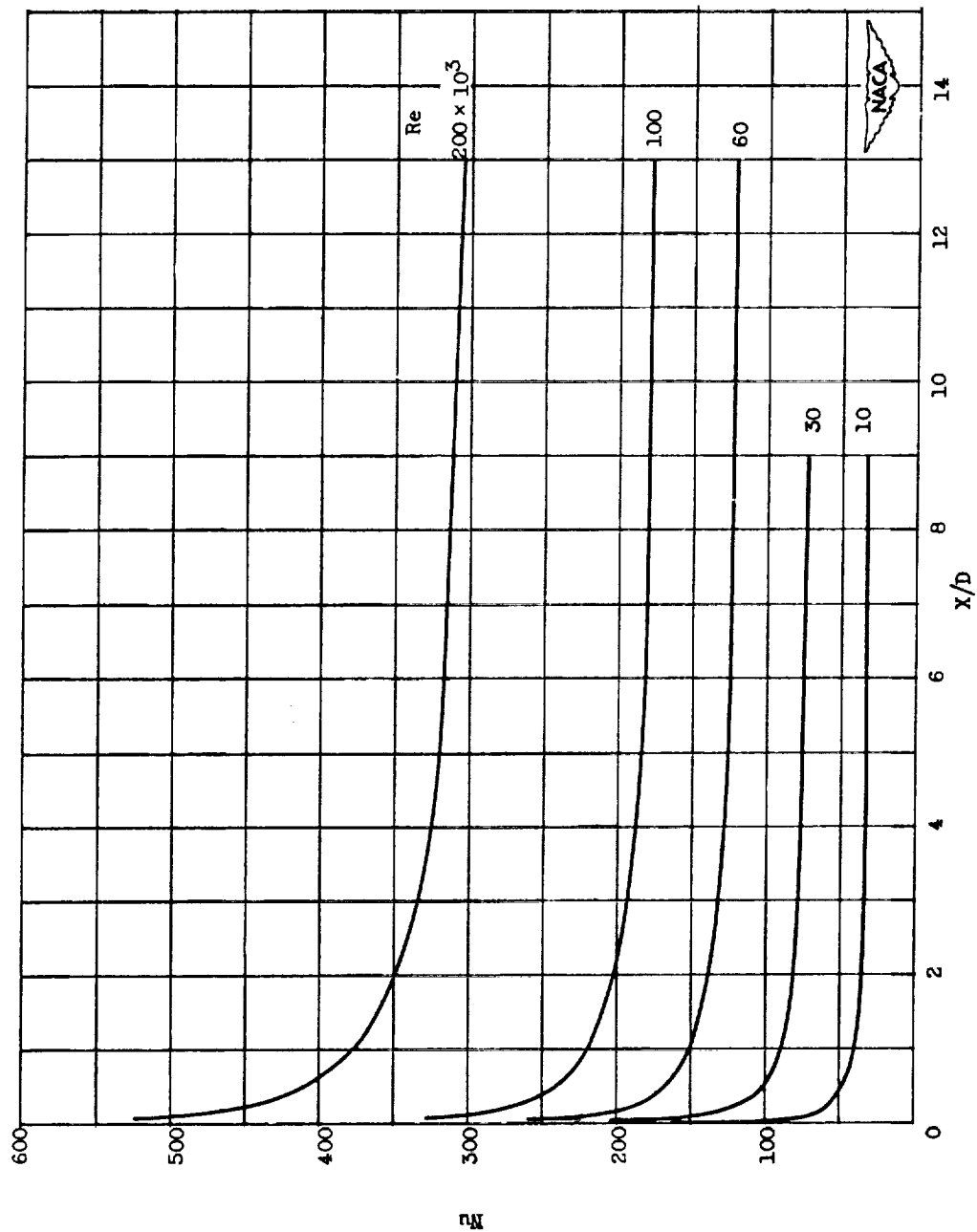


Figure 18. - Variation of Nusselt number with  $x/D$  and Reynolds number for gas flowing in a tube.  $Pr, 0.73$ . Uniform wall temperature, uniform initial temperature distribution, fully developed velocity distribution, and constant properties.

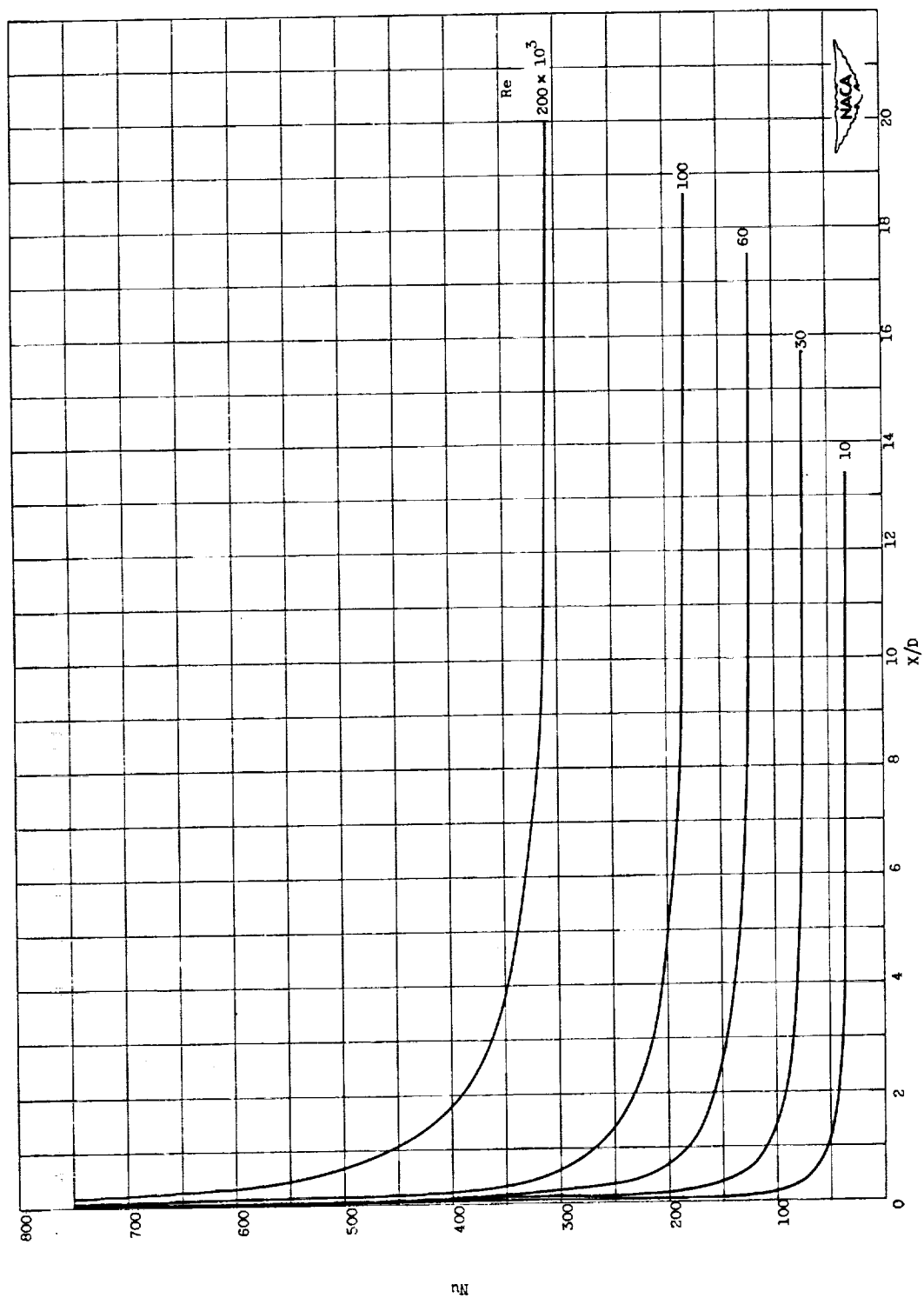
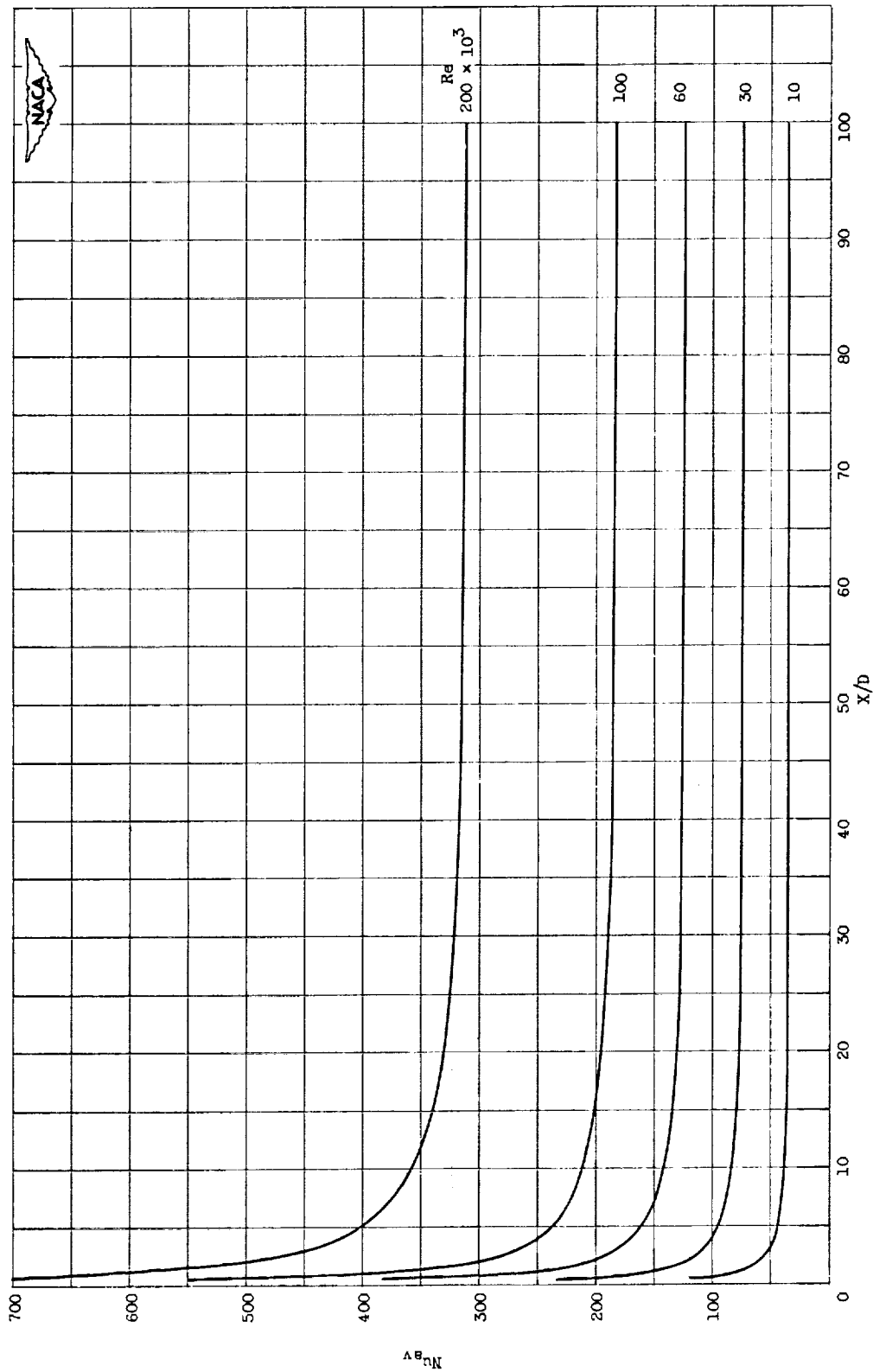


Figure 19. - Variation of Nusselt number with  $X/D$  and Reynolds number for gas flowing in a tube.  $Pr$ , 0.73. Uniform heat flux, uniform initial temperature and velocity distributions, and constant properties.

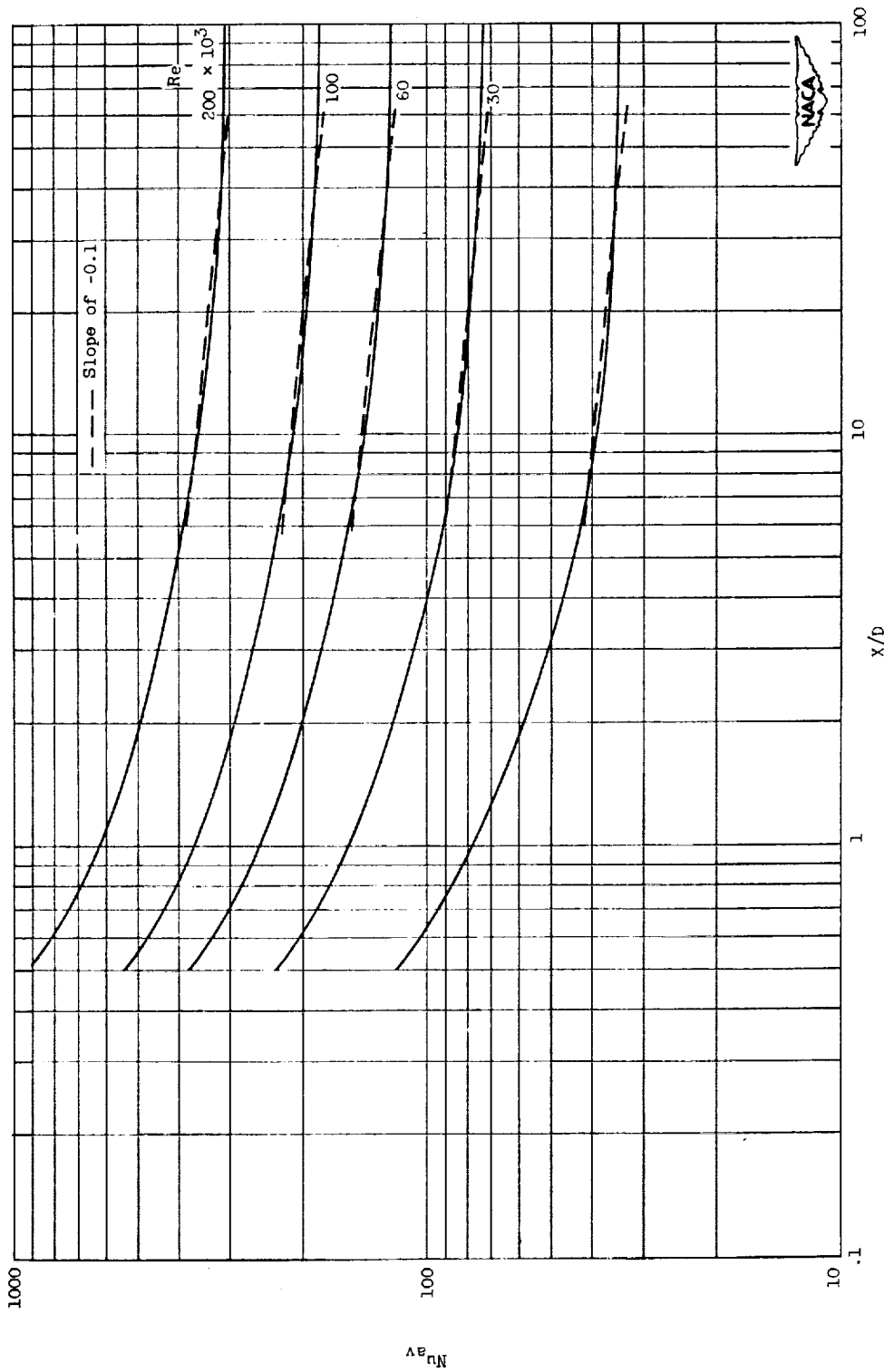
2857

CZ-10



(a) Rectangular Cartesian coordinates.

Figure 20. - Variation of average Nusselt number calculated from equation (25) with  $X/D$  and Reynolds number for gas flowing in a tube.  $Pr, 0.73$ . Uniform heat flux, uniform initial temperature and velocity distributions, and constant properties.



(b) Logarithmic coordinates.

Figure 20. - Concluded. Variation of average Nusselt number calculated from equation (25) with  $x/d$  and Reynolds number for gas flowing in a tube.  $Pr, 0.73$ . Uniform heat flux, uniform initial temperature and velocity distributions, and constant properties.

2857

CZ-10 back

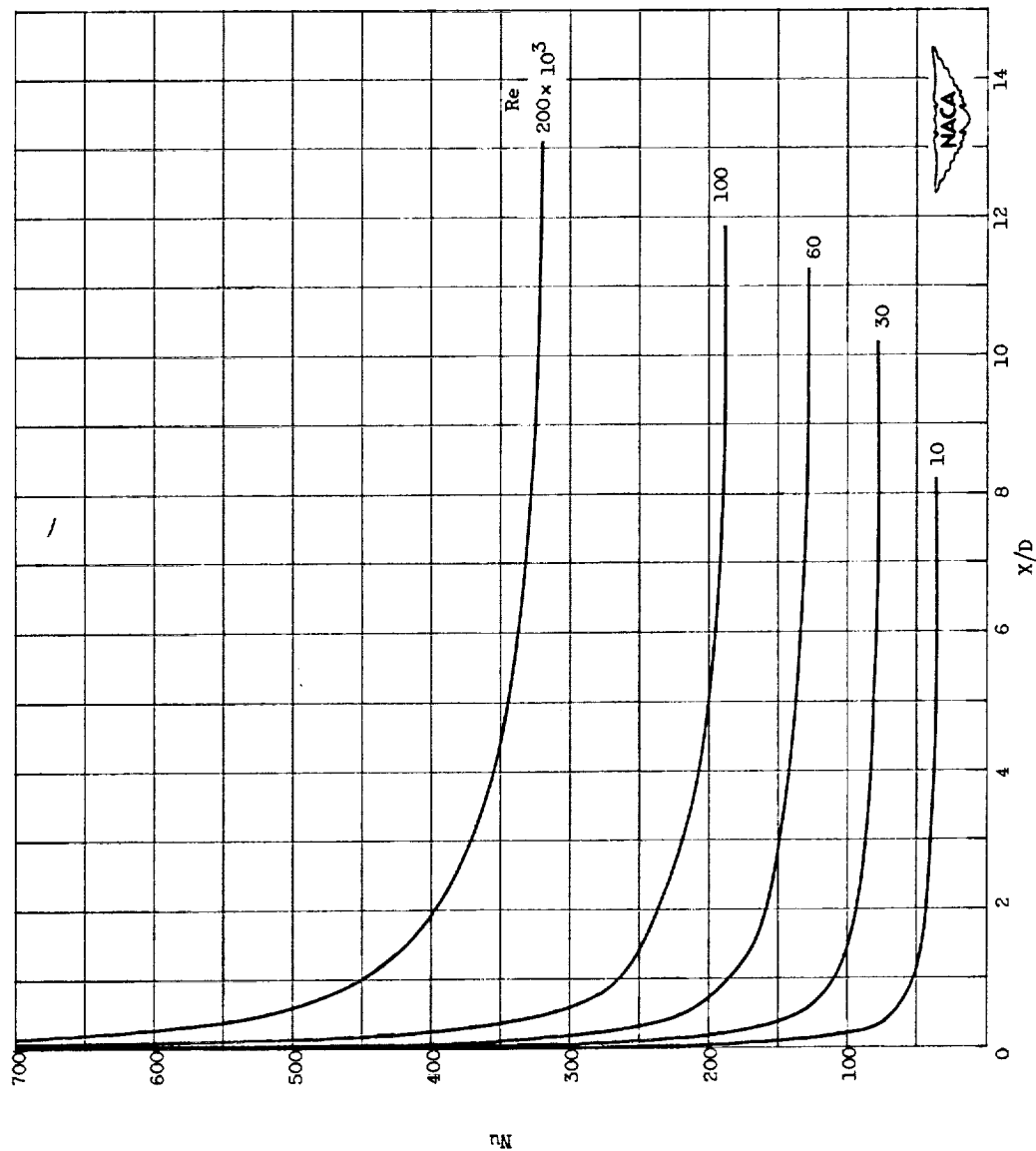


Figure 21. - Variation of Nusselt number with  $x/d$  and Reynolds number for gas flowing between parallel flat plates.  $Pr, 0.73$ . Uniform heat flux, uniform initial temperature and velocity distributions, and constant properties.

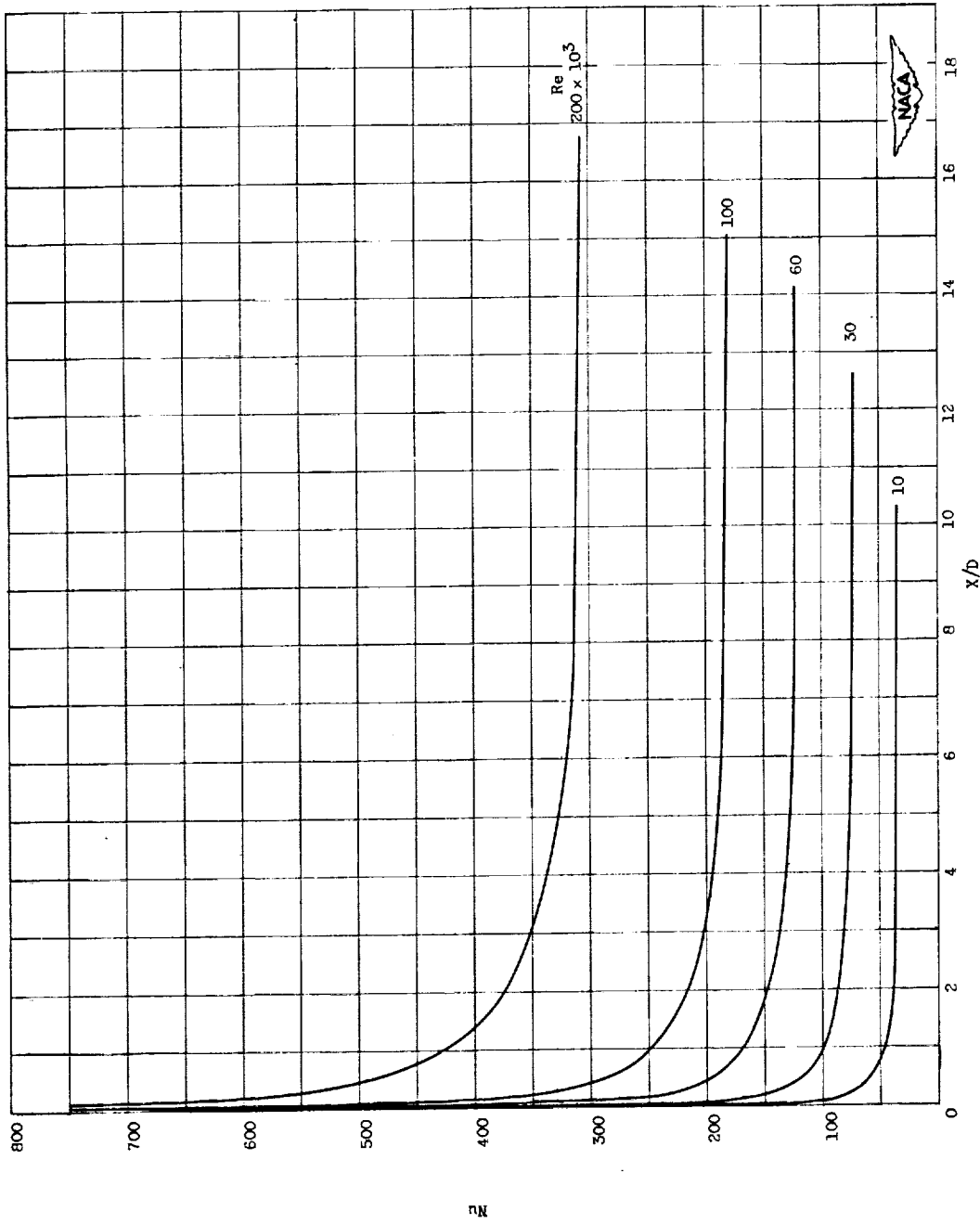


Figure 22. - Variation of Nusselt number with  $x/d$  and Reynolds number for gas flowing in a tube.  $Pr, 0.73$ . Uniform wall temperature, uniform initial velocity and temperature distributions, and constant properties.

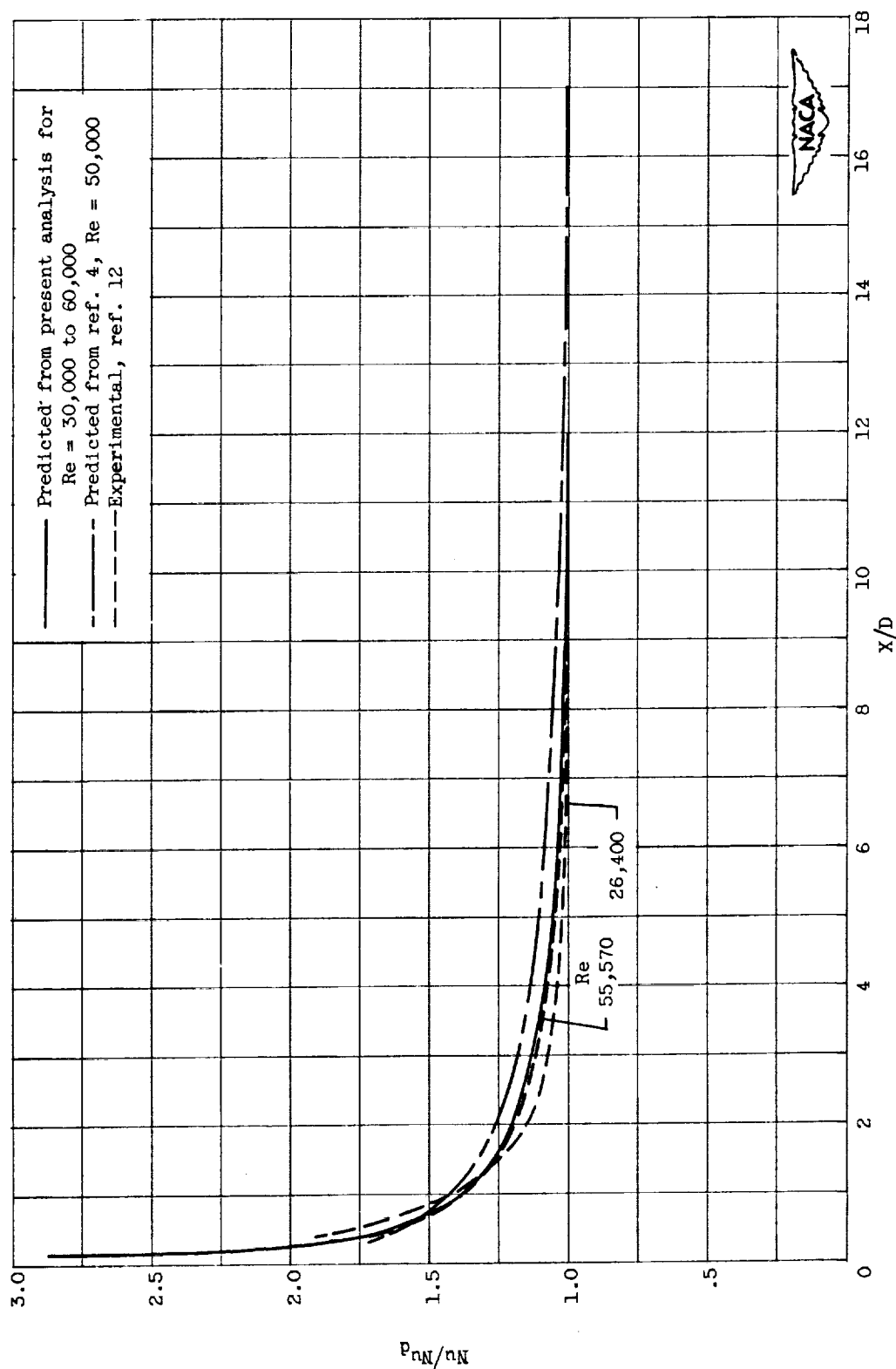


Figure 23. - Comparison of predicted and experimental results for air flowing in a tube.  $Pr, 0.73$ . Uniform wall temperature, uniform initial velocity and temperature distributions, and constant properties.

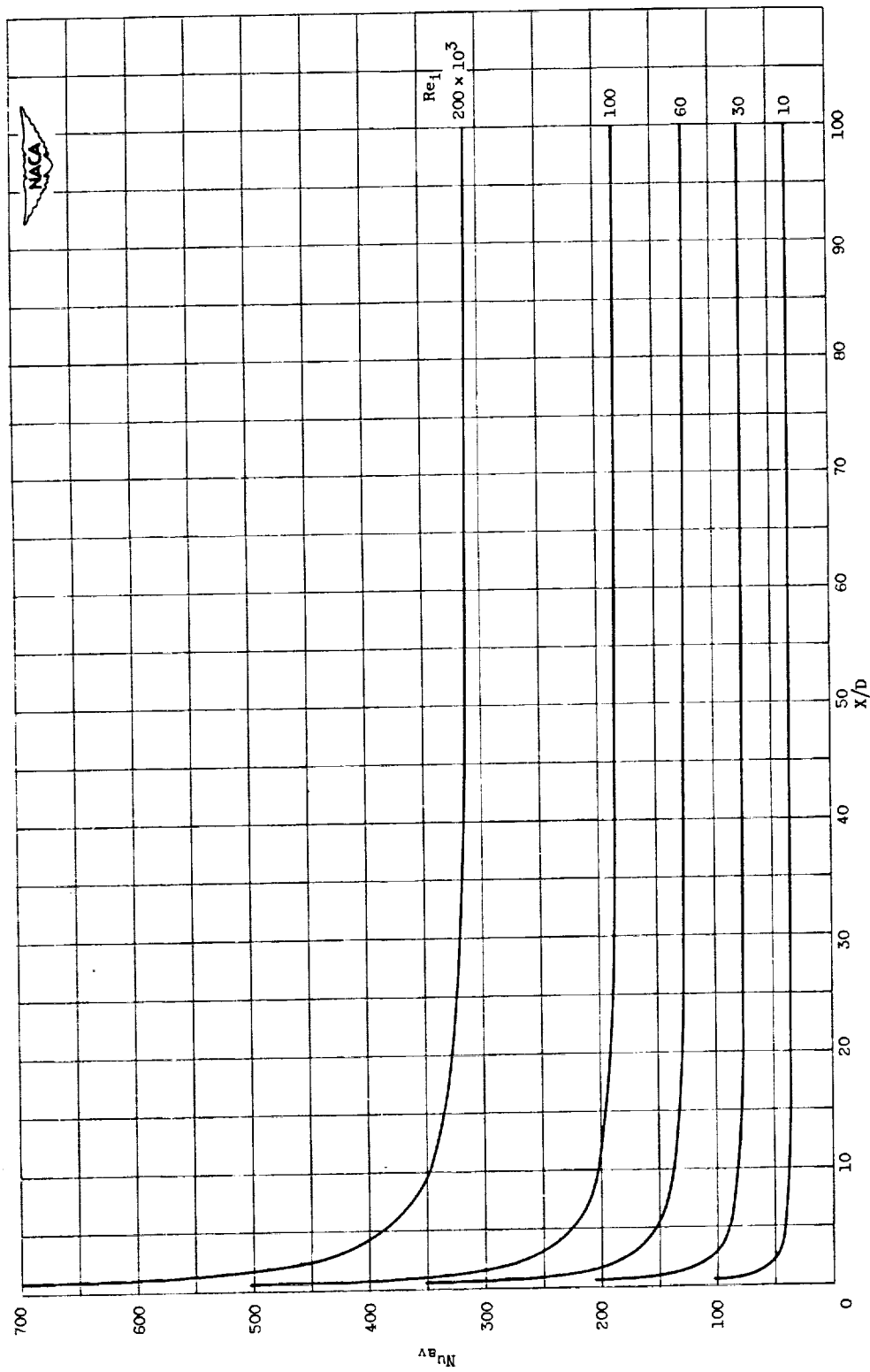


Figure 24. - Variation of average Nusselt number as calculated from equation (25) with  $x/d$  and Reynolds number for gas flowing in a tube.  $Pr, 0.73$ . Uniform wall temperature, uniform initial velocity and temperature distributions, and constant properties.



2857

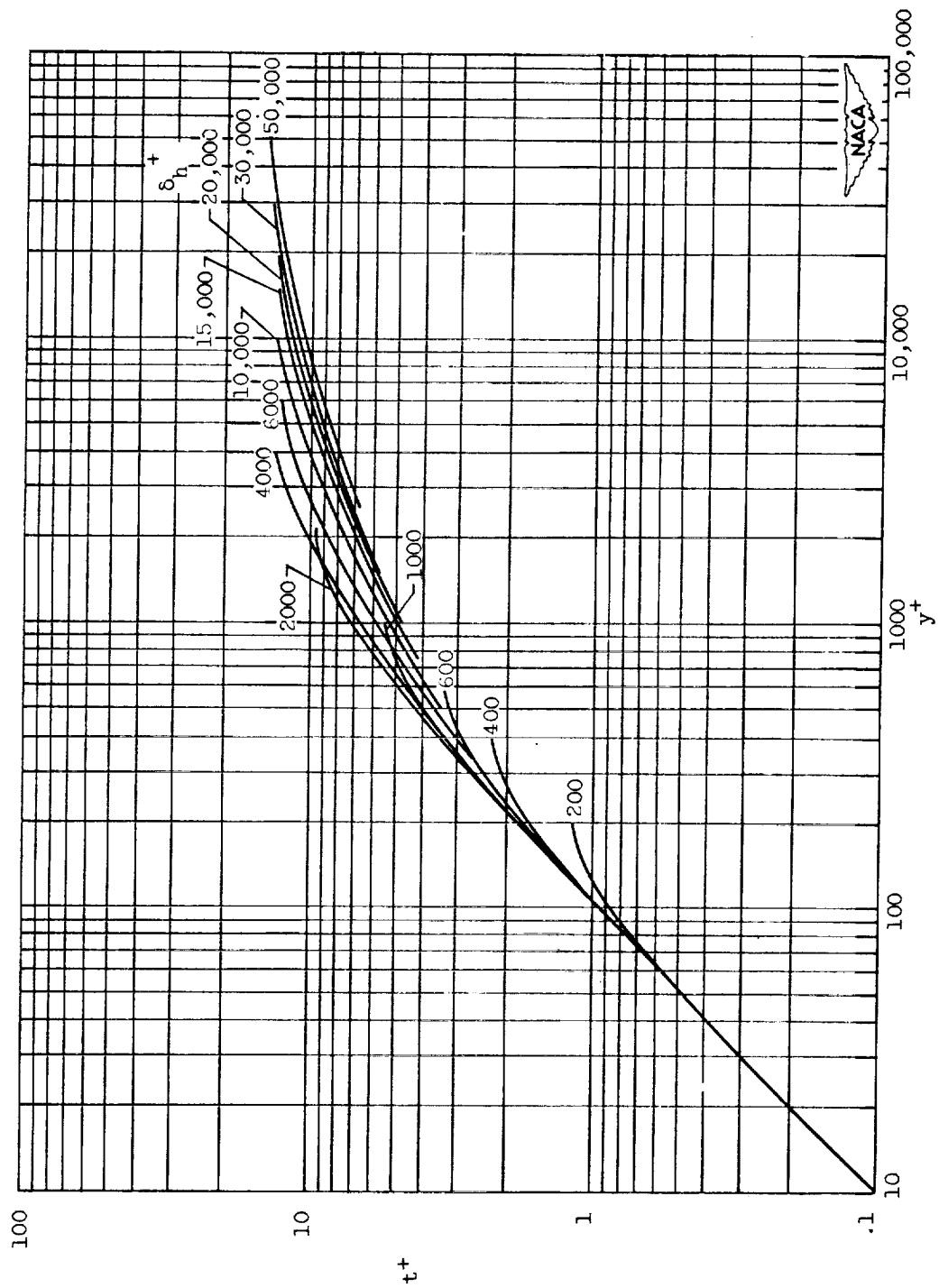


Figure 25. - Predicted generalized temperature distribution for flow of liquid metal with heat transfer. Data from reference 8.  $Pr, 0.01$ .

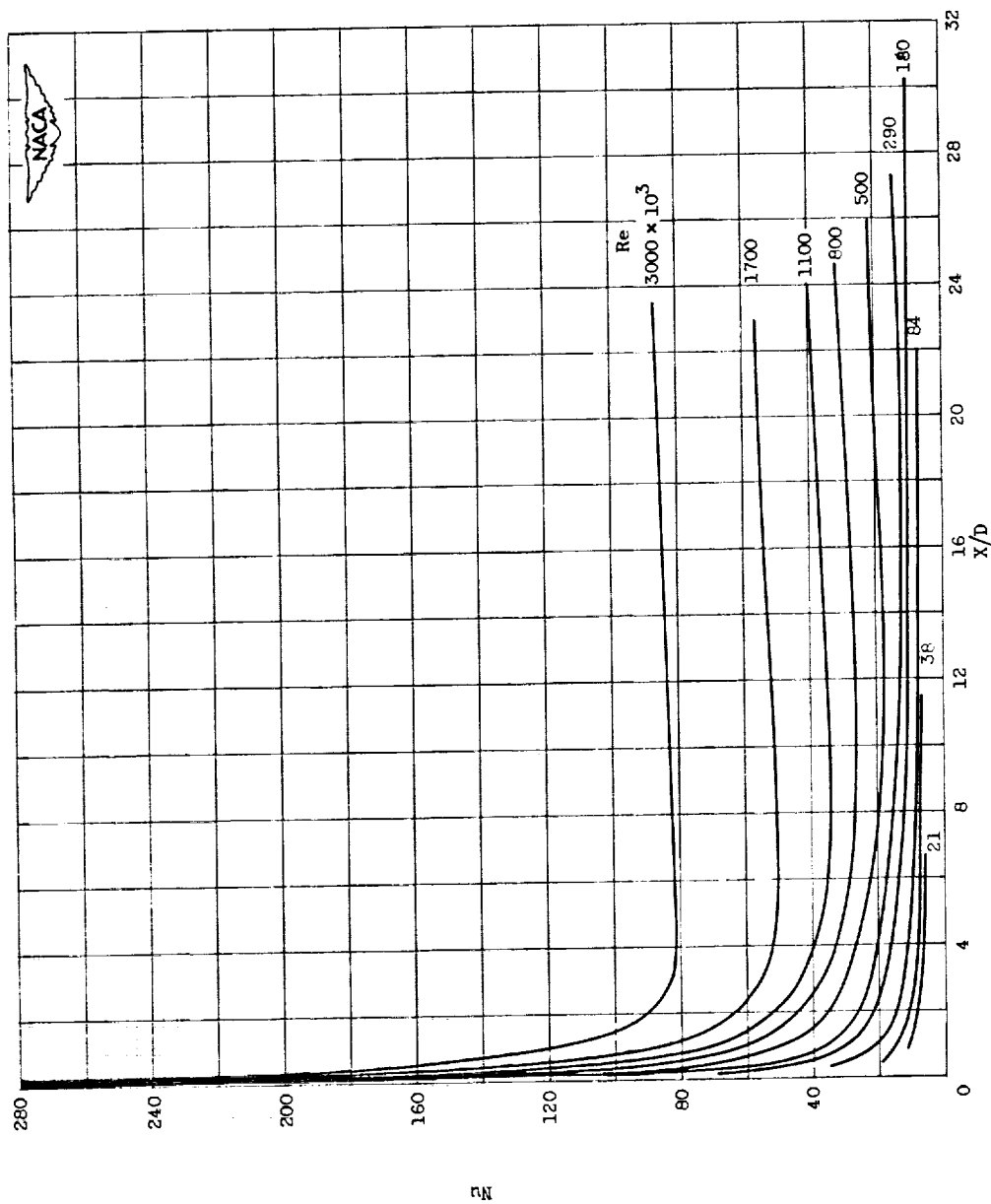


Figure 26. - Variation of Nusselt number with  $X/D$  and Reynolds number for liquid metal flowing in a tube. Prandtl number, 0.01. Uniform heat flux, uniform initial temperature distribution, fully developed velocity distribution, and constant properties.

2857 IT-ZO

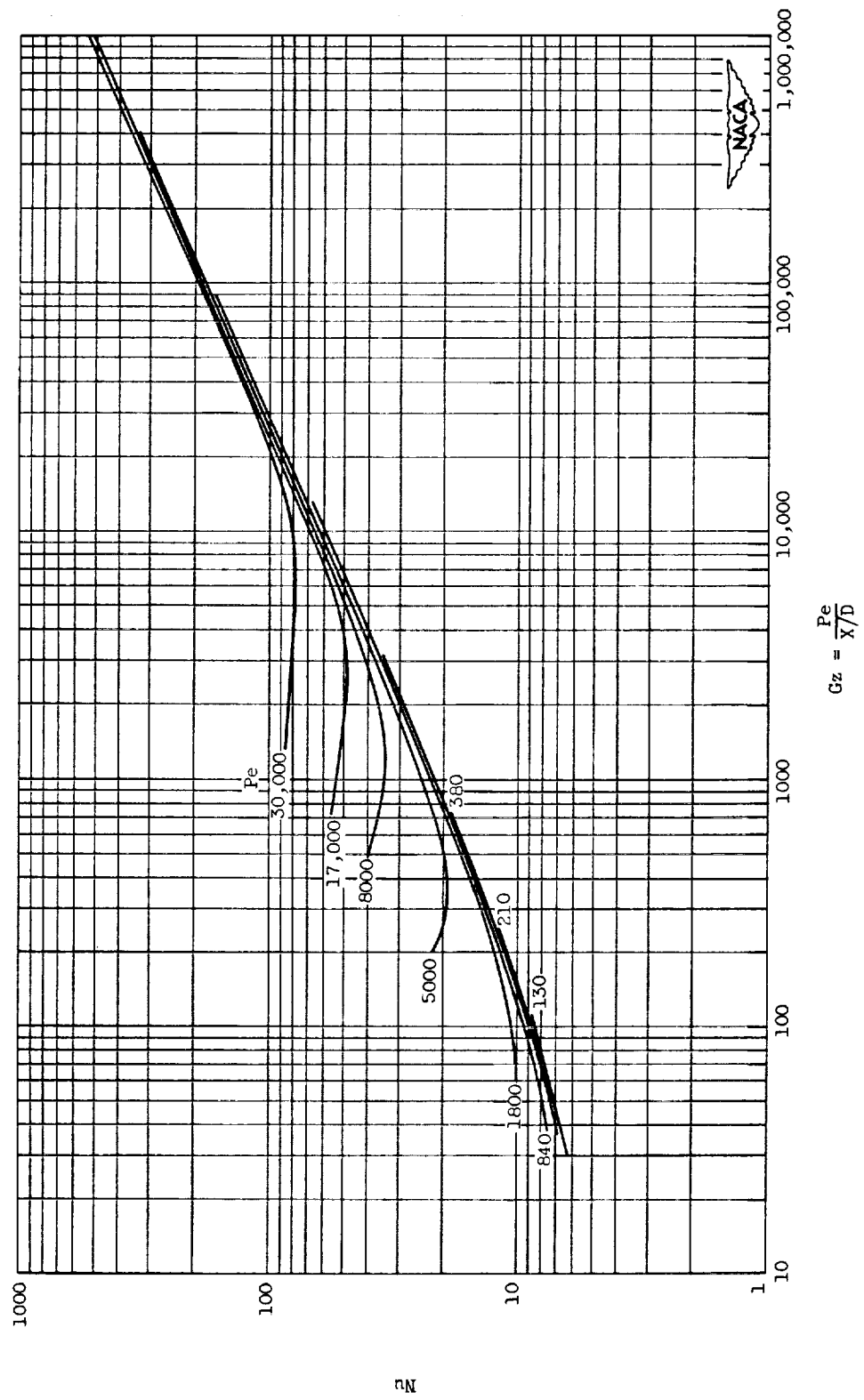


Figure 27. - Variation of Nusselt number with Graetz number and Peclet number for liquid metal flowing in a tube.  $Pr, 0.01$ . Uniform heat flux, uniform initial temperature distribution, fully developed velocity distribution, and constant properties.

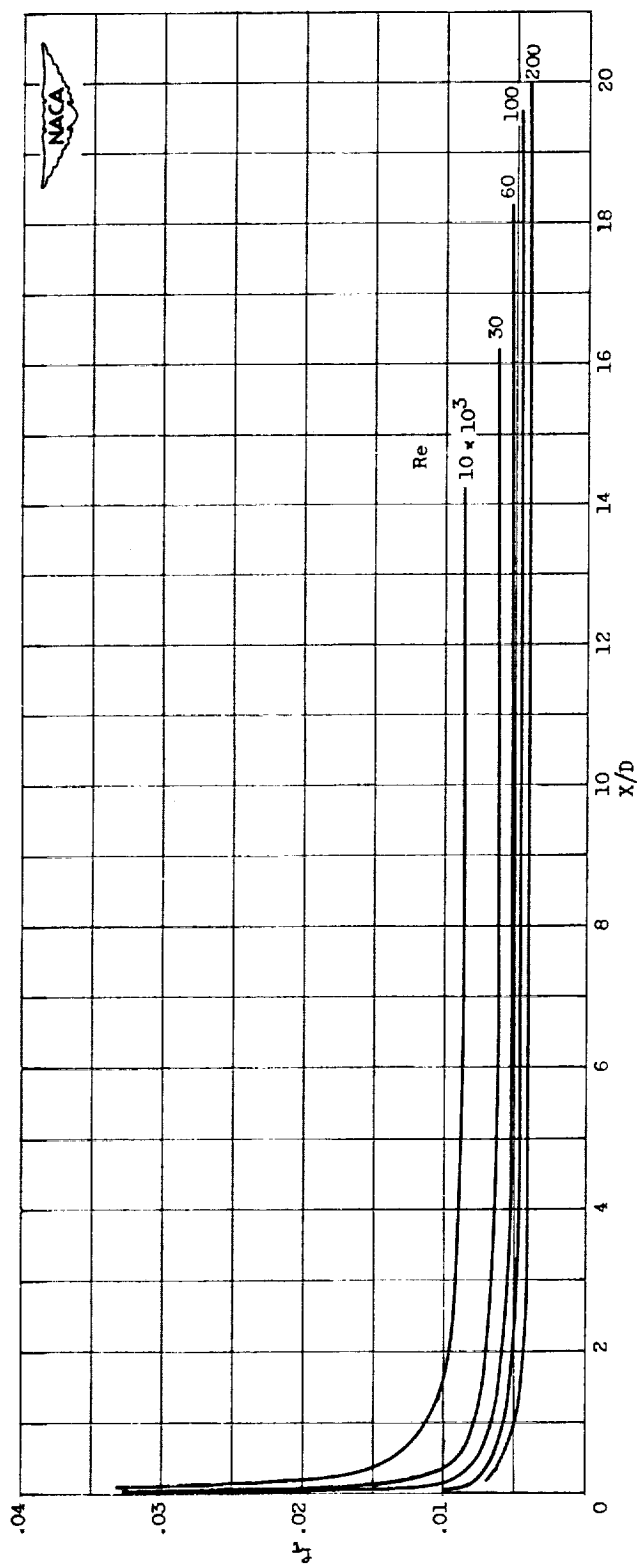


Figure 29. - Variation of friction factor based on wall shear stress with  $X/d$  and Reynolds number for flow in a tube. Constant properties.

2857

CZ-11 back

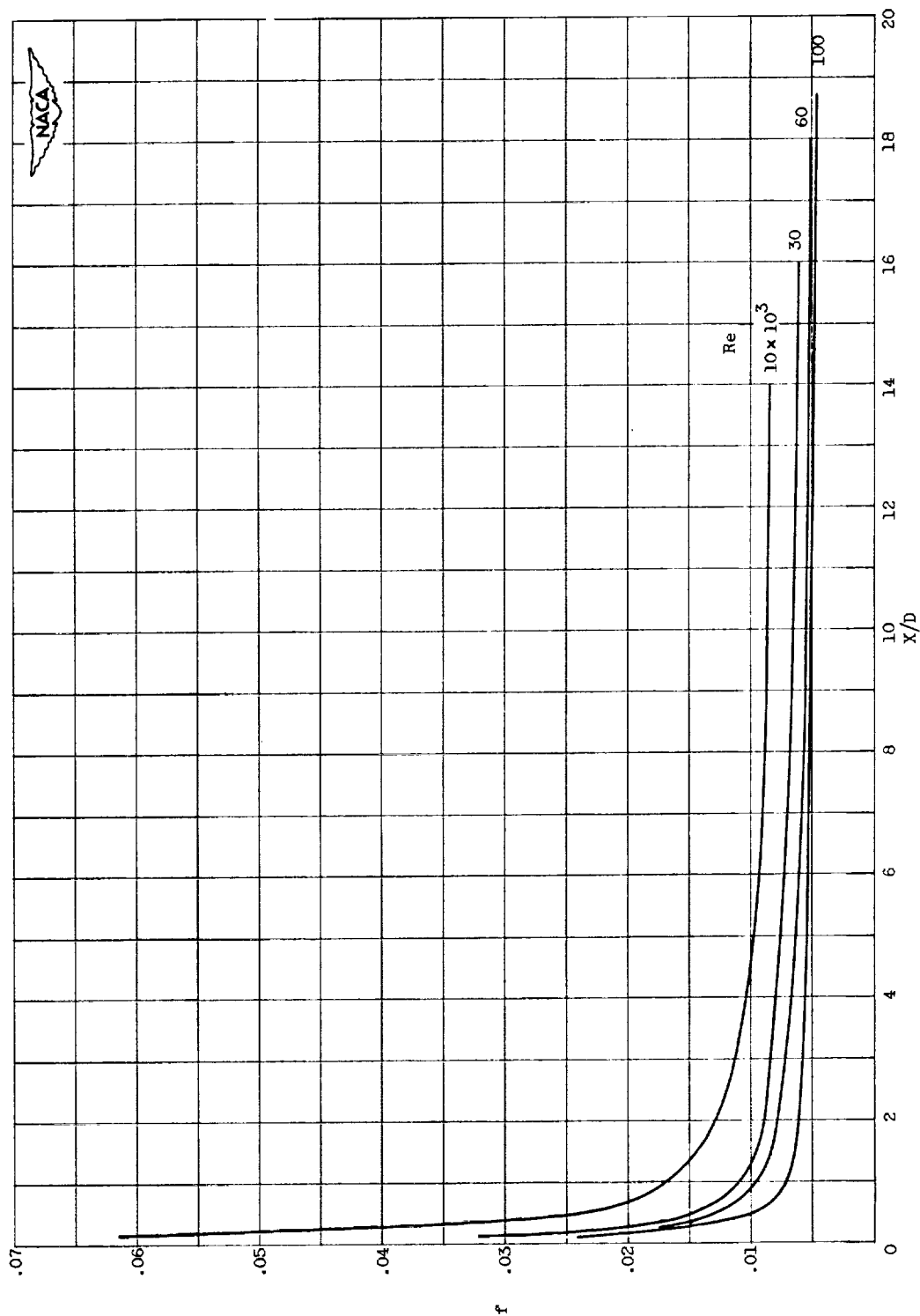


Figure 29. - Variation of friction factor based on static-pressure gradient with  $X/D$  and Reynolds number for flow in a tube. Constant properties.

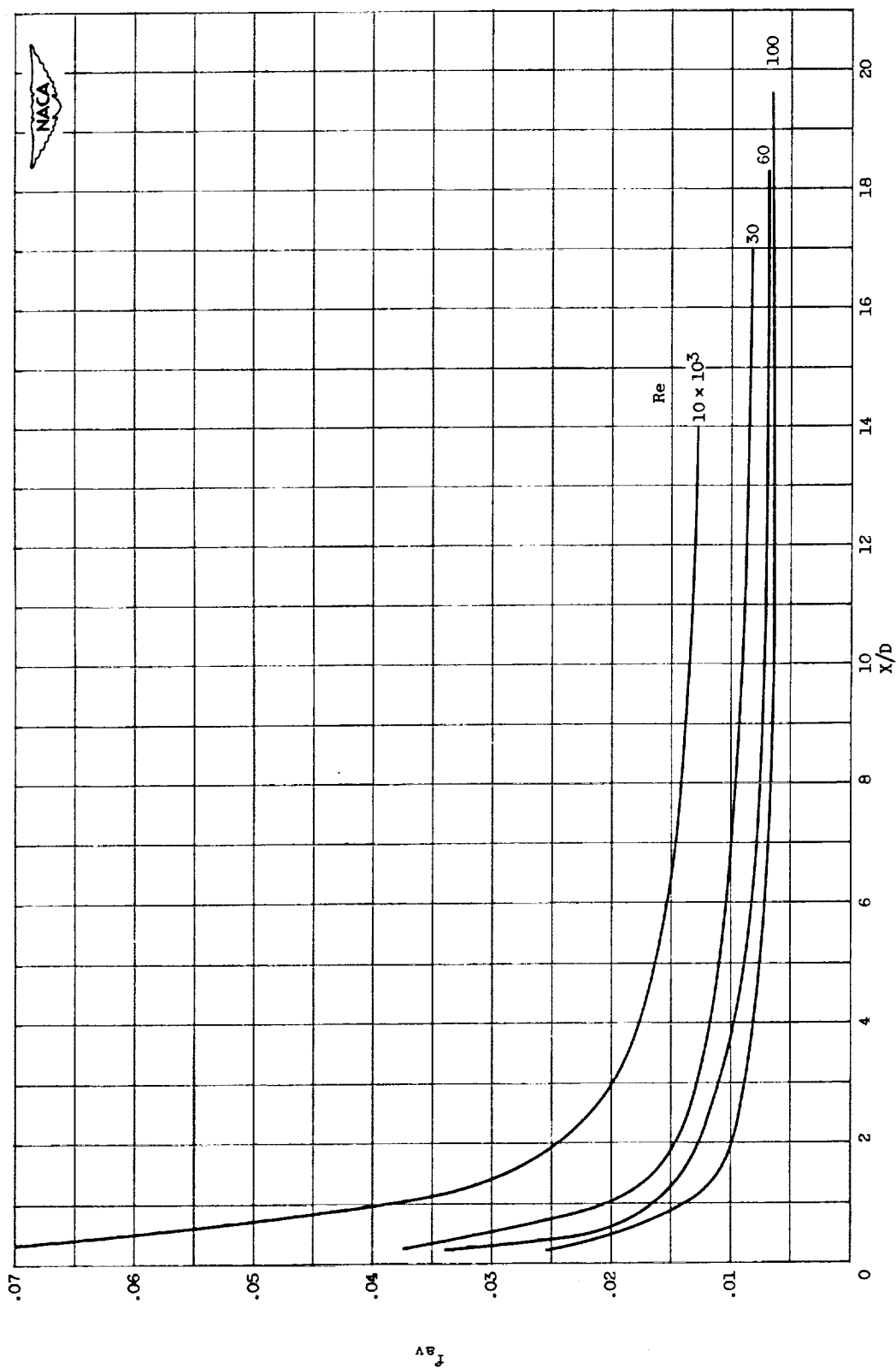


Figure 30. - Variation of average friction factor based on static-pressure drop with  $x/d$  for flow in a tube. Constant properties.

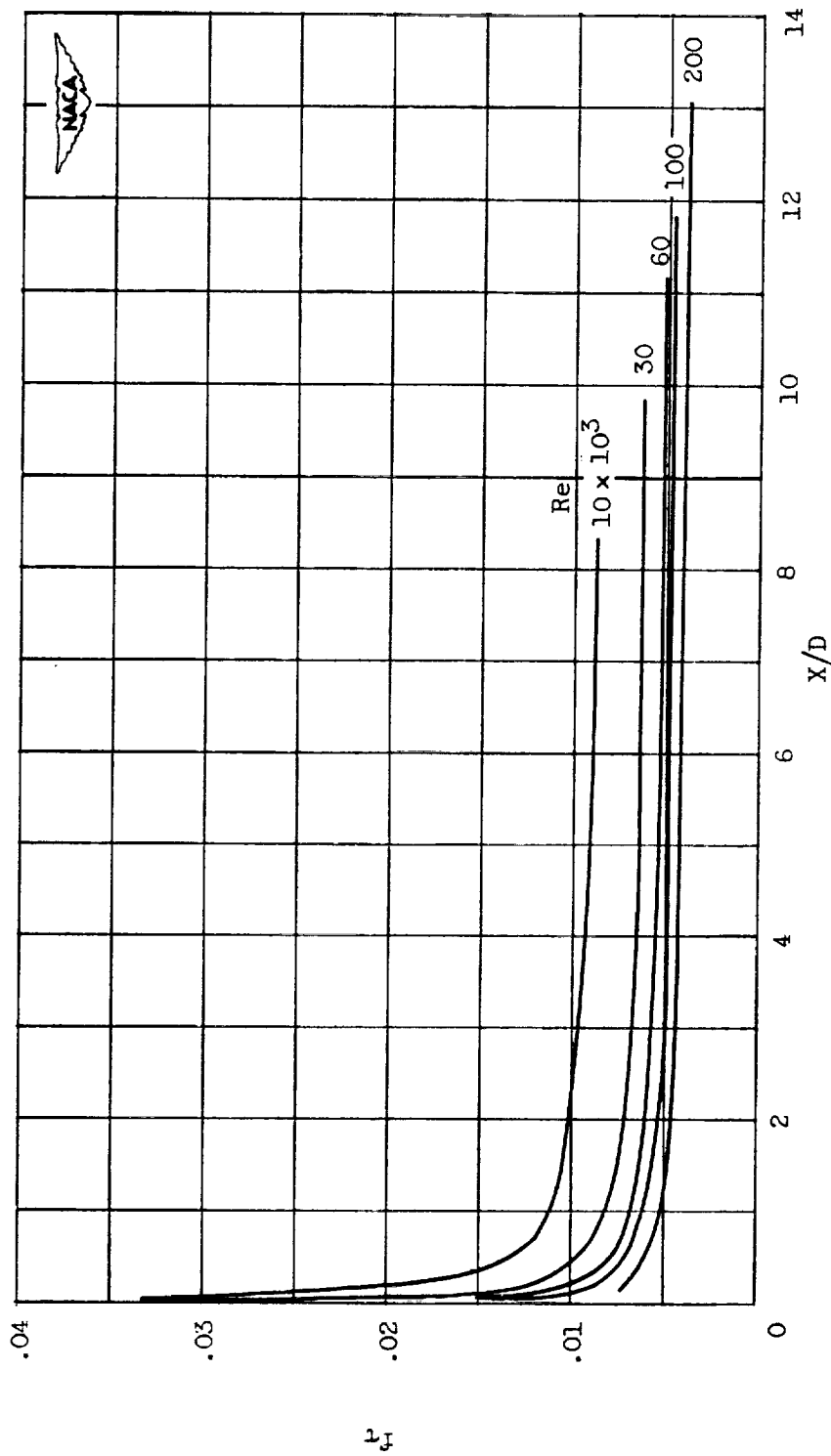


Figure 31. - Variation of friction factor based on wall shear stress with  $x/D$  and Reynolds number for flow between parallel flat plates. Constant properties.

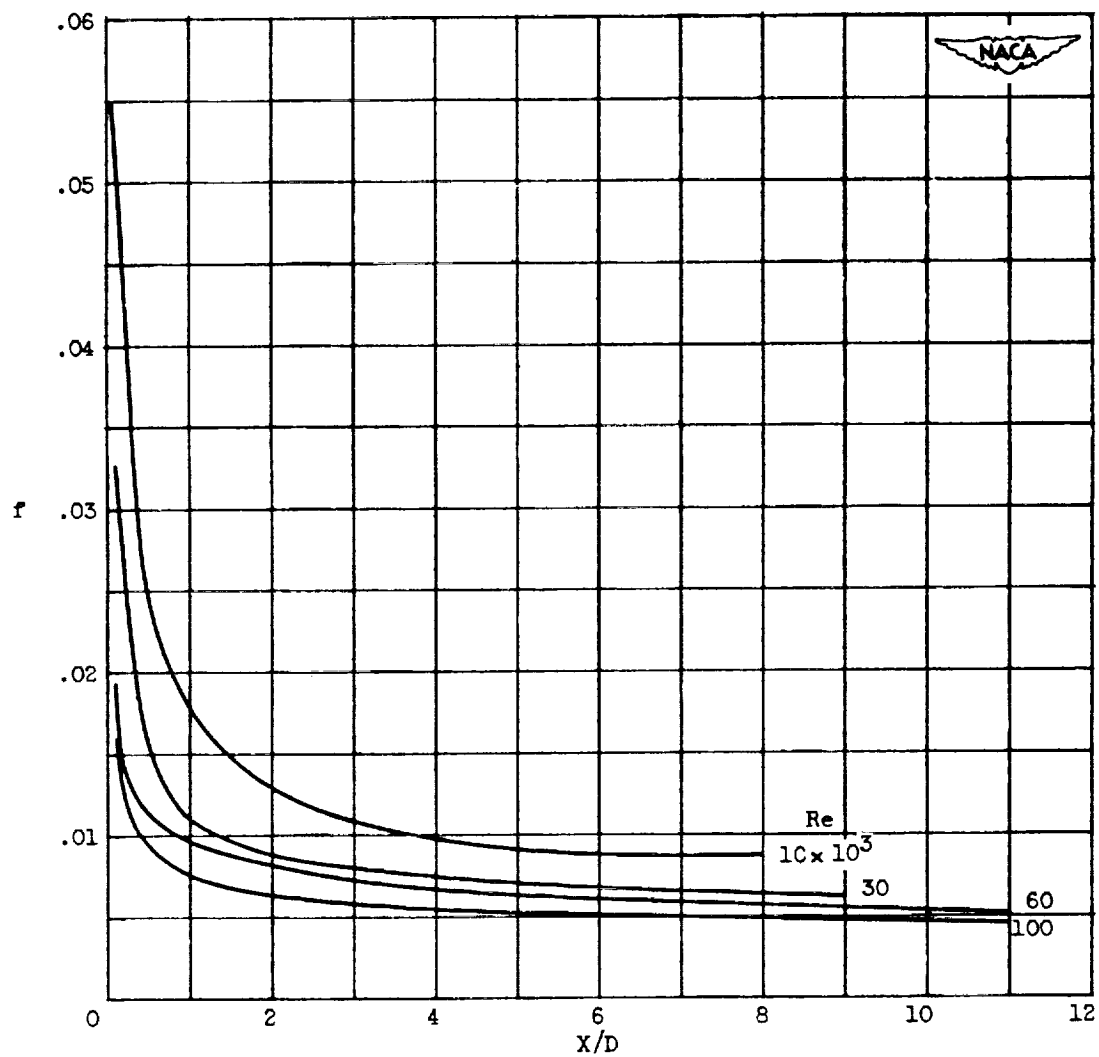


Figure 32. - Variation of friction factor based on static-pressure gradient with  $X/D$  and Reynolds number for flow between parallel flat plates. Constant properties.



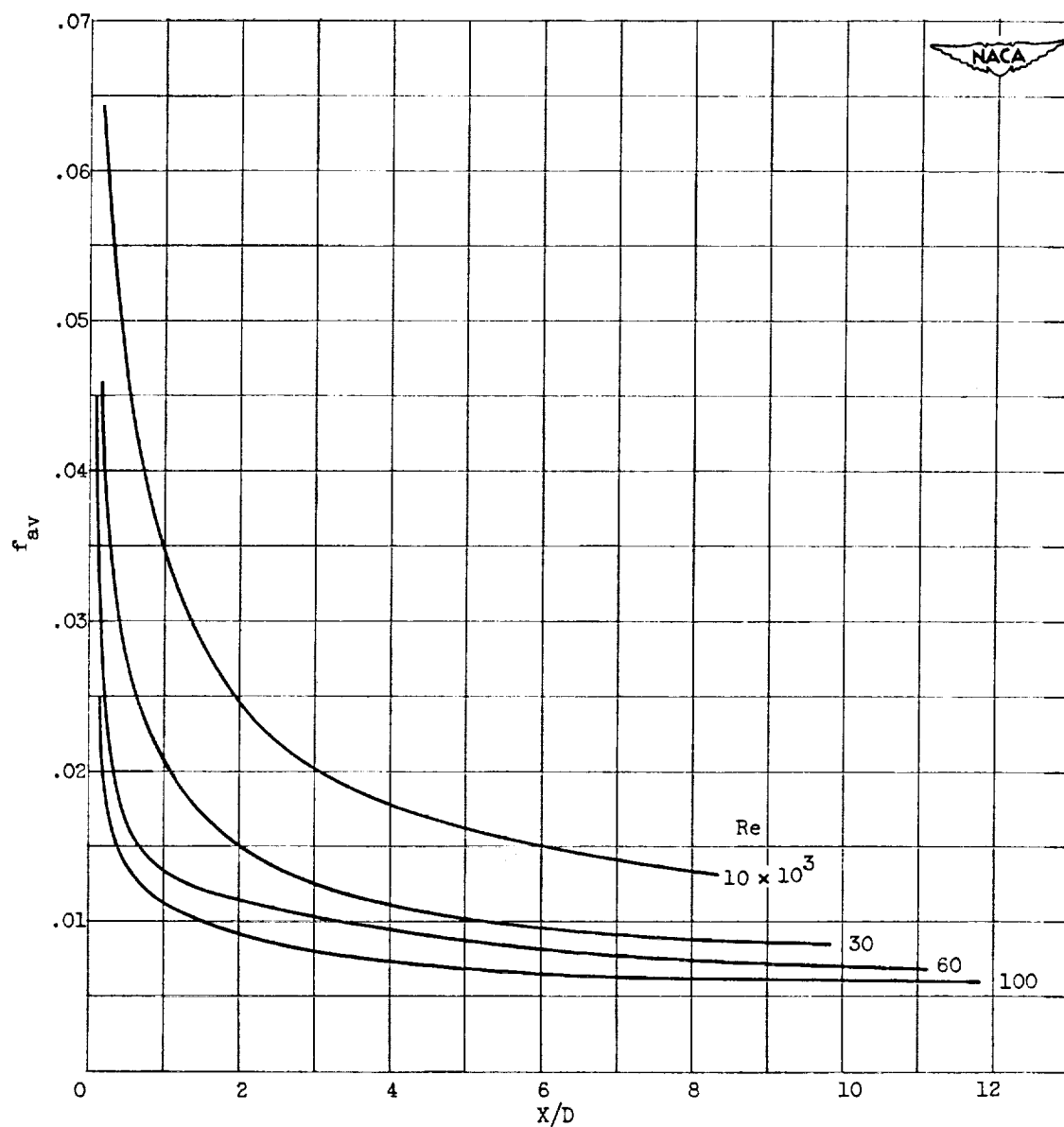


Figure 33. - Variation of average friction factor based on static-pressure drop with  $X/D$  and Reynolds number for flow between parallel flat plates. Constant properties.

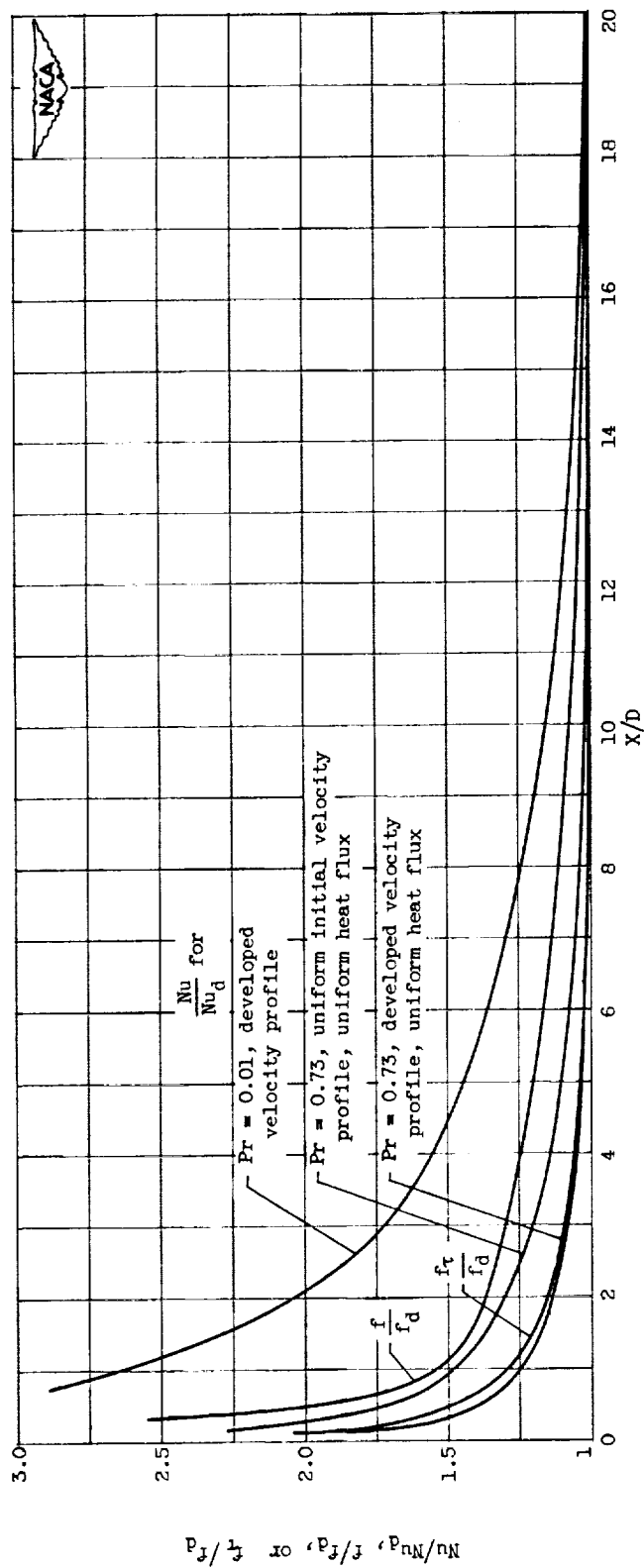


Figure 34. - Comparison of Nusselt numbers and friction factors for various cases. Constant properties. Reynolds number, 100,000.